B.Tech. (VII Sem.) 17EC27 - MICROWAVE ENGINEERING

Objective:

This course provides the knowledge on microwave communication in terms of various bands, advantages, applications.

The course will give an idea about microwave active and passive devices.

The course also gives the complete information regarding microwave bench setup and microwave measurements.

Course Outcomes (COs): At the end of the course, students will be able to

CO1: Understand the operation and use of Microwave solid state devices

CO2: Analyze the characteristics of Microwave tubes.

CO3: Apply the properties of S-parameters to waveguide components.

CO4: Evaluate the various microwave parameters using microwave bench setup.

UNIT-I

Introduction, Microwave Spectrum and Bands, Advantages and Applications of Microwaves.

Microwave Tubes: Limitations and Losses of conventional tubes at microwave frequencies. Microwave tubes – O type and M type classifications.

Klystron Tubes: Two Cavity Klystrons – Structure, Velocity Modulation Process and Applegate Diagram, Bunching Process– Expressions for o/p Power and Efficiency. Reflex Klystrons – Structure, Applegate Diagram and Principle of working, Mathematical Theory of Bunching, Power Output, Efficiency, o/p Characteristics.

What is microwave?

The term *microwave* is typically used for frequencies between 3 and 300 GHz, with a corresponding electrical wavelength between $\lambda = c/f = 10$ cm and $\lambda = 1$ mm, respectively.
A wavelength is the distance between the crests of waves.

The wave length of a signal which is represented by the Greek letter λ(lambda) is computed by dividing speed of light (C) by the frequency f

$$\lambda = \frac{v}{f} \quad \text{or} \quad f = \frac{v}{\lambda}$$

Where:

λ = wavelength in meters

v = velocity of radio wave (speed of light)

f = frequency of radio wave (in Hz, kHz or Mhz)

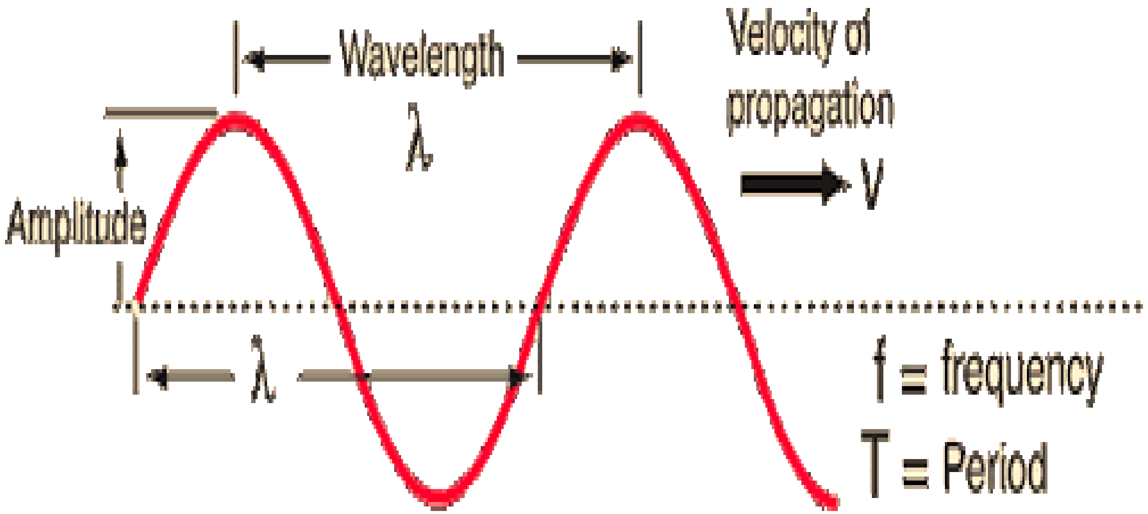

Find the wavelengths of (*a*) a 150-MHz, (*b*) a 430-MHz, (*c*) an 8-MHz, and (*d*) a 750-kHz signal.

a. $\lambda = \frac{300{,}000{,}000}{150{,}000{,}000} = \frac{300}{150} = 2\text{ m}$

b. $\lambda = \frac{300}{430} = 0.697\text{ m}$

c. $\lambda = \frac{300}{8} = 37.5\text{ m}$

d. For Hz (750 kHz = 750,000 Hz):

$$\lambda = \frac{300{,}000{,}000}{750{,}000} = 400\text{ m}$$

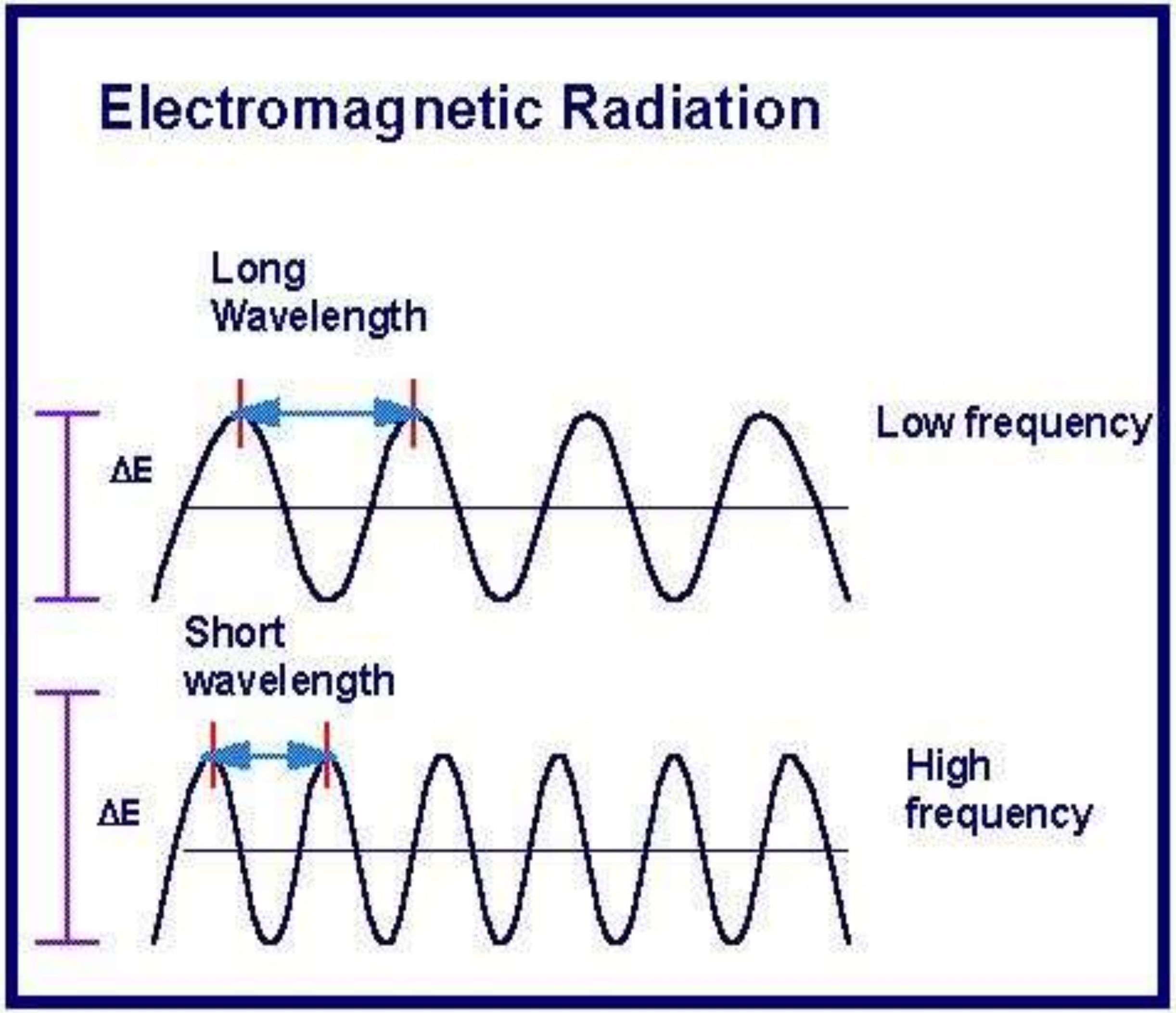

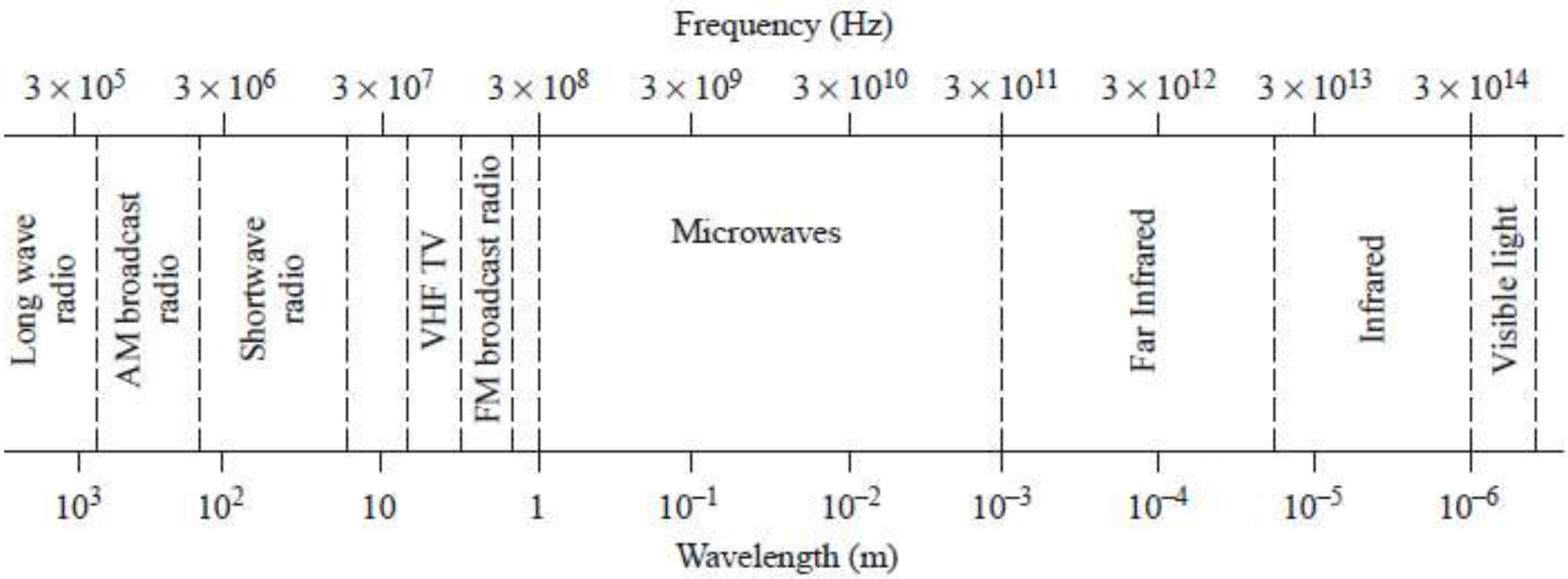
Frequency (Hz)
3 × 10^5
3 × 10^6
3 × 10^7
3 × 10^8
3 × 10^9
3 × 10^10
3 × 10^11
3 × 10^12
3 × 10^13
3 × 10^14
Long wave radio
AM broadcast radio
Shortwave radio
VHF TV
FM broadcast radio
Microwaves
Far Infrared
Infrared
Visible light
10^3
10^2
10
1
10^-1
10^-2
10^-3
10^-4
10^-5
10^-6
Wavelength (m)

Typical Frequencies	
AM broadcast band	535–1605 kHz
Short wave radio band	3–30 MHz
FM broadcast band	88–108 MHz
VHF TV (2–4)	54–72 MHz
VHF TV (5–6)	76–88 MHz
UHF TV (7–13)	174–216 MHz
UHF TV (14–83)	470–890 MHz
US cellular telephone	824–849 MHz
	869–894 MHz
European GSM cellular	880–915 MHz
	925–960 MHz
GPS	1575.42 MHz
	1227.60 MHz
Microwave ovens	2.45 GHz

Approximate Band Designations	
Medium frequency	300 kHz–3 MHz
High frequency (HF)	3 MHz–30 MHz
Very high frequency (VHF)	30 MHz–300 MHz
Ultra high frequency (UHF)	300 MHz–3 GHz
L band	1–2 GHz
S band	2–4 GHz
C band	4–8 GHz
X band	8–12 GHz
Ku band	12–18 GHz
K band	18–26 GHz
Ka band	26–40 GHz
U band	40–60 GHz
V band	50–75 GHz
E band	60–90 GHz

Table of frequency bands

Band	Frequency range
HF Band	3 to 30 MHz
VHF Band	30 to 300 MHz
UHF Band	300 to 1000 MHz
L Band	1 to 2 GHz
S Band	2 to 4 GHz
C Band	4 to 8 GHz
X Band	8 to 12 GHz
Ku Band	12 to 18 GHz
K Band	18 to 27 GHz
Ka Band	27 to 40 GHz
V Band	40 to 75 GHz
W Band	75 to 110 GHz
mm Band	110 to 300 GHz

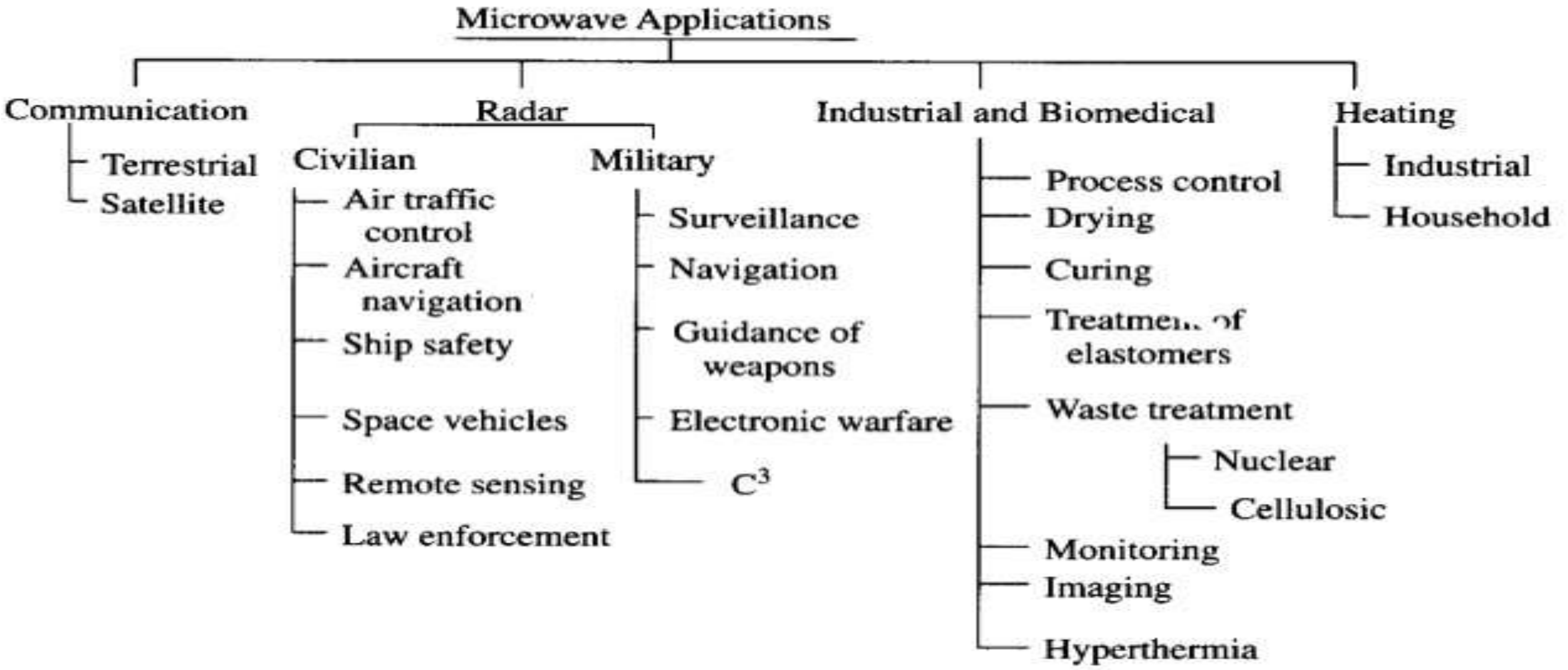
Microwave Applications
Communication
Terrestrial
Satellite
Radar
Civilian
Air traffic control
Aircraft navigation
Ship safety
Space vehicles
Remote sensing
Law enforcement
Military
Surveillance
Navigation
Guidance of weapons
Electronic warfare
C3
Industrial and Biomedical
Process control
Drying
Curing
Treatment of elastomers
Waste treatment
Nuclear
Cellulosic
Monitoring
Imaging
Hyperthermia
Heating
Industrial
Household

Application of different types of frequency bands

The main uses of the HF spectrum are:

- Military and governmental communication systems
- Aviation air-to-ground communications
- Amateur radio
- Over the horizon radar systems

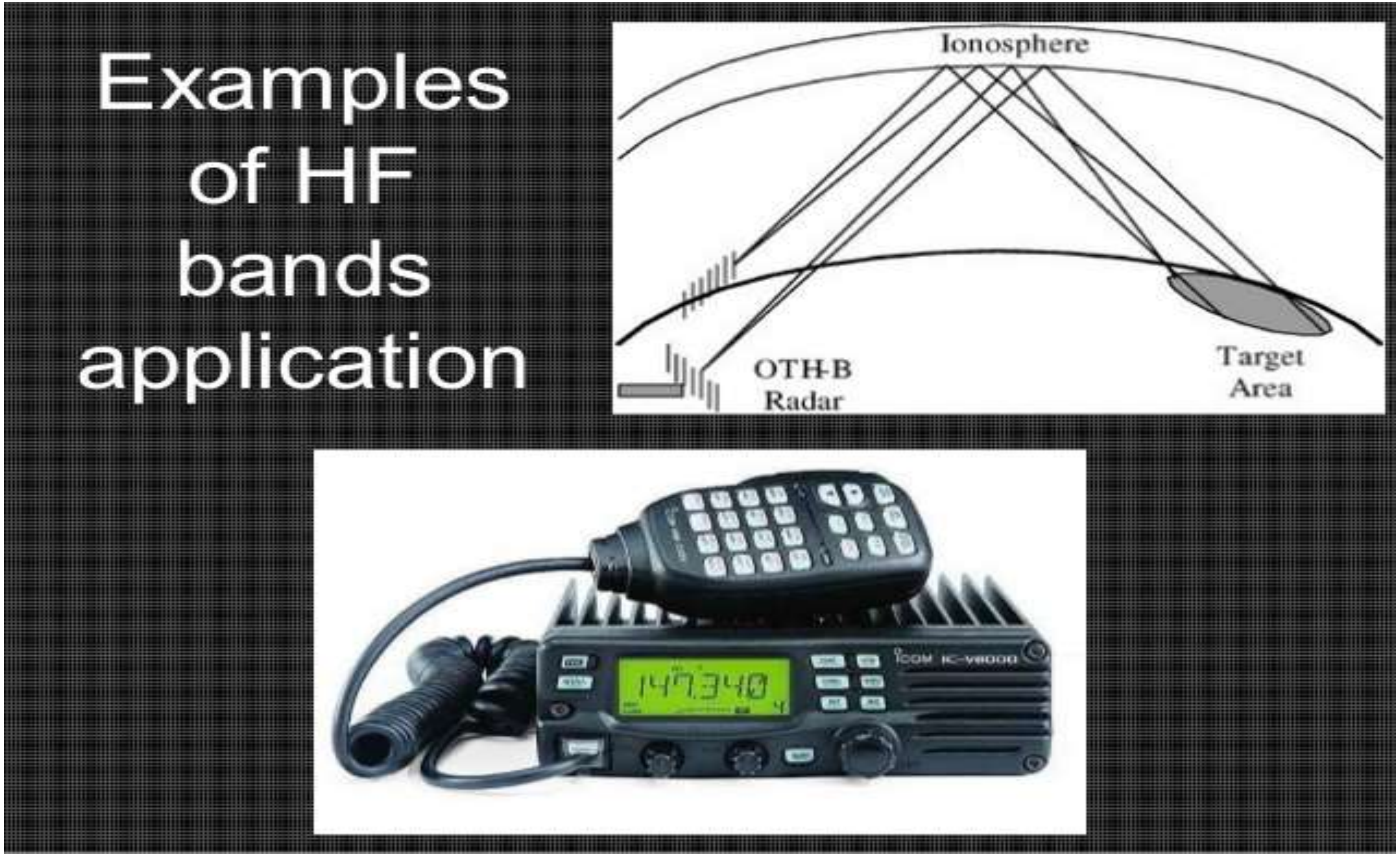
Examples of HF bands application
Ionosphere
OTH-B Radar
Target Area

Application of UHF band

300 – 420 MHz: Meteorology and federal two-way use
420 – 450 MHz: Government radiolocation and 70cm ham radio band
450 – 470 MHz: UHF Business Band, GMRS, FRS, public safety


Examples of UHF band applicatio
MOTOROLA
CDM1250
P1
P2
P3
P4

Application of L band

Astronomy
Digital Audio Broadcasting
Satellite navigation
Mobile service

Examples of L band application

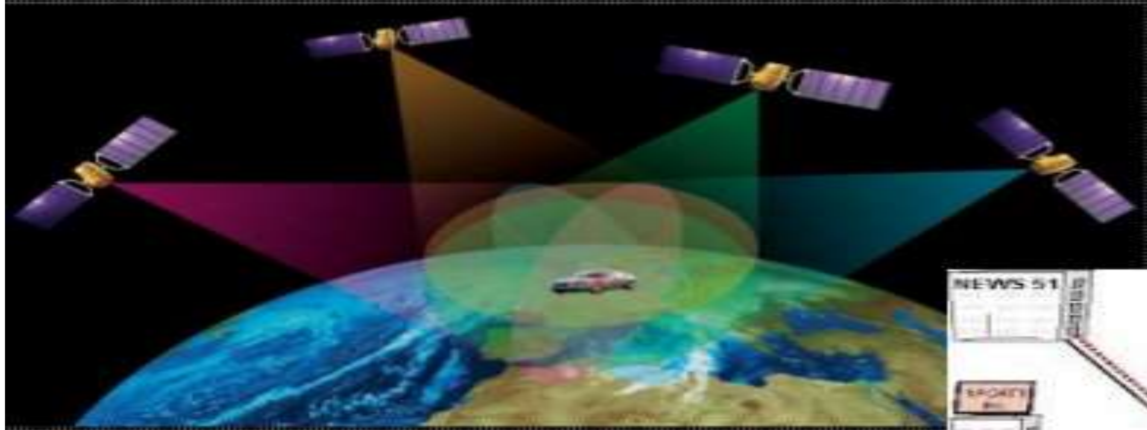

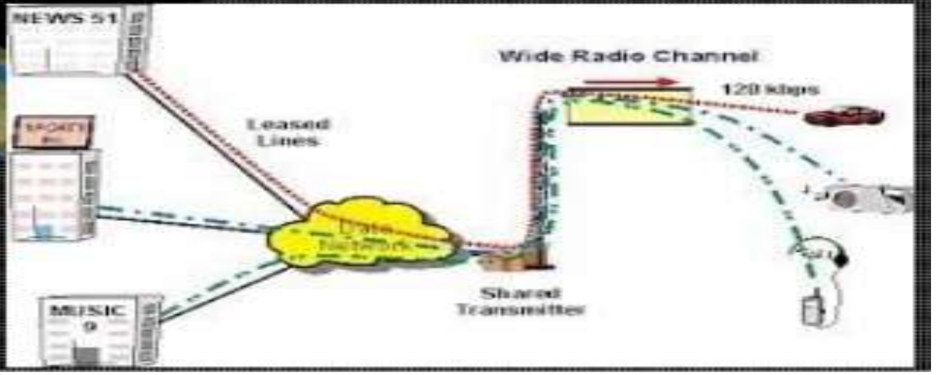

Application of S band

Weather radar
Surface ship radar
Some communications satellites.

Examples of S band application

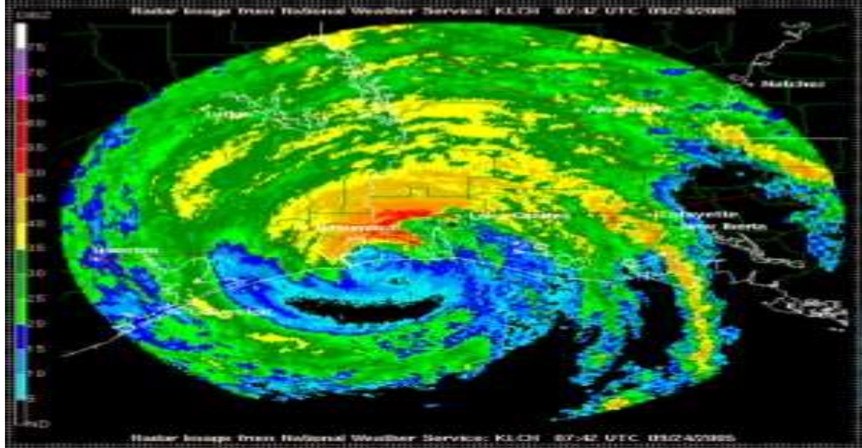

Application of C band

Microwave radio relay chains
Television receive-only satellite reception systems
802.11a Wi-Fi
Cordless telephone applications

Examples of C band application

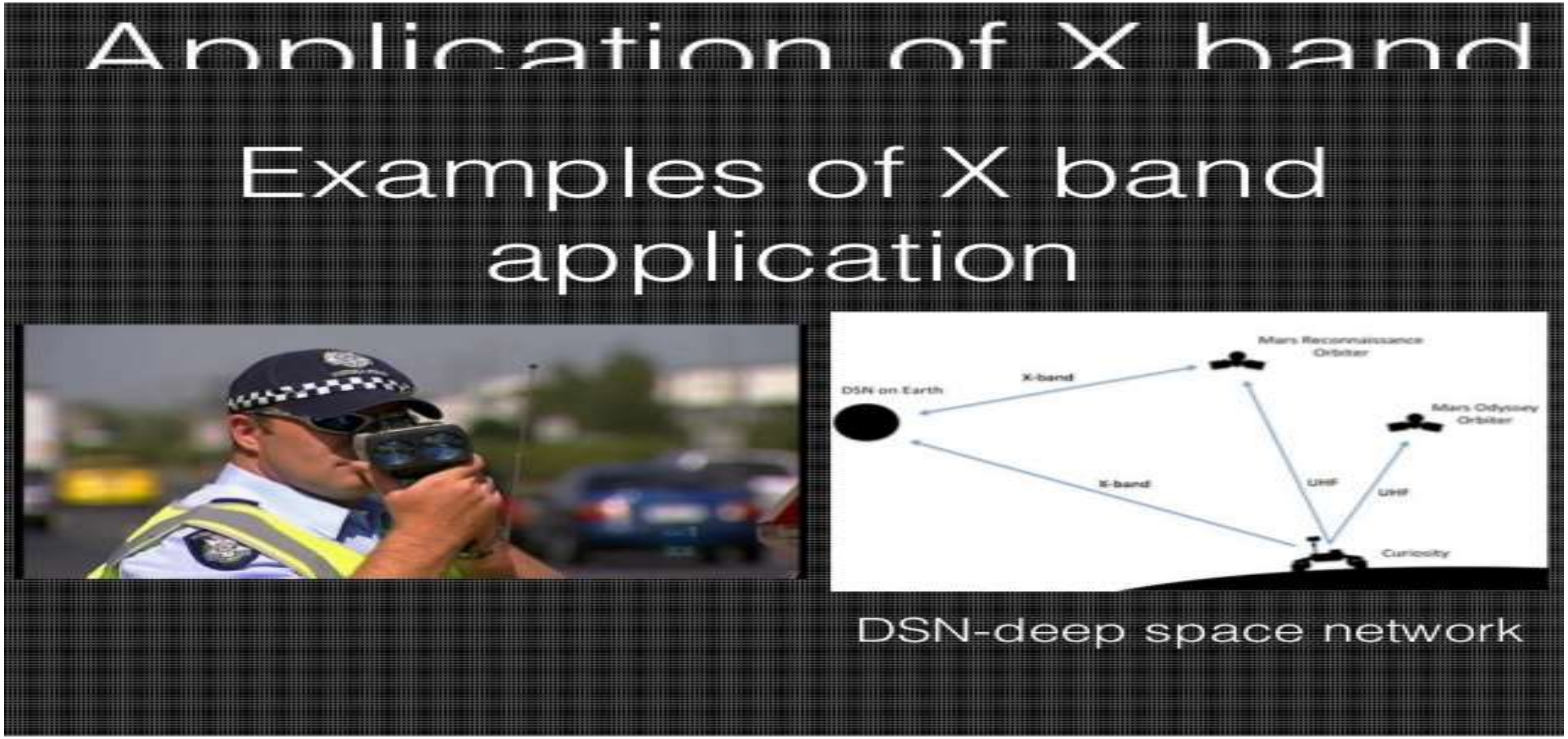
Application of X band
Examples of X band application
Mars Reconnaissance Orbiter
X-band
DSN on Earth
Mars Odyssey Orbiter
X-band
UHF
UHF
Curiosity
DSN-deep space network


Application of Ku band
Satellite communication
Vehicle speed detection
Examples of Ku band application
AirLNK™ B-LOS
End-to-End Beyond Line of Sight Communication
satellite
transceiving parabolic antenna
relay station
home antenna
Hertzian wave transmission
private broadcasting network
transmitting tower
local station
mobile unit
national broadcasting network
cable distributor
direct home reception
distribution by aerial cable network


Application of mm band
Almost all modern electronic devices
Examples of mm band application

Other Applications Of Microwaves

Terahertz Images Can Reveal Objects Concealed Under Cloth, Paper, Tape, Even Behind Walls

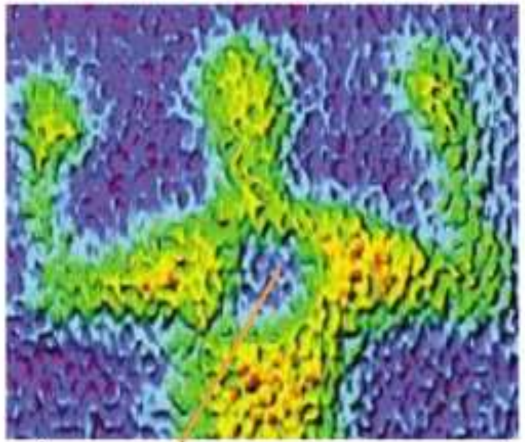

Objects Concealed Under clothes

Knife Wrapped in Newspaper

Homeland Security Applications

Potential Security Applications

- Detection of hidden weapons and explosives
- Detecting non-metallic weapons
- Postal screening of envelopes for bacteria
- Chem/bio detection

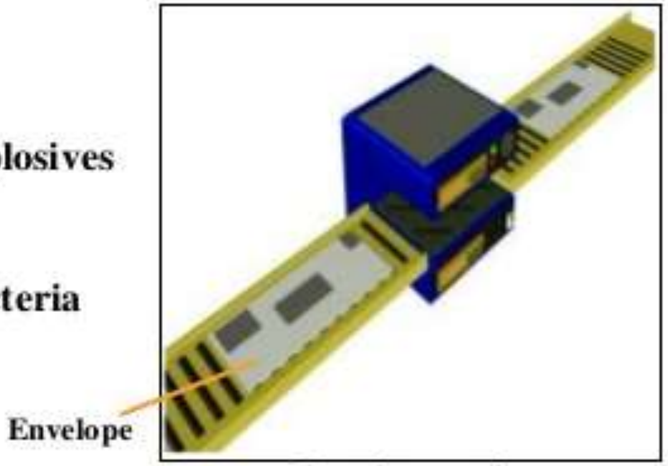

Postal screening

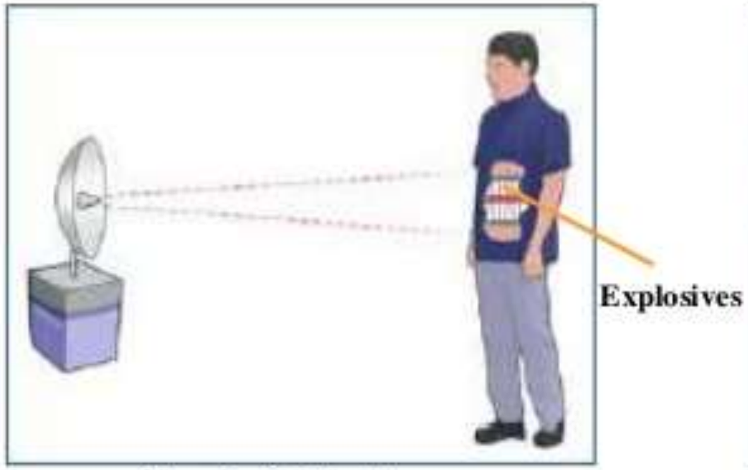

Stand-off detection

Security screening wand

Microwave Tubes: Limitations and Losses of conventional tubes at microwave frequencies.

Conventional Tubes

- Conventional Device tubes cannot be used for frequencies above 100MHz
- 1. Interelectrode capacitance
- 2. Lead Inductance effect
- 3. Transit time effect
- 4. Gain Bandwidth limitation
- 5. Effect of RF losses (Conductance, dielectric)
- 6. Effect due to radiation losses

Inter-electrode capacitance:

- Plays an important role in the operation of tubes at microwave frequency.
- It is due to active parts of tube structure, i.e., between the leads.
- As frequency increases, reactance of C_{gp}, C_{gk} and C_{pk} decreases and begins to short circuit the input and output voltages.

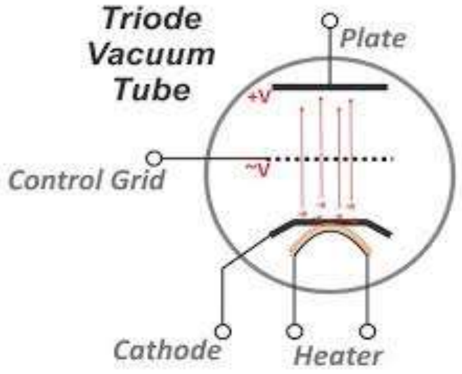

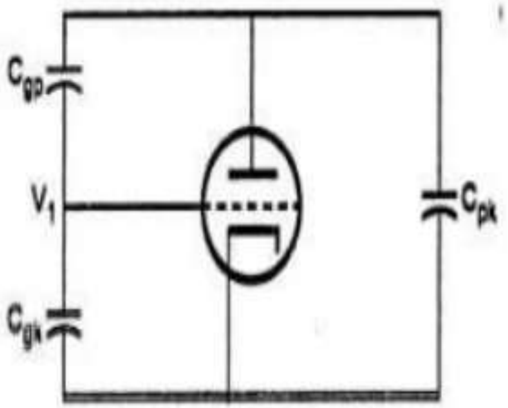

- This leads to reduction in amplification.
- These capacitances must be minimized.
- It can be achieved by increasing the distance between the electrodes or reducing the area of electrodes.

Lead Inductance:

- The leads have small but finite inductance.
- When the frequency increases the reactance of this becomes appreciable.
- They limit the performance of the tube by providing degenerative feedback.
- They can be minimized by using short lead tube.

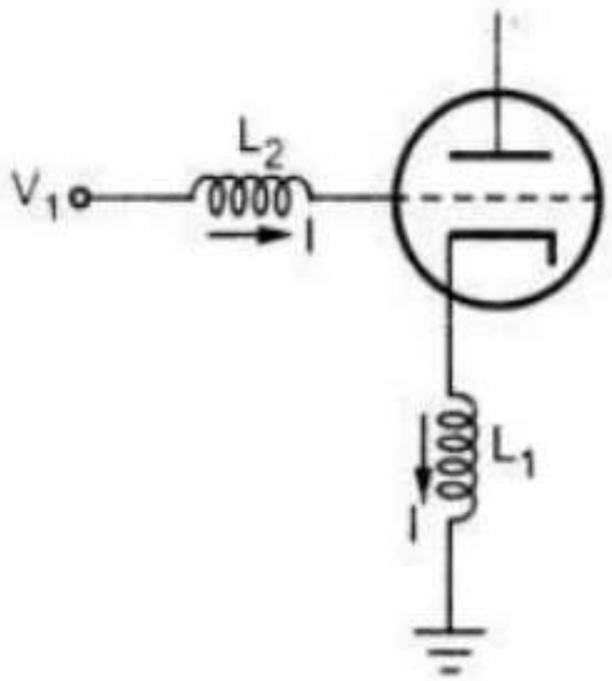

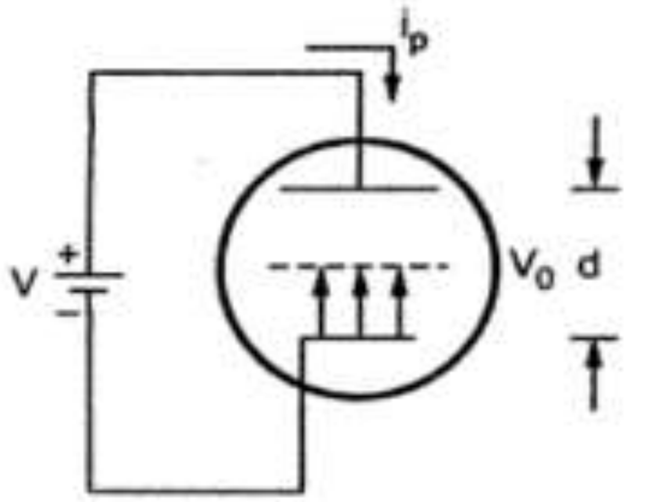

Fig. 3.1.5 Transit-time effect

iv) Transit time effect

- Transit time is the time required for electrons to travel from the cathode to the anode plate. If we consider the circuit of a simple vaccum tube as shown in Fig. 3.1.5. When 'd' is the distance between two plates, i_p is plate current, V is applied input voltage, V_0 is output voltage.

Calculation for Transit Time : By definition, Transit Time is given by :

$$\tau = \frac{d}{v_0} \quad \text{where } v_0 \text{ is velocity of electrons}$$

Static energy of electrons = eV

Kinetic energy of electrons = eV

Kinetic energy of electrons = $\frac{1}{2} m v_0^2$

We know that under equilibrium state the static energy of electrons is equal to kinetic energy of electrons.

$$eV = \frac{1}{2} m v_0^2$$

$$v_0 = \sqrt{\frac{2eV}{m}}$$

$$\tau = \frac{d}{\sqrt{\frac{2eV}{m}}}$$

- At low frequencies, the transit time effect is negligible because distance between anode and cathode is very small.
- But at higher freuqencies, the transit time is large as compared to the period of microwave signal. The potential between the cathode and grid may alternate from 10 to 100 times during the electron transmit.
- **Therefore the transit angle effect reduces the operating efficiency of the vacuum tube**

Gain bandwidth product = $A_{max} \cdot BW = \frac{g_m}{G} \times \frac{G}{C} = \frac{g_m}{C}$

As shown in above relation, the gain bandwidth product is independent of frequency. Higher gain for a given tube can be achieved only by using the narrow bandwidth. This restriction is applicable to its resonant circuit only.

Dielectric losses

- These are different insulating materials which are used as a glass envelope, silicon plastic encapsulations in different microwave devices. The loss in any of these material is in general related to power loss given by :

$$P = \pi f . V_0^2 \varepsilon_r \tan \sigma$$

where ε_r = Relative permittivity of dielectric

δ = Loss angle of dielectric

P = Power loss

3 Power Losses

- The power losses associated with a tube and circuit, tend to increase with frequency. At UHF current flows in the surface layers because of skin effect. The associated resistance and losses increase as square root of frequency.
- Insulating materials like glass have losses associated with molecular movements produced by the electric fields. These losses are called as **dielectric losses**.
- In addition, there are radiation losses from electrodes.
- The **resistance losses** can be reduced by increasing the area of surfaces carrying the current.
- Dielectric losses can be reduced by proper positioning of glass with respect to points of electric fields.

Microwave Tubes

- Microwave tubes are designed to overcome the principle limitations of conventional negative grid electron tubes. In microwave tubes the electron transit time is utilized for microwave oscillation or amplification. The principle uses an electron beam on which space-charge waves interact with electromagnetic fields in the microwave cavities to transfer energy to the output circuit of the cavity.
- There are basically two types of microwave tubes :

O-Type microwave tube

- Tubes in the O-type category are sometimes called linear or rectilinear beam tubes in recognition of the straight path taken by the electron beam. In this class of devices, both velocity and density modulation take place, creating the bunching effect. The electron bundles thus created have a period in the microwave region. Examples of O-type tubes include Klystrons and travelling-wave tubes (TWT).

M-Type microwave tube

- A principle feature of such tubes is that electrons travel in a curved path. Those tubes were designated M-type. These are crossed field devices where the static magnetic field is perpendicular to the electric field. e.g. Magnetrons.
- The O-type tubes differ from M-type in that electrons travel in a straight line under the influence of parallel electric and magnetic fields.

CLASSIFICATION OF MICROWAVE TUBES

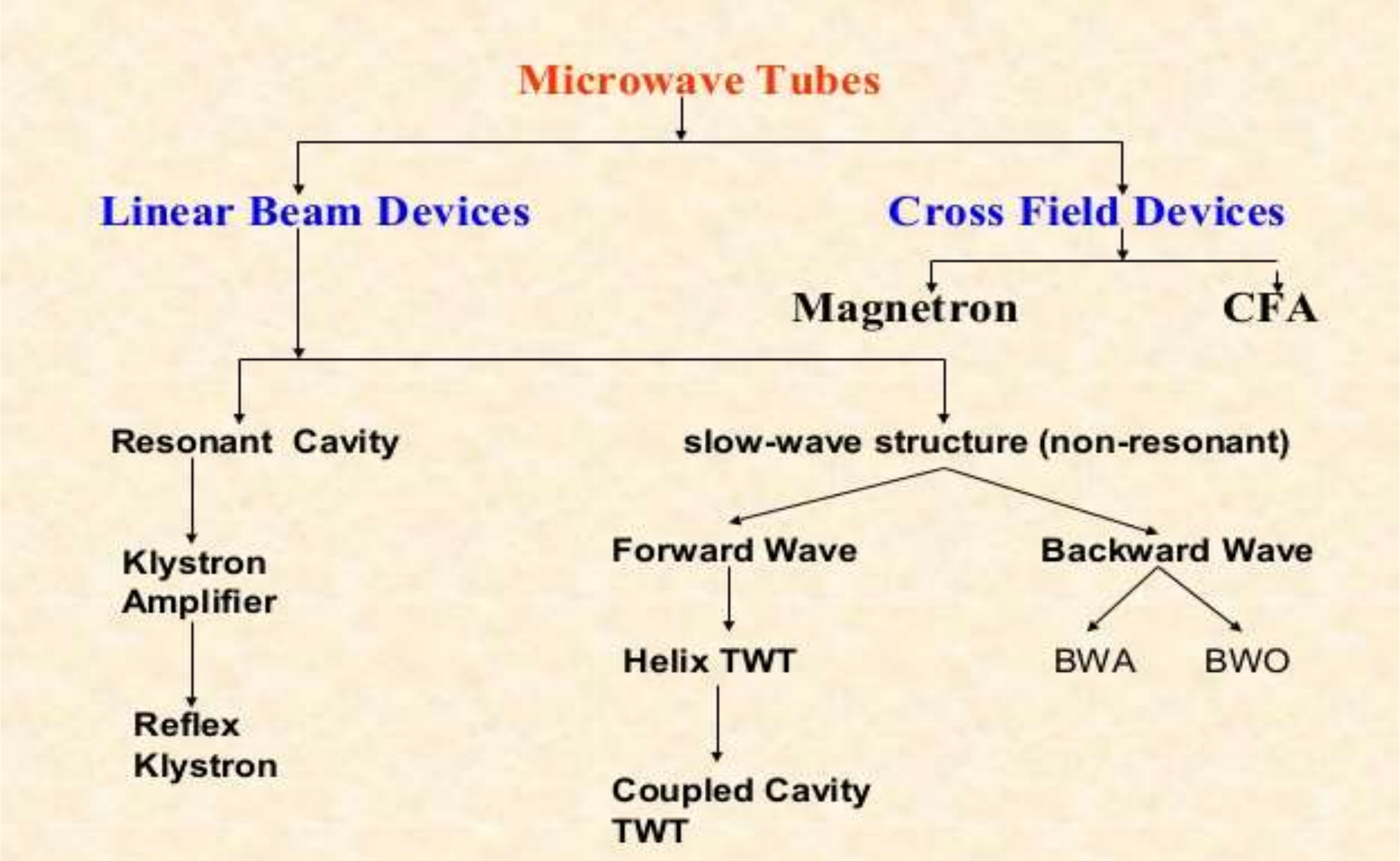

O-type Travelling tubes are suitable for amplification.

Classification of different O-type tubes is ,

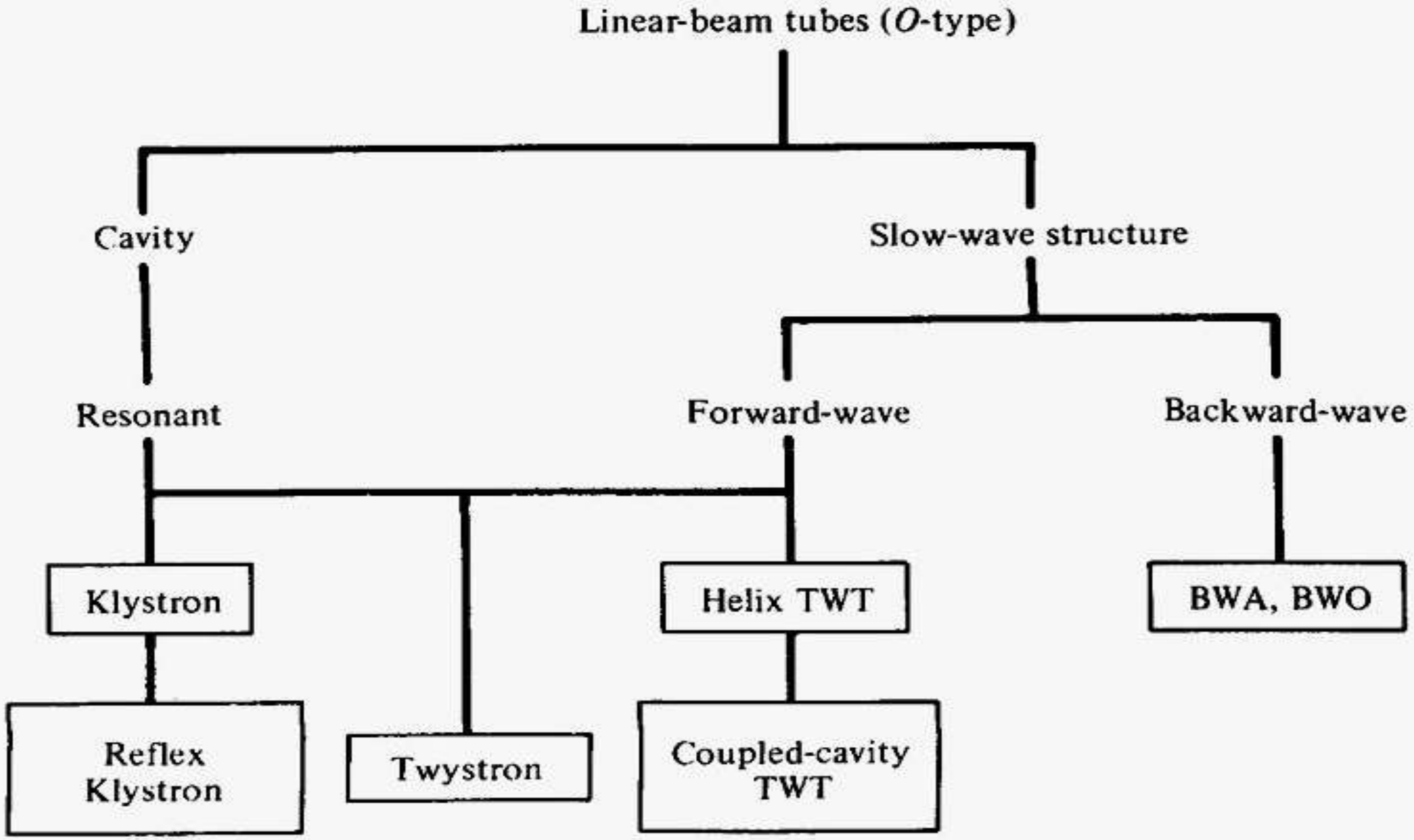

The classification of crossed-field tubes is,

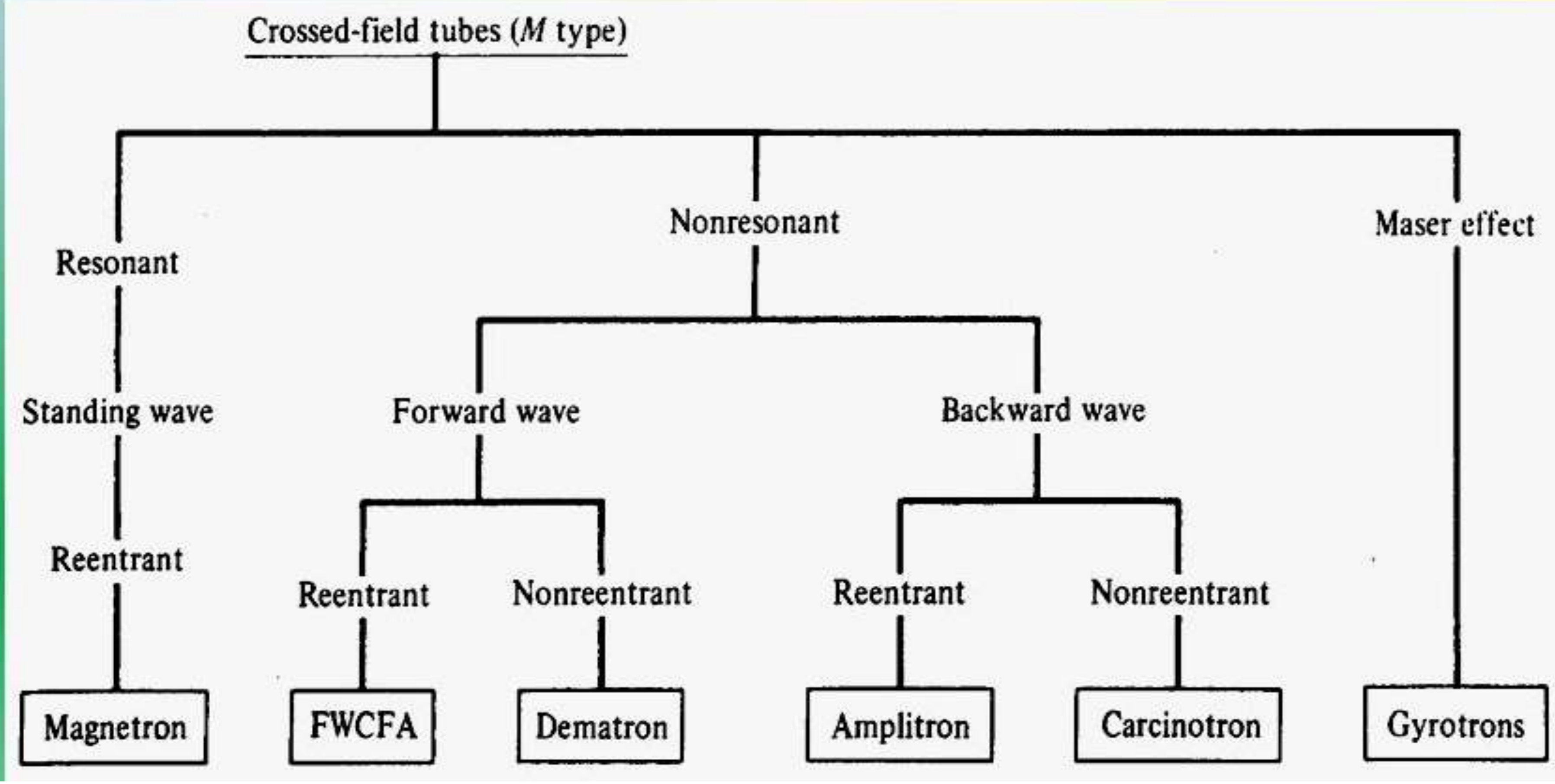

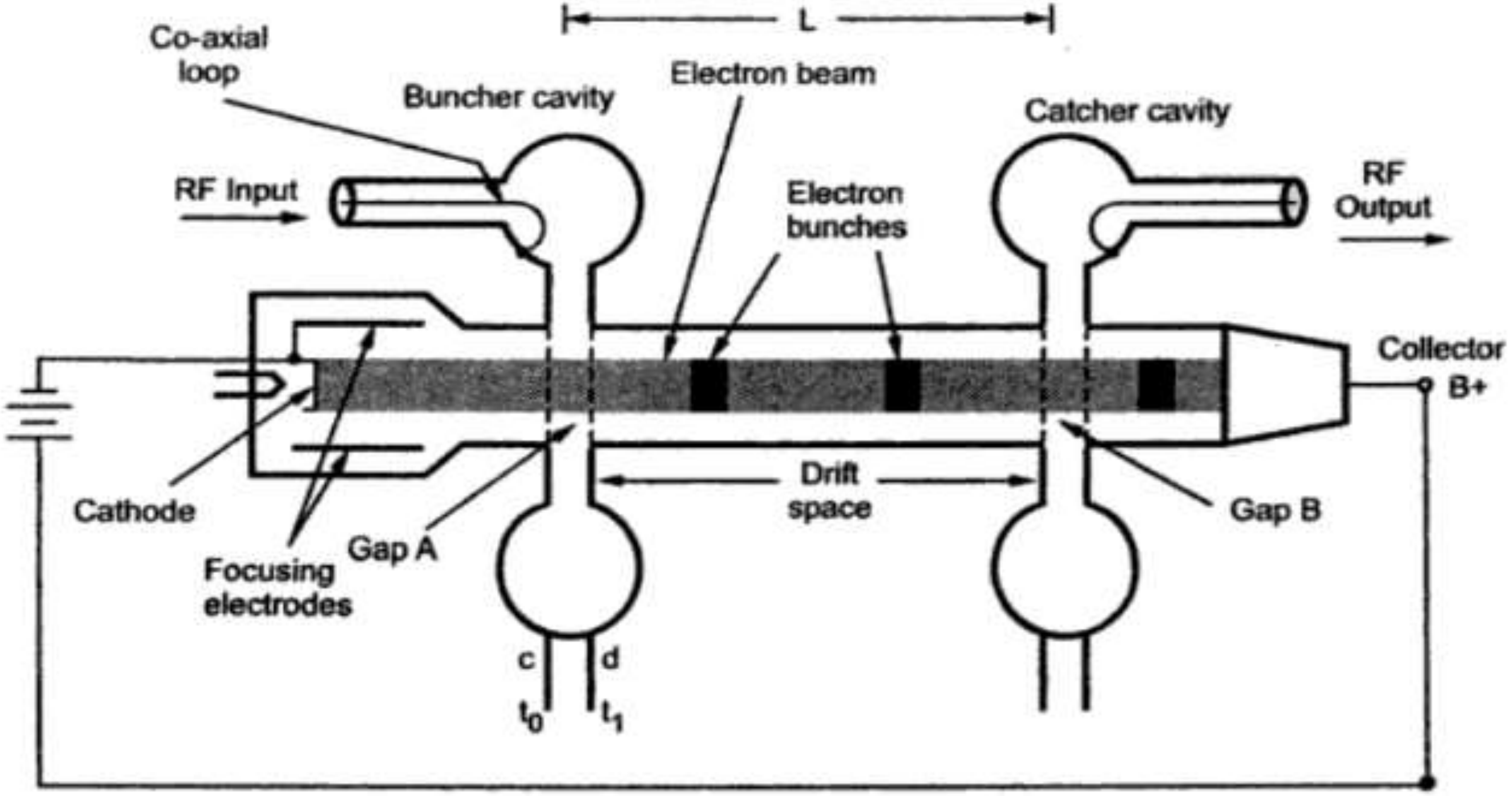

Fig. 5.3.1 Klystron amplifier schematic diagram

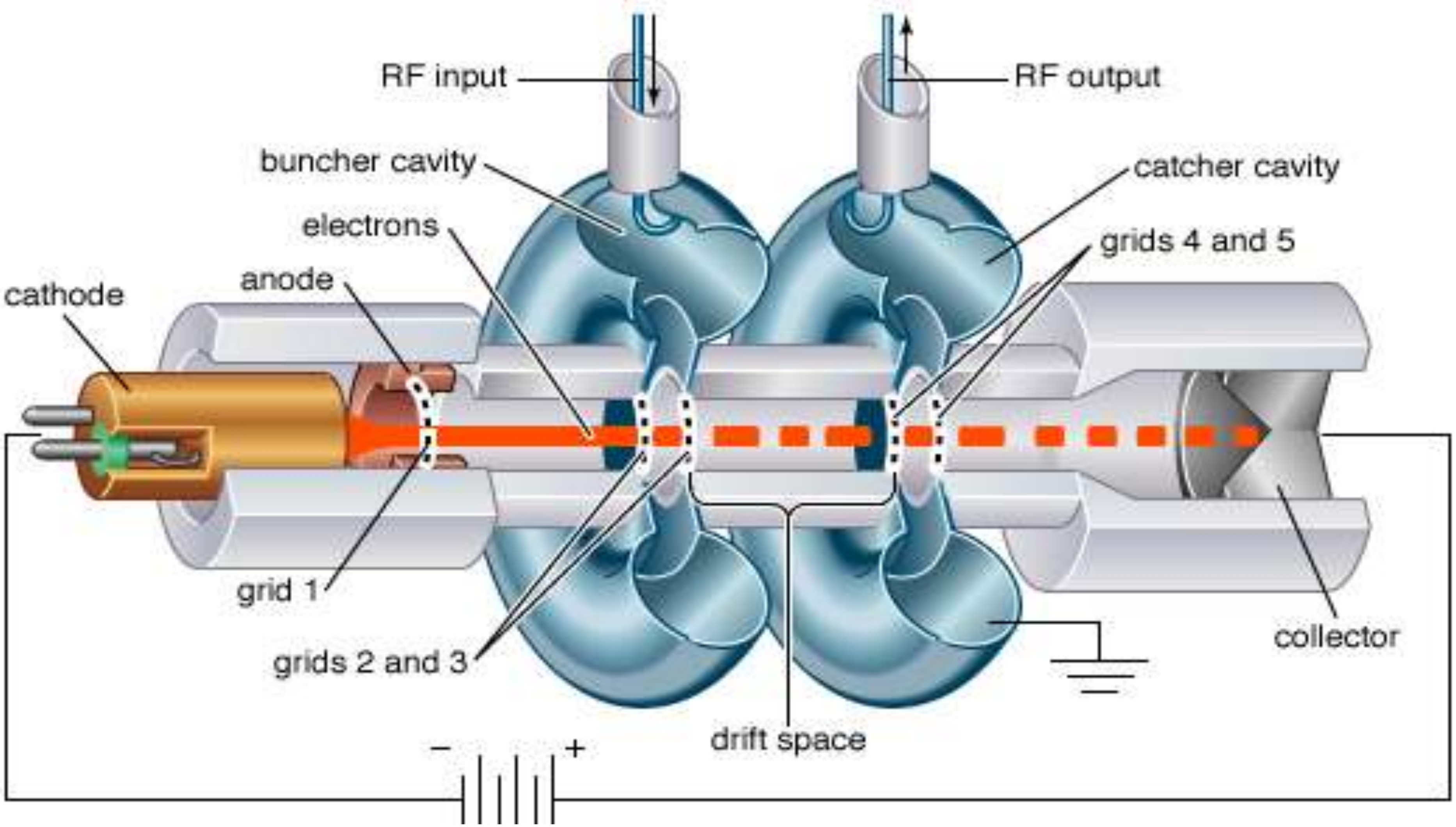
RF input
RF output
buncher cavity
catcher cavity
electrons
grids 4 and 5
anode
cathode
grid 1
grids 2 and 3
collector
drift space
−
+

5.3 Klystron

- Klystron is most widely used tube as amplifier at microwave frequencies. Klystron works on the principle of velocity and current modulation. There are two basic configurations of Klystron tubes.

i) Two cavity or multicavity Klystron- It is used as low power microwave amplifier.

ii) Reflex Klystron - It is used as low power microwave oscillator.

5.3.1 Two Cavity Klystron Amplifier

[a] Construction

- A two cavity Klystron amplifier consists of a cathode, focussing electrodes, two buncher grids separated by a very small distance forming a gap of two catcher grids with small gap B followed by a collector. The cavity close to the cathode is known as the **buncher cavity** or input cavity, which velocity modulates the electron beam. The other cavity is called the **catcher cavity** or output cavity it catches energy from the bunched electron beam. Fig. 5.3.1 shows schematic diagram of two cavity Klystron amplifier.

b) Operation

- Two cavity Klystron amplifier works on the principle of velocity and current modulation. A high velocity electron beam is formed, focussed and sent down along a glass tube to a collector electrode. The high velocity electron beam generated by cathode arrive at the first cavity with uniform velocity. The electron beam passes gap A in the buncher cavity to which RF signal to be amplified is applied and is then allowed to drift freely without any influence from RF fields until it reaches gap B in the output or catcher cavity. The separation between buncher grid and catcher grid is called **drift space**.

- The focussing electrode (first grid) controls the numbers of electron beam and serves to focus the beam. The velocity of electrons in the beam is determined by the beam accelerating potential. On having the region of first grid, the electrons pass through the grids of buncher cavity. The grids of the cavity allow the electrons to pass through, but limits the magnetic fields within the cavity. The space between the grids is referred to as **interaction space**. When the electrons travel through this space they are subjected to RF potentials at a frequency determined by the cavity resonant frequency or the input frequency. The amplitude of this RF potential between the grids is determined by the amplitude of the incoming signal in case of the amplifier, or by the amplitude of the feed-back signal from the second cavity it used as an oscillator.

The cavities are re-entrant type and are tunable.

Velocity Modulation and Bunching

Consider when there is no voltage across the gap ; electrons passing the gap are not affected and continue to collector with same constant velocity.

When an input is applied to the buncher cavity, an electron will pass gap A at the time when the voltage across this gap is zero and going positive, let this be the reference electron y. This reference electron is unaffected by the gap, and thus it is shown with the same slope on the applegate diagram of Fig. 5.3.2 as electrons passing the gap before any signal was applied to the buncher cavity.

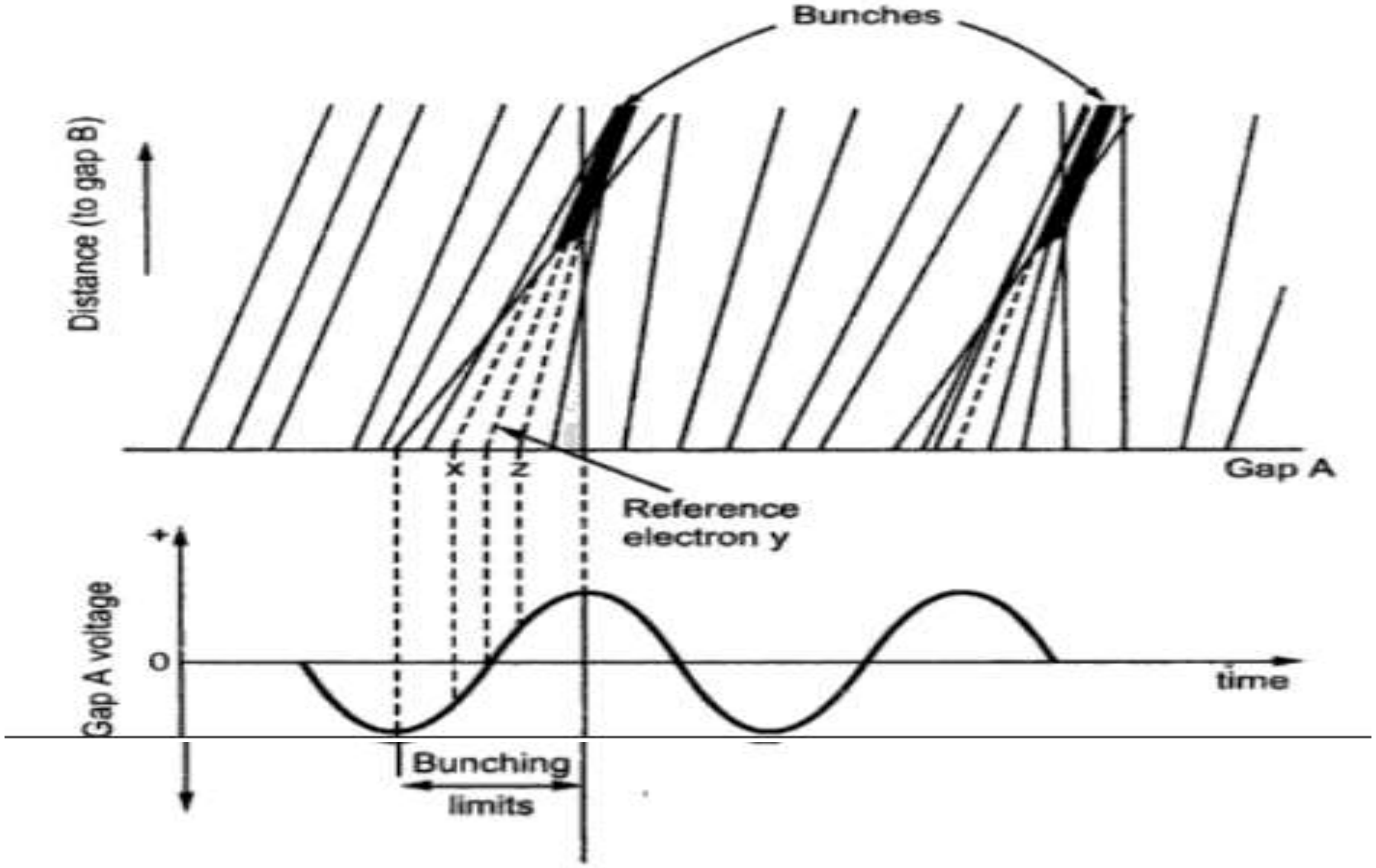

Fig. 5.3.2 Applegate diagram for Klystron amplifier

- Electron z, passes gap A slightly later than y as shown. In absense of gap voltage, both electrons would have continued past the gap with unchanged velocity. In presence of positive voltage across gap A, however electron z is accelerated slightly and given enough time, will catch up with the reference electron easily before gap B is approached.
- Similarly, electron x passes gap A slightly before the reference electron, and is retarded by the negative voltage, at that instant across the gap, since electron y was not so retarded, it has an excellent chance of catching electron x before gap B, this is shown in applegate diagram.

- As a result of these actions, the electrons gradually **bunch** together as they travel down the drift space. The variation in electron velocity in the drift space is known as **velocity modulation**. The density of the electrons in the second cavity gap varies cyclically with time. Such velocity modulation is not sufficient in itself for amplification, by Klystron. While bunching of electrons it exchanges energy with the slower electron, giving it some excess energy, and the two bunch together move with the average velocity of the beam. As the beam progresses further down along the drift space, the **bunching** becomes more complete, as more and more of the faster electrons catch up with bunches ahead. Eventually, the current passes the catch gap with quite pronounced bunches and, therefore varies cyclically with time, and this variation in current density (current modulation) enables the Klystron to have a significant gain.

- Applegate diagram shows that the bunching can occur only per cycle, centering on the reference electron. The limits of bunching are also shown, any electrons arriving after the second limit are not accelerated sufficiently to catch up with any electron passing through the gap A just before the first limit. Bunches, therefore, arrive at the catcher grid, once per cycle and then deliver this energy to this cavity. The catcher cavity is excited into oscillations at its resonant frequency (input frequency) and a large sinusoidal output can be obtained because of flywheel effect of the output resonator. Bunching therefore, depends upon the following parameters.

i) Drift space should be adjusted properly.

ii) Signal amplitude should be such that proper bunching takes place.

iii) DC anode voltage.

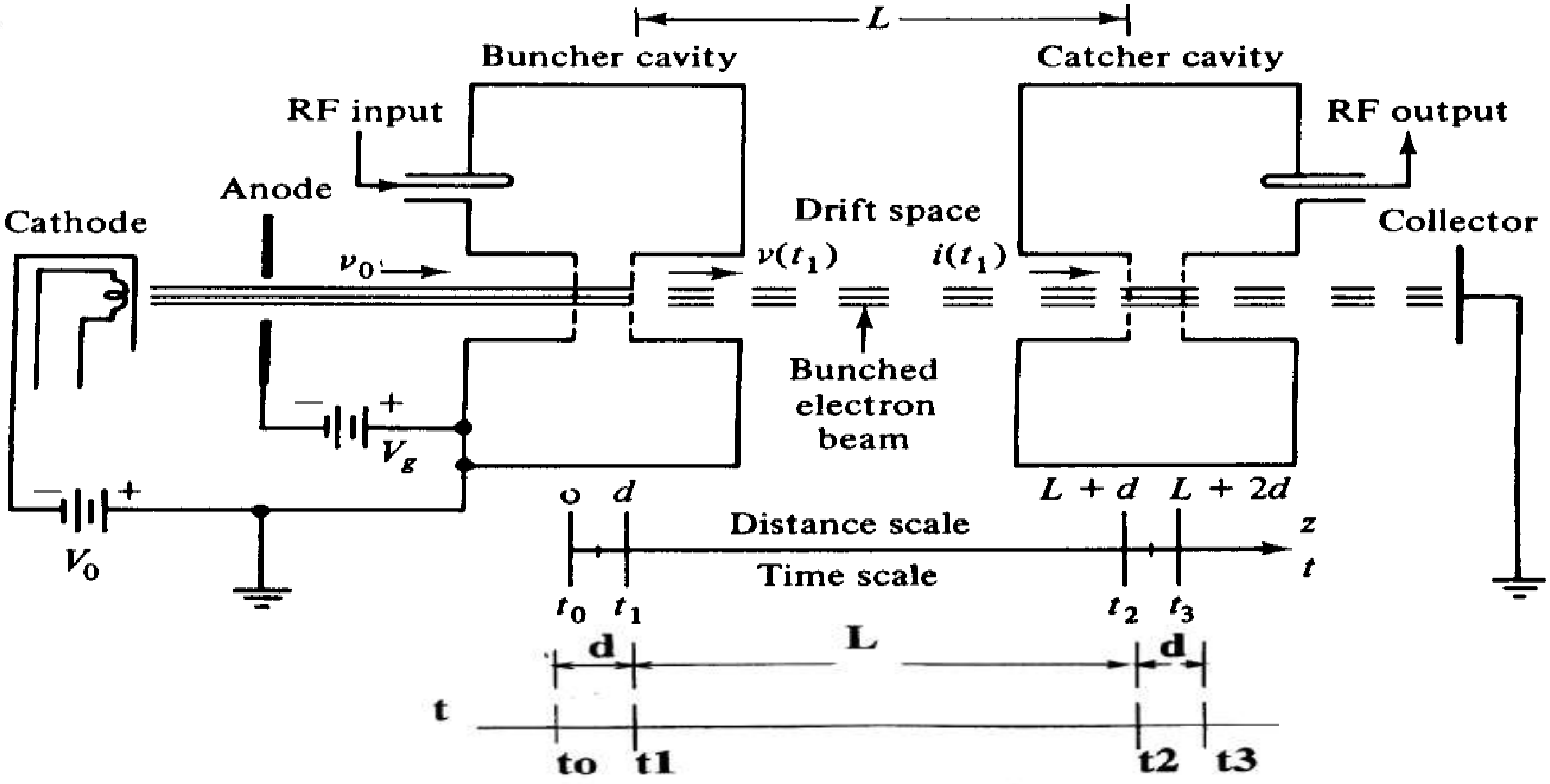

Fig 5.1 Schematic diagram of two cavity klystron

Components of two cavity klystron

Cathode: Source of electrons

Anode: for formation of electron beam

Bucher Cavity: A reentrat type resonator cavity which is kept at a +ve voltage of V_o w.r.t. cathode to effect acceleration of electrons. RF input voltage of $\mathbf{V_1}$ **Sin** $\boldsymbol{\omega t}$ is applied **to buncher** cavity.

Catcher cavity: The amplified output signal $\mathbf{V_2}$ **Sin** $\boldsymbol{\omega t}$ is obtained from this cavity.

Collector: The elctrons after transfer of enerty to catcher cavity are collected by the collector.

Let us define varous parameters used in the description and operation of two cavity klystron.

$\mathbf{V_o}$ = DC voltage between cathode and buncher cavity.

$\mathbf{V_1}$ = Amplitude of input RF signal, $\mathbf{V_{1} << V_o}$

$\boldsymbol{\omega = 2\pi f}$ = Input signal angular frequency. It is also equal to resonant frequency of both the cavities.

vo = Uniform velocity of electrons between cathode and buncher cavity. t_o = Time at which electrons enter the buncher cavity

t_1 = Time at which electrons leave the buncher cavity

t = Transit time of electrons in the buncher cavity = $t_1 - t_o$

θ_g = Angle /Phase vaiation of input signal during the tansit time = ωŤ

β = Beam Coupling Coefficient of the buncher / Catcher Cavity

When the electrons enter the buncher cavity with uniform velocity „ ***v*0** ‟ interact with the field due to input RF signal **V_1sin ωt**. The time varying field in the cavity cause the electrons to accelerate or decelerate and there by electrons undergo velocity modulation.

Let v(t_1) = Velocity of electrons at **t= t_1** at the output of buncher cavity

Let d = cavity with of buncher / catcher cavity

L = spacing between buncher and catcher cavities

L‟ is the design parameter for optimum performance of the klystron amplifier

t_2 = Time at which electrons enter the catcher cavity

t_3= Time at which electrons leave the catcher cavity

$$\tau \approx \frac{d}{v_o} = t_1 - t_0 \quad \textbf{(5.2)}$$

Because $V_1 << V_0$

Evaluation of $v(t_1)$ VELOCITY MODULATION

$v(t_1)$ is the instantaneous velocity of electrons which is a time varying quantity and primarily depends upon the average voltage in the gap during the time „*t* ‟ i.e. during the time period (transit) the electrons are influenced by the field.

V_{avg} = Average voltage in the gap during time **„*t* ‟**

$$V_{avg} = \frac{1}{\tau}\int_{t_0}^{t_1} V_1 \sin\omega t \; dt$$

$$= \frac{-V_1}{\omega\tau}\left[\cos\omega t\right]_{t_0}^{t_1}$$

$$V_{avg} = \frac{-V_1}{\omega\tau}\left[\cos\omega t_1 - \cos\omega t_0\right] = V_{avg} = \frac{V_1}{\omega\tau}\left[\cos\omega t_o - \cos\omega t_1\right]$$

Where $\tau = t_1 - t_0$

$$t_1 = t_0 + \tau = t_0 + \frac{d}{v_o}$$

$$V_{avg} = \frac{V_1}{\omega\tau}\left[\cos\omega t_0 - \cos\left(\omega t_0 + \frac{\omega d}{v_0}\right)\right]$$

Where $\theta_g = \omega\,\tau = \dfrac{\omega d}{v_0}$ (5.3)

$$V_{avg} = \frac{V_1}{\omega\tau}\left[\cos\omega t_0 - \cos(\omega t_0 + \theta_g)\right]$$

Let $A = \omega t_0 + \dfrac{\theta_g}{2}$

and $B = \dfrac{\theta_g}{2}$

Since cos (A-B) – cos (A+B) = 2 sin A sin B

$$V_{avg} = V_1\left\{\frac{\sin(\omega d/2v_0)}{\omega d/2v_0}\right\} \sin\left(\omega t_0 + \frac{\omega d}{2v_0}\right)$$

$$= V_1 \frac{\sin\theta_g/2}{\theta_g/2}\sin\left(\omega t_0 + \frac{\theta_g}{2}\right)$$

β_i = beam coupling coefficient of input (buncher) cavity by definition

$$\beta_i = \frac{\sin \theta_g / 2}{\theta_g / 2} \qquad (5.4)$$

$$V_{avg} = V_1 \beta_i \sin\left(\omega t_0 + \frac{\theta_g}{2}\right)$$

As we have seen earlier $v_0 = \sqrt{\frac{2eV_0}{m}}$

|||ly $u(t_1) = = \sqrt{\frac{2e}{m}} . \sqrt{V_1 \beta_i \sin\left(\omega t_0 + \frac{\theta_g}{2}\right) + V_0}$

$$= \sqrt{\frac{2e}{m} V_0 \left[1 + \frac{\beta_i V_1}{V_0} \sin\left(\omega t_0 + \frac{\theta_g}{2}\right)\right]}$$

Since $V_1 << V_0$, $\frac{\beta_i V_1}{V_0} << 1$

Using binomial expansion $\sqrt{1+x} = 1 + \frac{x}{2}$ *for* $x << 1$

$$v(t_1) = v_0\left[1 + \frac{\beta_i V_1}{2V_0}\sin\left(\omega t_0 + \frac{\theta_g}{2}\right)\right]$$

Since $\tau = t_1 - t_0$

$\theta_g = \omega\tau = \omega t_1 - \omega t_0$

$\omega t_0 = \omega t_1 + \omega t_0$

$\omega t_0 + \theta_g/2 = \omega t_1 - \theta_g + \theta_g/2 = \omega t_1 - \theta_g/2$

$$v(t_1) = v_0\left[1 + \frac{\beta_i V_1}{2V_0}\sin\left(wt_1 - \frac{\theta_g}{2}\right)\right] \quad (5.5)$$

$$v(t_1) = v_0\left[1 + \frac{\beta_i V_1}{2V_0}\sin\left(wt_0 + \frac{\theta_g}{2}\right)\right] \quad (5.6)$$

Bunching Process of Electrons

All the electrons in the beam will drift with a uniform velocity of "v_0" at $t = t_0$ i.e. at time of entry into the buncher cavity. For $t_2 > t > t_0$ i.e. in the cavity gap the velocity of electrons vary with time depending upon the instantaneous field $V_1 \sin wt$

Consider three arbitrary electrons a, b and c passing thro the gap when the field is –ve max, zero and +ve max respectively at time instances t**a, tb** and **tc**.

Consider three arbitrary electrons a, b and c passing thro the gap when the field is –ve max, zero and +ve max respectively at time instances t**a, tb** and **tc**.

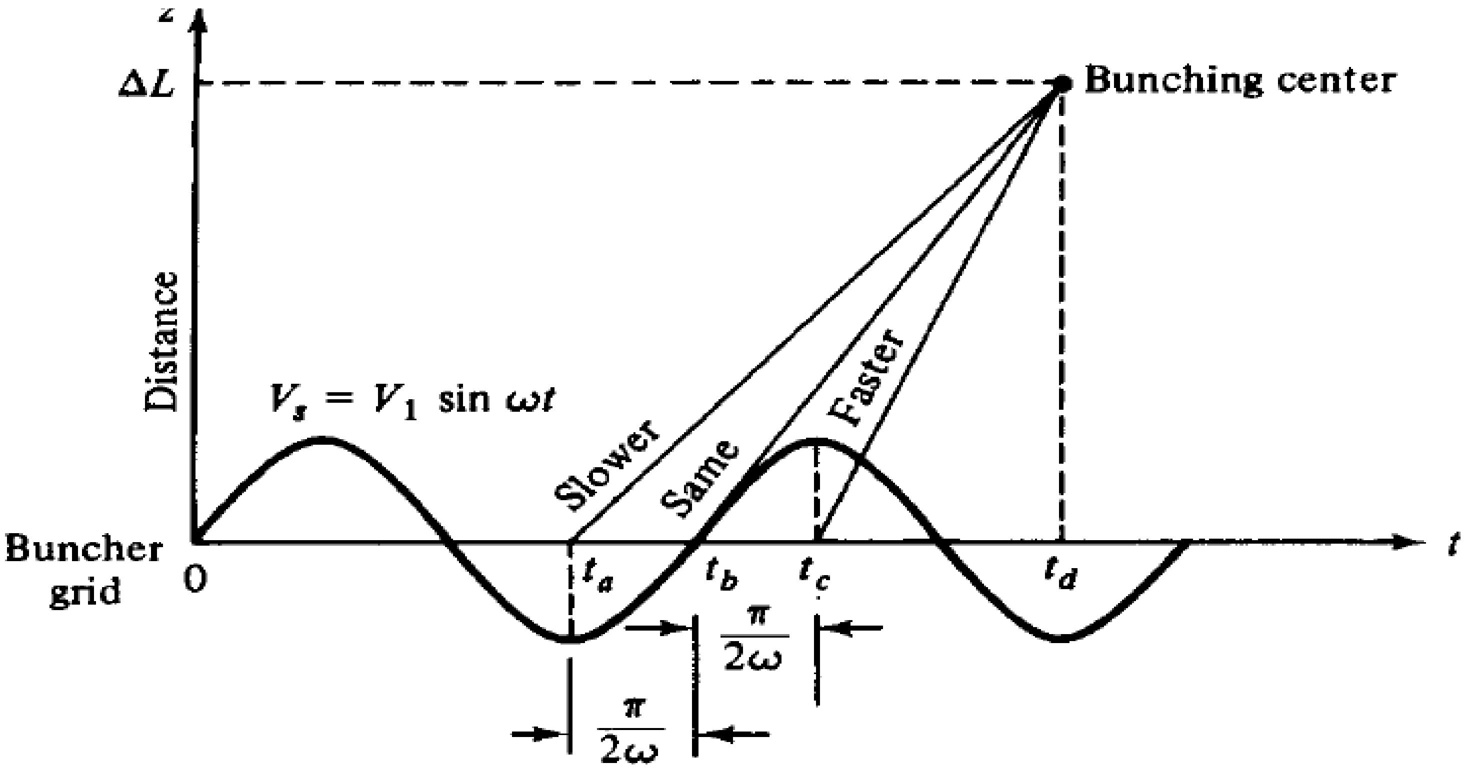

Fig 5.3 : Appligate diagram

Velocity of electron 'b' = $v_b = v_0$ (field zero)

Velocity of electron 'a' = $v_a < v_0 = v_{min}$ (-ve field)

Velocity of electron 'c' = $v_c > v_0 = v_0 = v_{max}$ (+ve field)

Let us consider that these three electrons draft with different velocities (bunch) together at $t = t_d$ at a length ΔL from buncher cavity.

$$\Delta L = v_{min}\,(t_d - t_a) \quad (5.7)$$

$$\Delta L = v_0\,(t_d - t_b) \quad (5.8)$$

$$\Delta L = v_{max}\,(t_d - t_c) \quad (5.9)$$

$$t_c - t_b = t_b - t_a = \pi / 2w \text{ (1/4 of time period)} \quad (5.10)$$

$$\Delta L = v_{min}(t_d - t_a) = v_{min}(t_d - t_b + \pi/2\omega) \qquad (5.7A)$$

$$\Delta L = v_{max}(t_d - t_c) = v_{max}(t_d - t_b - \pi/2\omega) \qquad (5.8A)$$

We have $v(t_1) = v_0\left[1 + \frac{\beta_i V_1}{2V_0}\sin\left(\omega t_0 + \frac{\theta_g}{2}\right)\right]$

From above equation

$$v_{max} = v(t_1)| = v_0\left(1 + \frac{\beta_i V_1}{2V_0}\right) \qquad (5.11)$$

$$v_{\min} = v(t_1) = v_0\left(1 - \frac{\beta_i V_1}{2V_0}\right) \qquad (5.12)$$

Substituting equation 12, 11 in equation 7A and 8A

$$\Delta L = v_0(t_d - t_b) + \left[v_0\frac{\pi}{2\omega} - \frac{v_0\beta_i V_1}{2V_0}(t_d - t_b) + \frac{v_0\beta_i V_1}{2V_0}\frac{\pi}{2\omega}\right] \qquad (5.13)$$

$$\Delta L = v_0(t_d - t_b) + \left[-v_0\frac{\pi}{2\omega} + \frac{v_0\beta_i V_1}{2V_0}(t_d - t_b) + \frac{v_0\beta_i V_1}{2V_0}\frac{\pi}{2\omega}\right] \qquad (5.14)$$

Subtracting Eqn 5.14 from Eqn 5.13

$$v_0 \frac{\pi}{2\omega} - v_0 \frac{\beta_i V_1}{2V_0}(t_d - t_b) - v_0 \frac{\beta_i V_1}{2V_0} \frac{\pi}{2\omega} = 0$$

$$\frac{v_0 \beta_i V_1}{2V_0}(t_d - t_b) = v_0 \frac{\pi}{2\omega} 1 + v_0 \frac{\beta_i V_1}{2V_0} \frac{\pi}{2\omega}$$

$$\frac{v_0 \beta_i V_1}{2V_0}(t_d - t_b) = v_0 \frac{\pi}{2\omega}\left[1 + \frac{\beta_i V_1}{2V_0}\right] \approx \frac{v_0 \pi}{2\omega}$$

$$\text{since} \quad \frac{\beta_i V_1}{2V_0} << 1$$

$$t_d - t_b = \frac{\pi V_0}{w \beta_i V_1} \qquad (5.15)$$

From Equation 5.8 and 5.15

$$\Delta L = v_0 \frac{\pi V_0}{w\beta_i V_1} \quad 5.16$$

$$\Delta L = v_0 (t_d - t_b) \quad (5.8)$$

$$L_{optimum} = \frac{3.682 v_0 V_0}{\omega \beta_i V_1}$$

Equation 5.16 gives the design parameter for spacing between buncher and catcher cavities.

Let T= Transit time for on electron travel distance „

L‟ (function of „t‟) L = spacing between two cavities

Let T_0 = Transit time for electron when the field in buncher cavity is i.e. $v(t_1) = v0$

$$T_0 = \frac{L}{v_0} \qquad T = \frac{L}{v(t_1)}$$

Substituting for $v(t_1)$ from equation 5

$$T = \frac{L}{v_0\left[1 + \frac{\beta_i V_1}{2V_0}\sin\left(\omega t_1 - \frac{\theta_g}{2}\right)\right]}$$

$$T = \frac{L}{v_0}\left[1 + \frac{\beta_i V_1}{2V_0}\sin\left(\omega t_1 - \frac{\theta_g}{2}\right)\right]^{-1}$$

Using binomial expansion $(1+x)^{-1} = 1-x$ for $x<<1$ and $V_1<<V_0$, $T_0 = L/v_0$

$$T = T_0\left[1 - \frac{\beta_i V_1}{2V_0}\sin\left(\omega t_1 - \frac{\theta_g}{2}\right)\right] \qquad (5.19)$$

Multiplying above equation by 'ω'

$$\omega T = \omega T_0\left[1 - \frac{\beta_i V_1}{V_0}\sin\left(\omega t_1 - \frac{\theta_g}{2}\right)\right] \qquad (5.20)$$

Let θ_0 = Angular variation in the signal during time 'T_0'

$\theta_0 = \omega T_0$

$$\omega T = \omega T_0 - \frac{\omega T_0 \beta_i V_1}{V_0} \sin\left(\omega t_1 - \frac{\theta_g}{2}\right)$$

$$\omega T = \theta_0 - X \sin \omega t_1 - \frac{\theta_g}{2}$$

$$where \;\; X = \frac{\beta_i V_1}{2V_0} \theta_0$$

X is called Bunching parameter of Klystron

Expression for output current i2‟ ac current in the catcher cavity:

Let charge **dQ0‟** pass through the buncher gap at a time interval **dt0** and we will assume the same amount of charge passes through the catcher gap later in time interval **dt2**

dQ0 = I0 dt0

$$dQ_0 = I_0 |dt_0| = i_2 |dt_2| \qquad (5.22)$$

$$\tau = t_1 - t_0$$

$$t_1 = t_0 + \check{T}$$

$$T = t_2 - t_1, \qquad T = t_2 - (t_0 + \check{T})$$

$$T = t_2 - t_1 = T_0\left[1 - \frac{\beta_i V_1}{2V_0}\sin\left(\omega t_1 - \frac{\theta_g}{2}\right)\right]$$

$$t_2 = t_0 + \tau + T_0\left[1 - \frac{\beta_i V_1}{2V_0}\sin\left(\omega t_1 - \frac{\theta_g}{2}\right)\right]$$

$$\omega t_2 = \omega t_0 + \omega\tau + \omega T_0\left[1 - \frac{\beta_i V_1}{2V_0}\sin\left(\omega t_1 - \frac{\theta_g}{2}\right)\right]$$

$$\omega t_2 = \omega t_0 + \theta_g + \theta_0 - \frac{\theta_0 \beta_i V_1}{2V_0} \sin\left(\omega t_0 + \frac{\theta_g}{2}\right)$$

$$we\ have\ X = \frac{\theta_0 \beta_i V_1}{V_0}$$

$$\omega t_2 = \omega t_0 + \theta_g + \theta_0 - X \sin\left(\omega t_0 + \frac{\theta_g}{2}\right)$$

θ_g, θ_0 are constants w.r.t. 't'

$$\omega \frac{dt_2}{dt_0} = \omega - \omega X \cos\left(\omega t_0 + \frac{\theta_g}{2}\right) and$$

$$dt_2 = dt_0\left[1 - X \cos\left(\omega t_0 + \frac{\theta_g}{2}\right)\right] \quad (5.23)$$

From equation 22 and 23

$$I_0[dt_0] = i_2|dt_2| = i_2\ dt_0\left|1 - X\cos\left(\omega t_0 + \frac{\theta_g}{2}\right)\right]$$

$$i_2\ (t_0) = \frac{I_0}{1 - X\cos\left(\omega t_0 + \frac{\theta_g}{2}\right)} \qquad (5.24)$$

$$where\ X = \frac{\beta_i V_1}{2V_0}\theta_0$$

$$I_t = \frac{I_o}{(1 - X\cos\omega t_1)}$$

I_t is clearly a periodic function of ωt, it can be expanded in a Fourier series, as follows

$$I_t = I_0\left[\frac{1}{|1 - X\cos\omega t_{11}|} + \frac{1}{|1 - X\cos\omega t_{12}|} + \ldots\right]$$

$$I_t = I_o + \sum_{\sigma_0 + \pi}^{\infty}[a_n \cos n(\omega t_2 - \theta_0) + b_n \sin n(\omega t_2 - \theta_0)]$$

$$a_n = 1/\pi \int I_t \cos n(\omega t_2 - \theta_0) d(\omega t_2)$$

$$a_n = \frac{I_0}{\pi}\int_{-\pi}^{\pi} \cos n(\omega t_1 - X\sin\omega t_1) d(\omega t_1) \longrightarrow I_o dt_1 = I_t dt_2$$

$$a_n = 2J_n(nX)$$

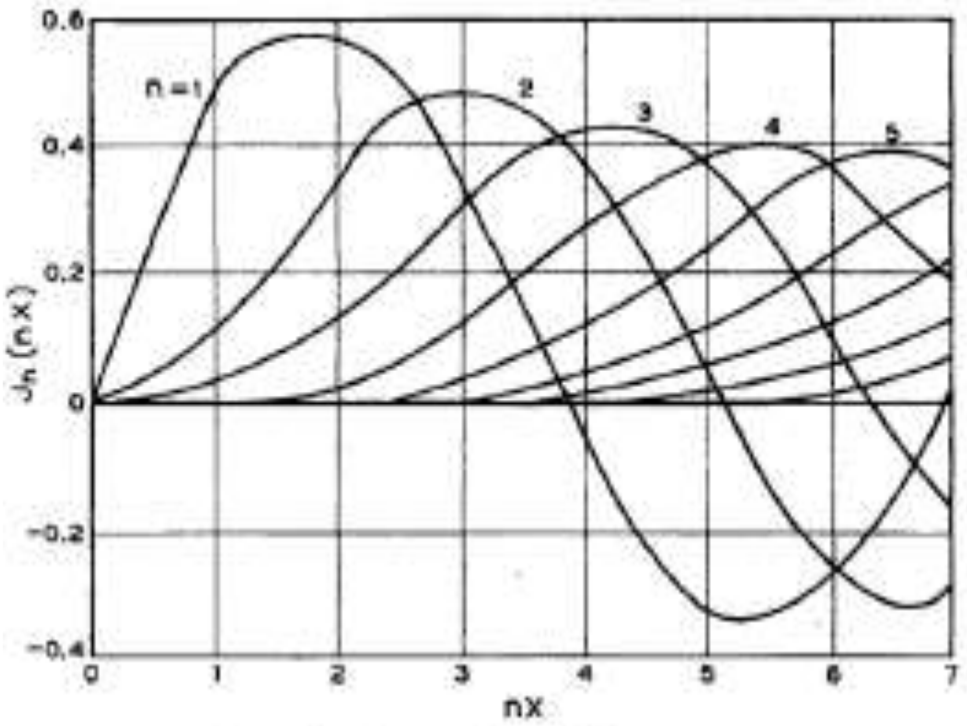

Bessel functions of various orders. The maximum value of J_1 occurs at $X = 1.84$ and is equal to 0.582.

Therefore, the catcher rf current I_t can be written as the following series

$$I_t = I_0 + 2I_0 \sum_{1}^{\infty} J_n(nX) \cos n(\omega t_1 - \theta_0)$$

The n = 1 harmonic (the fundamental) is simply,

$$I_1 = 2I_0 J_1(X) \cos(\omega t - \theta_0)$$

$$i_2 = I_0 + \sum_{n=1}^{\infty} 2I_0 \beta_0 J_n(\times) \cos n\omega(t_2 - \tau - T_0)$$

$$i_2 = I_0 + \sum_{n=1}^{\infty} 2I_0\beta_0 J_n(\times)\cos n\omega(t_2 - \tau - T_0)$$

$$I_f = 2I_0 J_1(X)\beta_0 \cos w\ (t_2 - \tau - T_0)$$

$$I_2 = 2\beta_0 I_0 J_1(X)$$

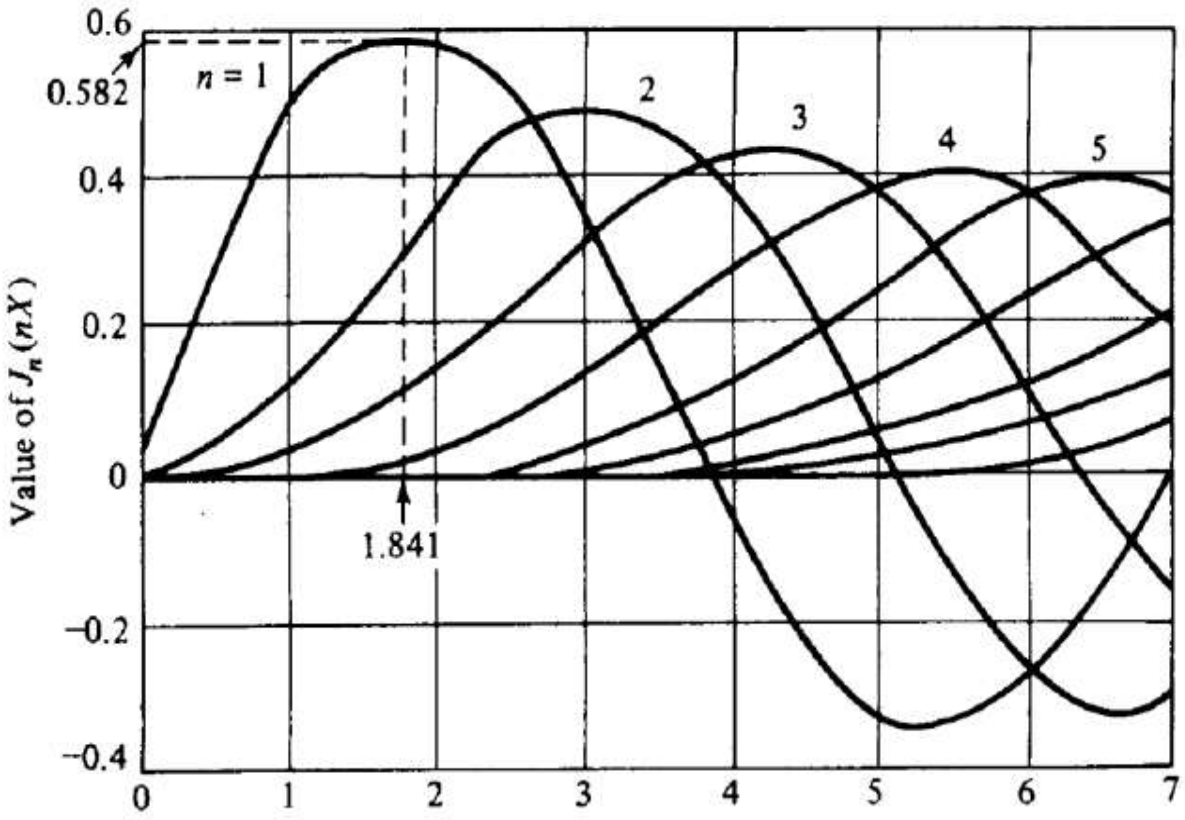

Fig 5.4: Bessel function J_n (nX)

$J_1(X)$ is maximum at X = 1.841 i.e. $J_1(1.841)$ = 0.582 from Bessel function

$$X = \frac{\beta_i V_1}{2V_0}\theta_0 = \frac{\beta_i V_1}{2V_0} w \frac{L}{v_0}$$

Where X = Bunching parameter of Klystron

$L \rightarrow L_{optimum}$ as $X \rightarrow 1.841$

$$Loptimum = \frac{2 \times 1.841 \times V_0 \times v_0}{\beta_i V_1 \omega} = \frac{3.682 v_0 V_0}{\omega \beta_i V_1}$$

Calculation for output power (P_{out})

- At catcher cavity, If V_2 is amplitude of voltge at time t_2, then RF voltage is :

  RF voltage $= V_2 \sin \omega t_2$

- If the charge on a electron is e, then total energy given by the electron to the bunch :

  Total energy $= - eV_2 \sin \omega t_2$

- If one RF cycle (Refer Fig. 5.3.4), the total phase angle between time instant t_1 to t_2 is 2π. The average power which is given to RF field in one cycle :

$$P_{ar} = \frac{1}{2\pi} \int_{\omega t_1 = 0}^{\omega t_2 = 2\pi} (-e \cdot V_2 \sin \omega t_2)\, d\omega t_1 \quad \text{...(19)}$$

- Due to drift space between two cavities, the transit time for velocity modulated electron is given by :

$$T = t_2 - t_1 = \frac{L}{v_1} = \frac{L}{\left[v_0 \left(1 + \frac{V_1}{V_0}\right) \sin \omega t_1\right]^{1/2}}$$

- By using Binomial expansion

$$T = t_2 - t_1 = \frac{L}{v_0}\left[1 - \frac{V_1}{2V_0}\sin\omega t_1\right]$$

- If we multiply by ω on both sides :

$$\omega T = \omega(t_2 - t_1) = \frac{\omega L}{v_0}\left[1 - \frac{V_1}{2V_0}\sin\omega t_1\right]$$

- As we know $\frac{\omega L}{v_0} = \theta_g = 2\pi N$ is transit angle without RF voltage V_1 in buncher cavity where N is the number of electron transit cycles in drift space.

$$\omega t_2 = \omega t_1 + \theta_g\left[1 - \frac{V_1}{2V_0}\sin\omega t_1\right] \qquad \text{...(20)}$$

$$P_{av} = -\frac{eV_2}{2\pi}\int_0^{2\pi}\sin\left[\omega t_1 + \theta_g\left(1 - \frac{V_1}{2V_0}\sin\omega t_1\right)\right]d\omega t_1$$

$$P_{av} = -\frac{eV_2}{2\pi}\int_0^{2\pi} \sin\left[\omega t_1 + \theta_g - \theta_g \frac{V_1}{2V_0}\sin\omega t_1\right] d\omega t$$

above equation is Bessel function equation and its solution given below

$$\int_0^{2\pi} \sin\left[(\omega t + \theta_g) - \theta_g \frac{V_1}{2V_0}\sin\omega t_1\right] d\omega t_1 = 2\, J_1\,(X)\,\sin\theta$$

- In solution, $J_1\,(X)$ is first order Bessel function for the argument of bunching parameter 'X' given in equation (18).

From Bessel function tables, it is clear that for $X = 1.84$, the maximum value of $J_1\,(X) = 0.58$.

$$P_{max} = -I\,V_2\,(0.58)\,\sin\theta_g$$

$$\sin\theta_g = -1 \quad \text{when } \theta_g = 2\pi n - \frac{\pi}{2} \qquad \ldots(21)$$

- The output power of two cavity Klystron is given by :

$$P_{out} = P_{max} = 0.58\, I \,.\, V_2 \quad \left(At\ \theta_g = 2\pi n - \frac{\pi}{2} \right) \qquad ...(22)$$

Efficiency (η)

- It is the ratio of the output power to input power Klystron

$$\eta = \frac{P_{out}}{P_{in}}$$

$$P_{in} = V_0 \,.\, I \quad (\because \text{Input power is dc input without RF signal})$$

From equation (22)

$$\eta = \frac{0.58\ I.V_2}{V_0 I} = \frac{0.58\, V_2}{V_0} \qquad (V_2 << V_0)$$

- The maximum efficiency of Klystron is 58% for maximum power transfer, the electron gun anode voltage required is given by :

$$\left(\frac{V_1}{V_0}\right)_{max} = \frac{2X}{\theta_g} \quad \text{from equation (18)}$$

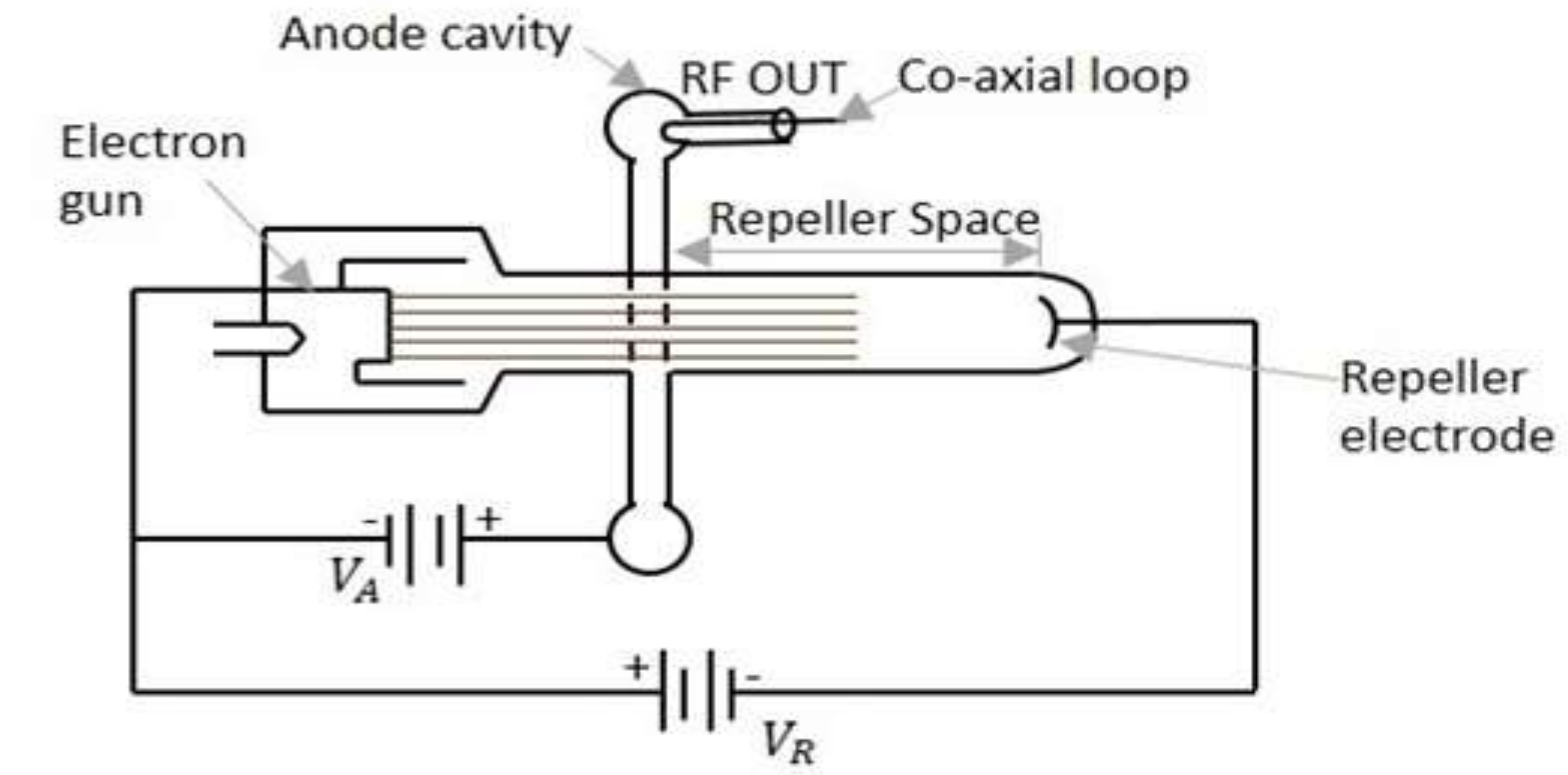

Constructional details of Reflex Klystron

Construction of Reflex Klystron:

The electron gun emits the electron beam, which passes through the gap in the anode cavity. These electrons travel towards the Repeller electrode, which is at high negative potential. Due to the high negative field, the electrons repel back to the anode cavity. In their return journey, the electrons give more energy to the gap and these oscillations are sustained. The constructional details of this reflex klystron is as shown in the following figure.

It is assumed that oscillations already exist in the tube and they are sustained by its operation. The electrons while passing through the anode cavity, gain some velocity.

Operation of Reflex Klystron:

The operation of Reflex Klystron is understood by some assumptions. The electron beam is accelerated towards the anode cavity.

Let us assume that a reference electron e_r crosses the anode cavity but has no extra velocity and it repels back after reaching the Repeller electrode, with the same velocity. Another electron, let's say e_e which has started earlier than this reference electron, reaches the Repeller first, but returns slowly, reaching at the same time as the reference electron.

We have another electron, the late electron e_l, which starts later than both e_r and e_e, however, it moves with greater velocity while returning back, reaching at the same time as er and **ee.**

Now, these three electrons, namely e_r, e_e and e_l reach the gap at the same time, forming an **electron bunch**. This travel time is called as **transit time**, which should have an optimum value. The following figure illustrates this.

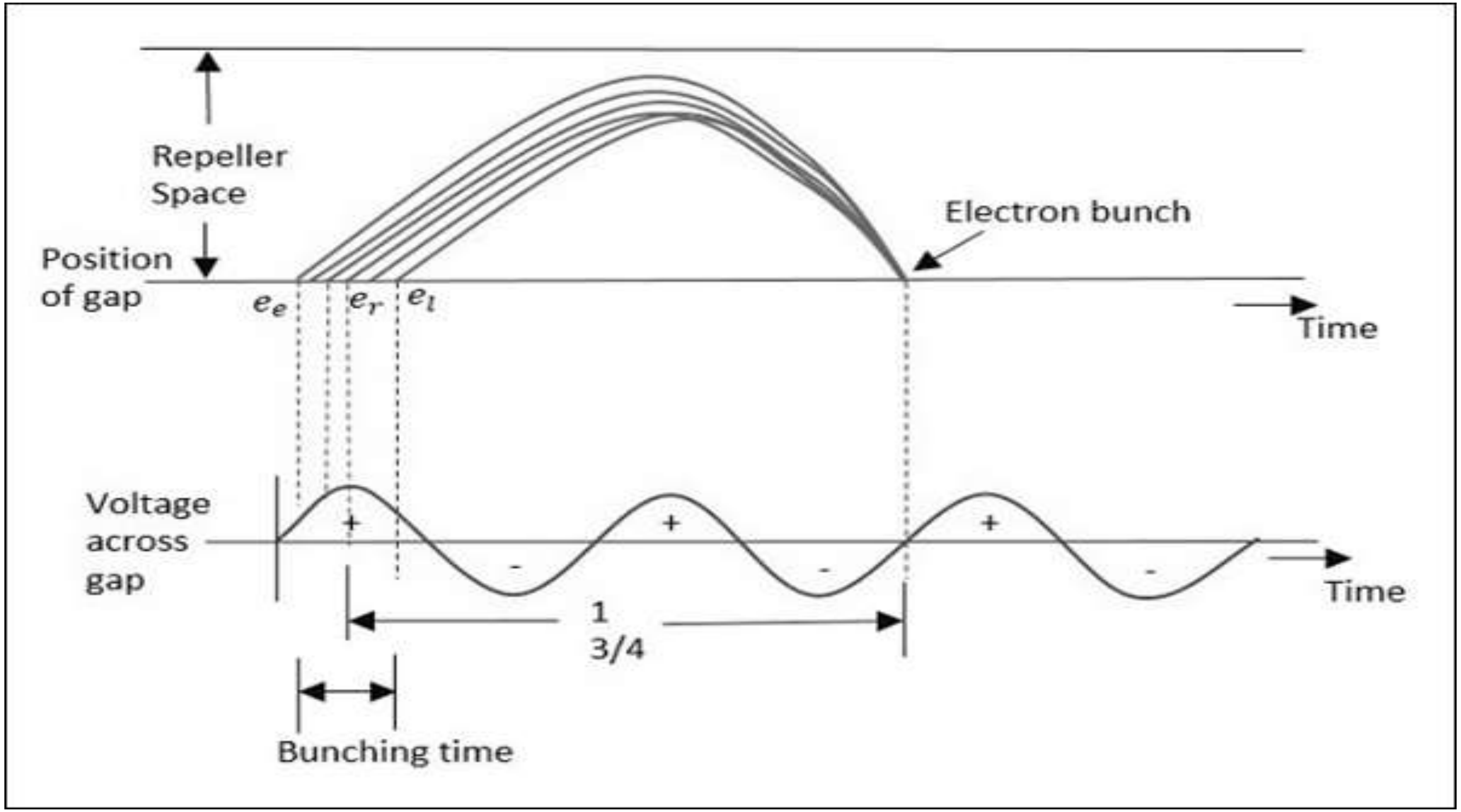

Fig: **Appligate diagram**

The anode cavity accelerates the electrons while going and gains their energy by retarding them during the return journey. When the gap voltage is at maximum positive, this lets the maximum negative electrons to retard.

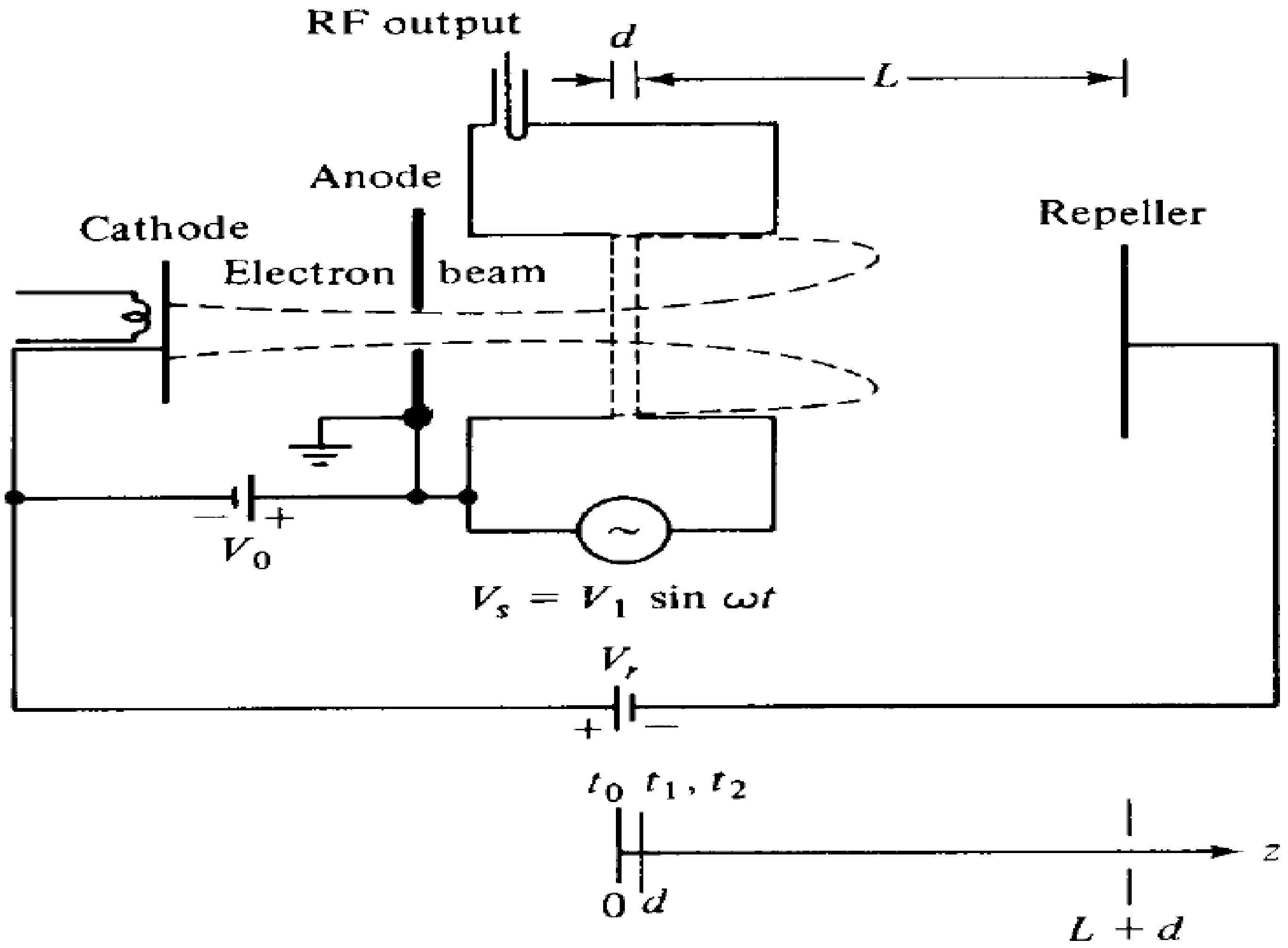

Fig 5.6: Schematic digram of Reflex Klystron

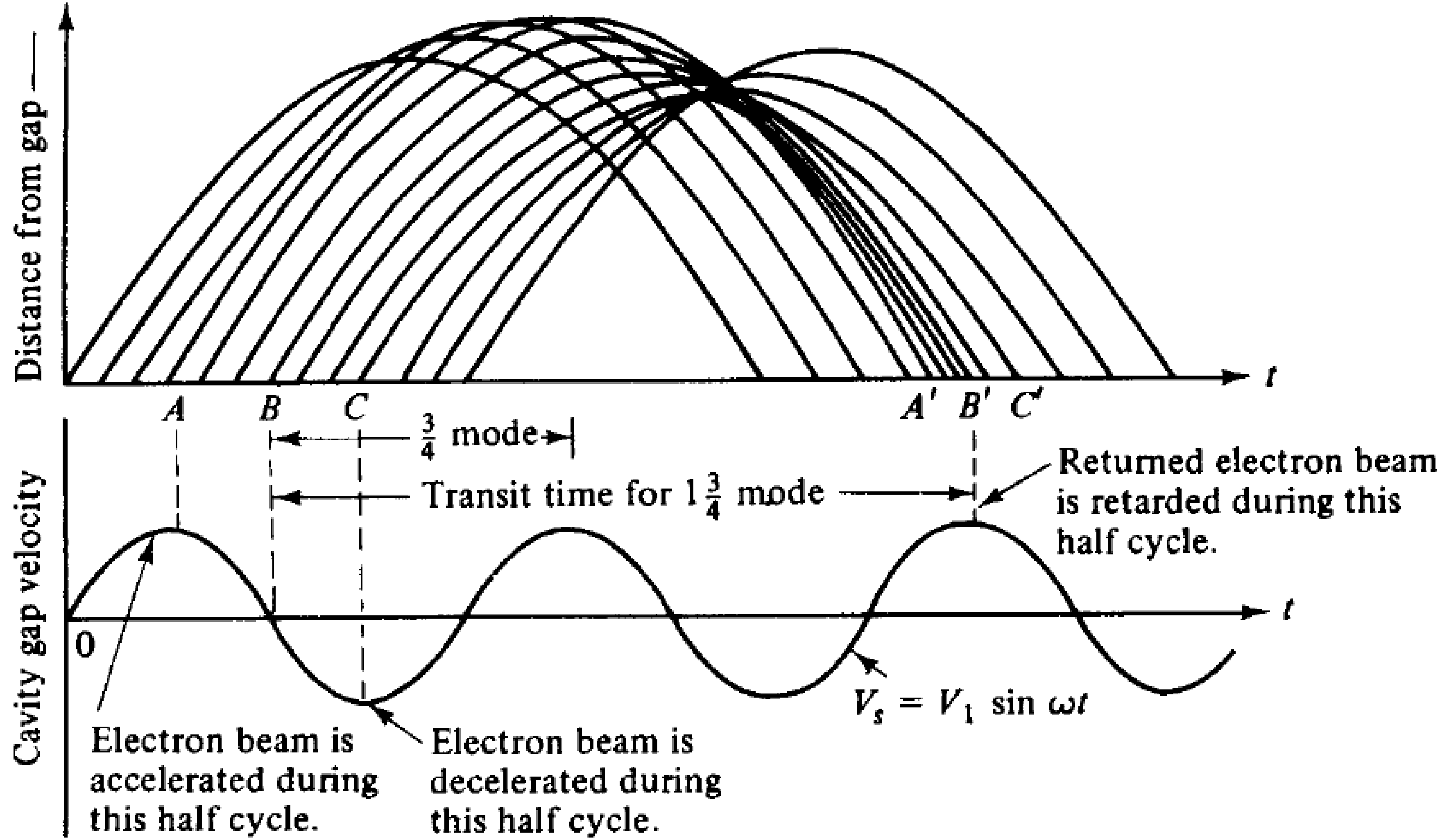
Distance from gap
t
A
B
C
A′
B′
C′
3/4 mode
Transit time for 1 3/4 mode
Returned electron beam is retarded during this half cycle.
Cavity gap velocity
0
t
$V_s = V_1 \sin \omega t$
Electron beam is accelerated during this half cycle.
Electron beam is decelerated during this half cycle.

Formation of electron beam with uniform velocity v_0 up to civility resonator is

$$v_0 = 0.593 \times 10^6 \sqrt{V_0} \ \ m/s$$

Some electrons are accelerated by the accelerating field (during +ve cycle of RF field) and enter the repeller space with greater velocity compared to the electrons with unchanged velocity, some electrons are decelerated by the decelerating field (during –ve cycle of RF field) and enter repeller space with less velocity

$$v(t_1) = v_0\left[1 + \frac{\beta_i V_1}{2V_0}\sin\left(wt_1 - \frac{\theta_g}{2}\right)\right]$$

$$E = \frac{V_r + V_0 + V_1 \sin wt}{L}$$

The force equation for an electron in the repeller region is given by

$$m\frac{d^2z}{dt^2} = -eE = -e\frac{[V_r + V_0 + V_1 \sin wt]}{L}$$

Since V1<<V0, V1<<Vr

$$m\frac{d^2z}{dt^2} = -e\frac{(V_r + V_0)}{L}$$

$$\frac{dz}{dt} = \frac{-e(V_r + V_0)}{mL}\int_{t1}^{t} dt = \frac{-e(V_r + V_0)}{mL}(t - t_1) + K_1$$

at t = t_1, z = d,
v(t_1) = dz / dt
K_1 = dz/ dt = v(t_1)

$$z = \frac{-e(V_0 + V_r)}{mL}\int_{t_1}^{t}(t - t_1)dt + \int_{t_1}^{t} v(t_1)dt$$

$$z = -e\frac{(V_0 + V_r)}{2mL}(t - t_1)^2 + v(t_1)(t - t_1) + K_2$$

At t= t_1, z= d K_2 = d

$$z = -e\frac{(V_0 + V_r)}{2mL}(t - t_1)^2 + v(t_1)(t - t_1) + d$$

$$z = -e\frac{(V_0 + V_r)}{2mL}(t - t_1)^2 + v(t_1)(t - t_1) + d$$

At t= t_1, z= d $K_2 = d$

At t = t_2 electrons returns of cavity after retardation at t = t_2, z=d substituting this in above equation.

$$d = \frac{-e(V_0 + V_r)}{2mL}(t_2 - t_1)^2 + v(t_1)(t_2 - t_1) + d$$

$$o = \frac{-e(V_0 + V_r)}{2mL}(t_2 - t_1)^2 + v(t_1)(t_2 - t_1)$$

Let T be rannd trip transit time = t_2-t_1

$$O = (t_2 - t_1)\left[\frac{-e(V_0 + V_r)}{2mL}(t_2 - t_1)^2 + v(t_1)\right]$$

$$\frac{e\left(V_0+V_r\right)}{2mL}(t_2-t_1)=v(t_1)$$

$$T'=t_2-t_1=\frac{2mL}{e\left(V_0+V_r\right)}v(t_1)$$

Let $\omega T_0 = \theta_0$

$$=T_0'\left[1+\frac{\beta_i V_i}{2V_0}\sin wt_1-\frac{\theta_g}{2}\right]$$

$$where\ \ T_0'=\frac{2mL}{e\left(V_0+V_r\right)}v_0 \qquad where\ X=\frac{\beta_i V_1}{2V_0}\theta_0$$

T'_0 is a function of V_r

$\omega(t_2-t_1) = \omega T$

$$\theta' = \omega T' = \omega T'_0 + \omega T'_0 \frac{\beta_i V_i}{2V_0} \sin\left(wt_1 - \frac{\theta_g}{2}\right)$$

Let $\omega T_0 = \theta_0$

$$where\ X' = \frac{\beta_i V_1}{2V_0}\theta' \qquad \theta' = \theta'_0 + X' \sin\left(wt_1 - \frac{\theta_g}{2}\right)$$

Where X' is bunching parameter of Reflex Klystron

Power output and efficiency of Reflex Klystron

Maximum magnitude of fundamental component current in the cavity I_2

$$I_2 == 2I_0\beta_i J_1(\times^1)$$

V_2 = output voltage of the cavity = V_1

$$V_1 = V_2 = 2I_0\beta_i J_1(\times^1)R_{sh}$$

$$output \;\; power = P_{az} = i_{rms}^2 . R_{sh} = \left(\frac{2I_0\beta_i J_1(\times^1)}{\sqrt{2}}\right)^2 R_{sh}$$

$$P_{ac} = 2I^2{}_0\beta^2{}_i J_1{}^2(\times^1)R_{sh}$$

$$X^1 = \frac{\beta_i V_1}{2V_0}\theta_0 = \frac{\beta_i V_1}{2V_0}\left(2\pi n - \frac{\pi}{2}\right)$$

$$\frac{V_1}{V_0} = \frac{2X^1}{\beta_i\left(2\pi n - \frac{\pi}{2}\right)}$$

$$P_{ac} = V_1 . I_0 \beta_i J_1(x^1)$$

$$\frac{P_{ac}}{P_{dc}} = Power \ \ Efficiency \ = \ \eta = \frac{V_1 I_0 \beta_i J_1(x^1)}{V_0 I_0} = \frac{V_1}{V_0}.\frac{\beta_i J_1(x^1)}{I_0} = \frac{2X^1 J_1(x^1)}{\left(2\pi n - \frac{\pi}{2}\right)}$$

$$\eta = \frac{2X^1 J_1(x^1)}{\left(2\pi n - \frac{\pi}{2}\right)}$$

The product $X_1 J_1(X^1)$ is maximum at $X^1 = 2.408$, $J_1(X^1) = 0.52$

$X^1 J_1(X^1)_{max} = 1.25$ at $X^1 = 2.408$

$$\eta_{max} = \frac{2 \times 1.25}{\left(2\pi n - \frac{\pi}{2}\right)}$$

At n = 2 (n=1 too short a value) η_{max} = 0.227 or 22.7

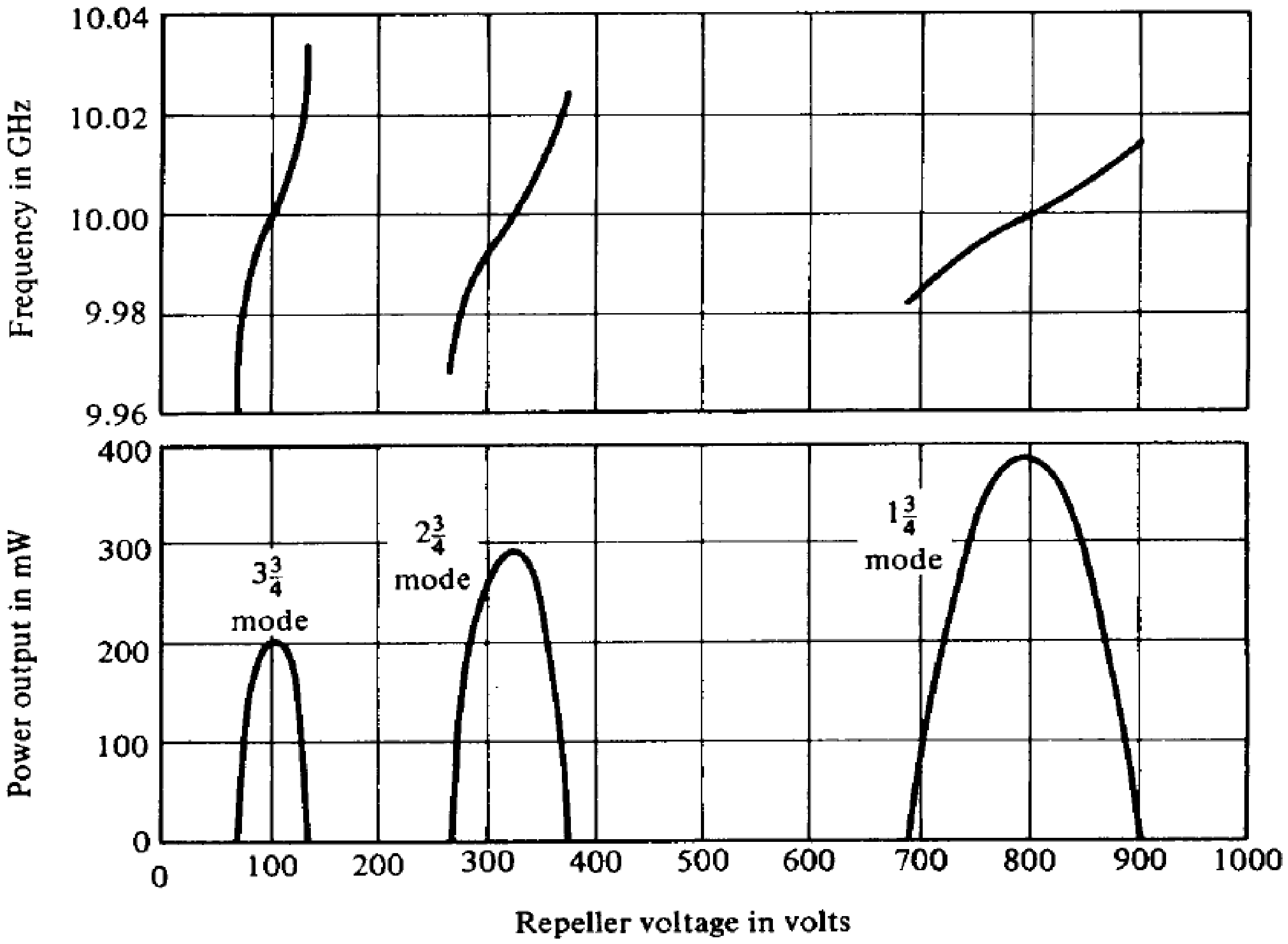

10.04
10.02
10.00
9.98
9.96
Frequency in GHz
400
300
200
100
0
Power output in mW
$3\frac{3}{4}$ mode
$2\frac{3}{4}$ mode
$1\frac{3}{4}$ mode
0
100
200
300
400
500
600
700
800
900
1000
Repeller voltage in volts

B.Tech. (VII Sem.) 17EC27 - MICROWAVE ENGINEERING

UNIT-II

Helix TWT: Significance, Types and Characteristics of Slow Wave Structures; Structure of TWT and Amplification Process, Axial Electric Field, Convection Current, Propagation Constants, Gain Considerations.

M-Type Tubes : Introduction, Cross-field effects, Magnetrons – Different Types, 8-Cavity Cylindrical Travelling Wave Magnetron: Hull Cut-off and Hartee Conditions, Modes of Resonance and PI-Mode Operation, o/p characteristics, Frequency Pulling and Frequency Pushing, Strapping.

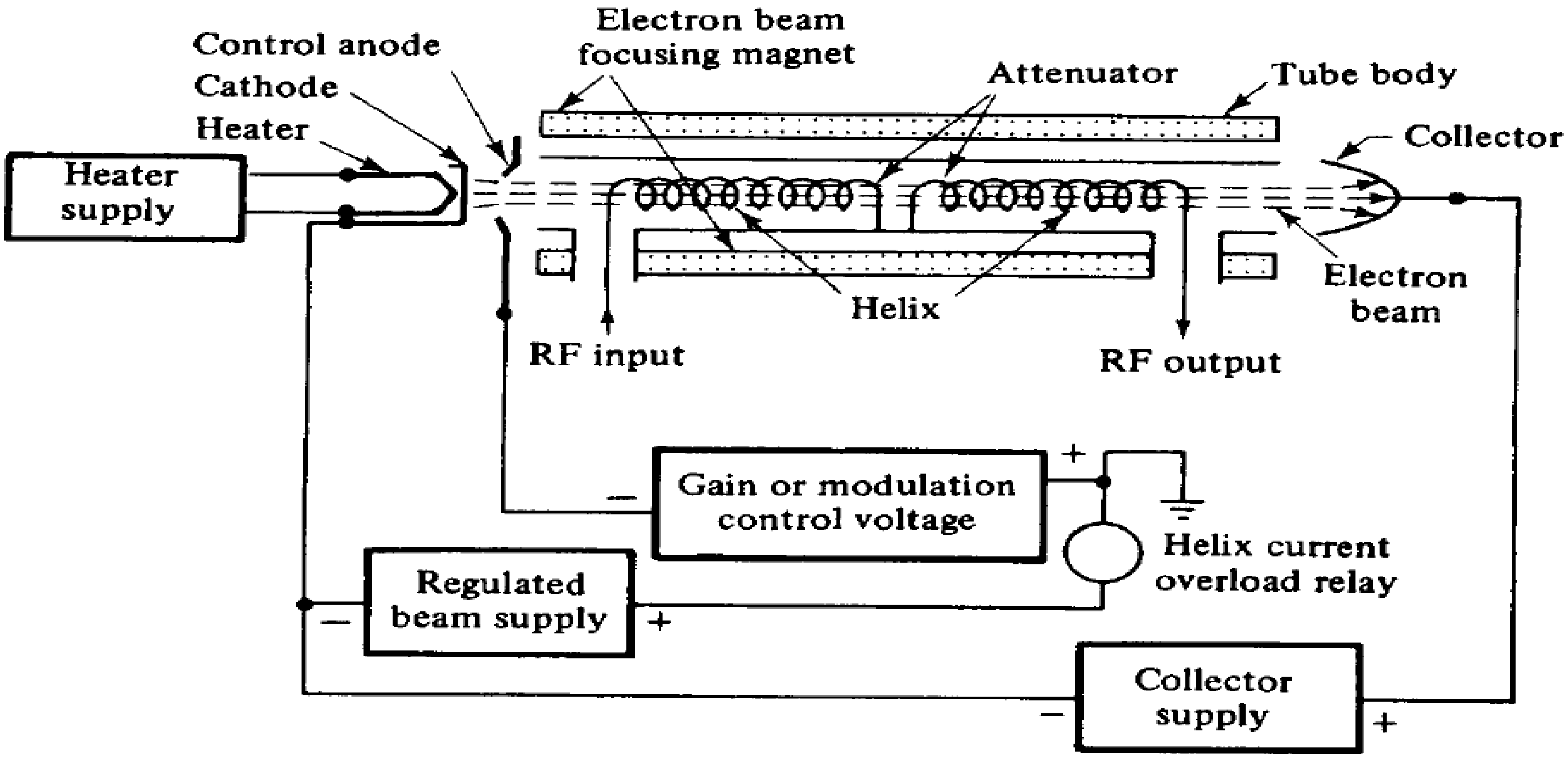

(a)

schematic diagram of helix

https://www.youtube.com/watch?v=vgR2YcVB6pI

https://www.youtube.com/watch?v=pC3Ek6YSBgM

Travelling Wave Tube Amplifier: High gain > 40 dB, Low NF < 10 dB ,Wide Band Frequency range:0.3 – 50 GHz

Contains electron gun, RF interaction circuit, electron beam focusing magnet, collector
Amplify a weak RF input signal many thousands of times

a) Electron gun
_ To get as much electron current flowing into as small a region as possible without distortion or fuzzy edges

b) RF interaction circuit
_ Interaction structures : helix, ring bar, ring loop, coupled cavity
_ RF circuit – complex trade off analysis, based on many interlocking parameters
_ Low power level : helix
_ Medium power level : ring loop, ring bar
_ Power level & frequency increased: RF losses on the circuit become more appreciate able.

c) Electron beam focusing
_ A magnetic field – to hold the electron beam together as it travels through the interaction structure of the tube

d) The collector
_ To dissipate the electrons in the form of heat as they emerge from the slow wave structure

ever, there are some major differences between the TWT and the klystron:

1. The interaction of electron beam and RF field in the TWT is continuous over the entire length of the circuit, but the interaction in the klystron occurs only at the gaps of a few resonant cavities.
2. The wave in the TWT is a propagating wave; the wave in the klystron is not.
3. In the coupled-cavity TWT there is a coupling effect between the cavities, whereas each cavity in the klystron operates independently.

A helix traveling-wave tube consists of an electron beam and a slow-wave structure. The electron beam is focused by a constant magnetic field along the electron beam and the slow-wave structure. This is termed an O-type traveling-wave tube. The slow-wave structure is either the helical type or folded-back line. The applied signal propagates around the turns of the helix and produces an electric field at the center of the helix, directed along the helix axis. The axial electric field progresses with a velocity that is very close to the velocity of light multiplied by the ratio of helix pitch to helix circumference. When the electrons enter the helix tube, an interaction takes place between the moving axial electric field and the moving electrons. On the average, the electrons transfer energy to the wave on the helix. This interaction causes the signal wave on the helix to become larger. The electrons entering the helix at zero field are not affected by the signal wave; those electrons entering the helix at the accelerating field are accelerated, and those at the retarding field are decelerated. As the electrons travel further along the helix, they bunch at the collector end. The bunching shifts the phase by $\pi/2$. Each electron in the bunch encounters a stronger retarding field. Then the microwave energy of the electrons is delivered by the electron bunch to the wave on the helix. The amplification of the signal wave is accomplished. The characteristics of the traveling-wave tube are:

Frequency range: 3 GHz and higher
Bandwidth: about 0.8 GHz
Efficiency: 20 to 40%
Power output: up to 10 kW average
Power gain: up to 60 dB

Slow-Wave Structures

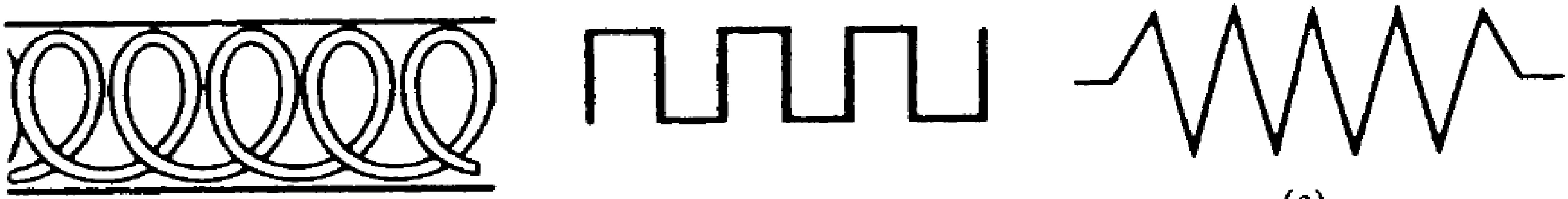

(a) (b) (c)

Slow-wave structures. (a) Helical line. (b) Folded-back line. Zigzag line.

(d)

(e)

(d) Interdigital line. (e) Corrugated waveguide.

Slow-wave structures are special circuits that are used in microwave tubes to reduce the wave velocity in a certain direction so that the electron beam and the sig-

Signal wave can interact

The commonly used slow-wave structure is a helical coil with a concentric con ducting cylinder

It can be shown that the ratio of the phase velocity v_p along the pitch to the phase velocity along the coil is given by

$$\frac{v_p}{c} = \frac{p}{\sqrt{p^2 + (\pi d)^2}} = \sin\psi \qquad (9\text{-}5\text{-}1)$$

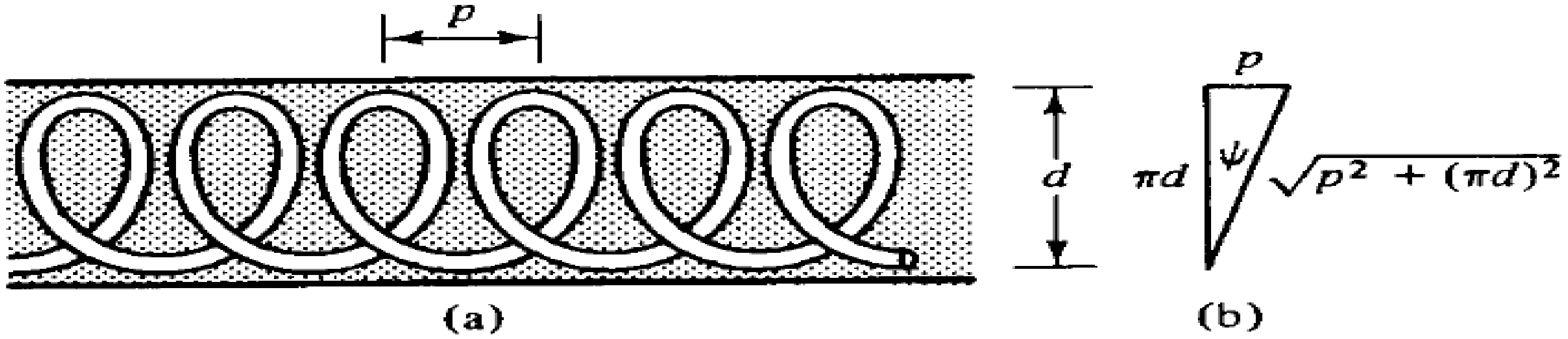

ure 9-5-3 Helical slow-wave structure. (a) Helical coil. (b) One turn of helix.

where $c = 3 \times 10^8$ m/s is the velocity of light in free space
p = helix pitch
d = diameter of the helix
ψ = pitch angle

In general, the helical coil may be within a dielectric-filled cylinder. The phase velocity in the axial direction is expressed as

$$v_{p\epsilon} = \frac{p}{\sqrt{\mu\epsilon[p^2 + (\pi d)^2]}} \tag{9-5-2}$$

For a very small pitch angle, the phase velocity along the coil in free space is approximately represented by

$$v_p \approx \frac{pc}{\pi d} = \frac{\omega}{\beta} \tag{9-5-3}$$

Figure 9-5-4 shows the ω-β (or Brillouin) diagram for a helical slow-wave structure. The helix ω-β diagram is very useful in designing a helix slow-wave structure. Once β is found, v_p can be computed from Eq. (9-5-3) for a given dimension of the helix. Furthermore, the group velocity of the wave is merely the slope of the curve as given by

$$v_{gr} = \frac{\partial \omega}{\partial \beta} \tag{9-5-4}$$

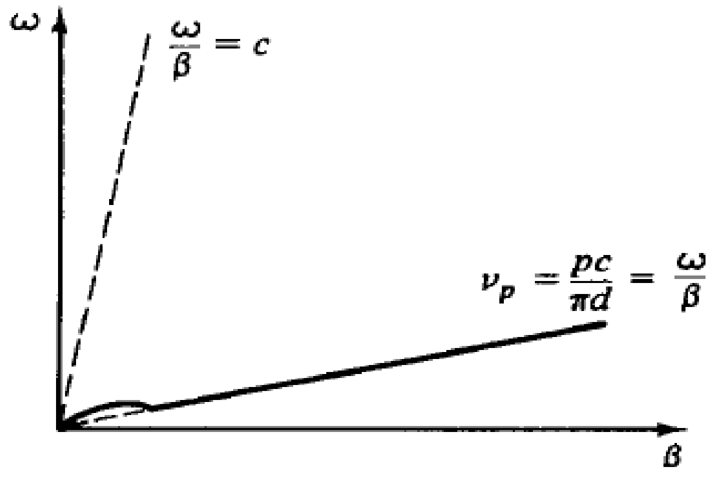

Figure 9-5-4 ω-β diagram for a helical structure.

In general, the field of the slow-wave structure must be distributed according to Floquet's theorem for periodic boundaries. Floquet's periodicity theorem states that:

> The steady-state solutions for the electromagnetic fields of a single propagating mode in a periodic structure have the property that fields in adjacent cells are related by a complex constant.

Mathematically, the theorem can be stated

$$E(x, y, z - L) = E(x, y, z)e^{j\beta_0 L} \tag{9-5-5}$$

where $E(x, y, z)$ is a periodic function of z with period L. Since β_0 is the phase constant in the axial direction, in a slow-wave structure β_0 is the phase constant of average electron velocity.

Amplification Process

The electrons entering the retarding field are decelerated and those in the accelerating field are accelerated. They begin forming a bunch centered about those electrons that enter the helix during the zero field. This process is shown in Fig. 9-5-7.

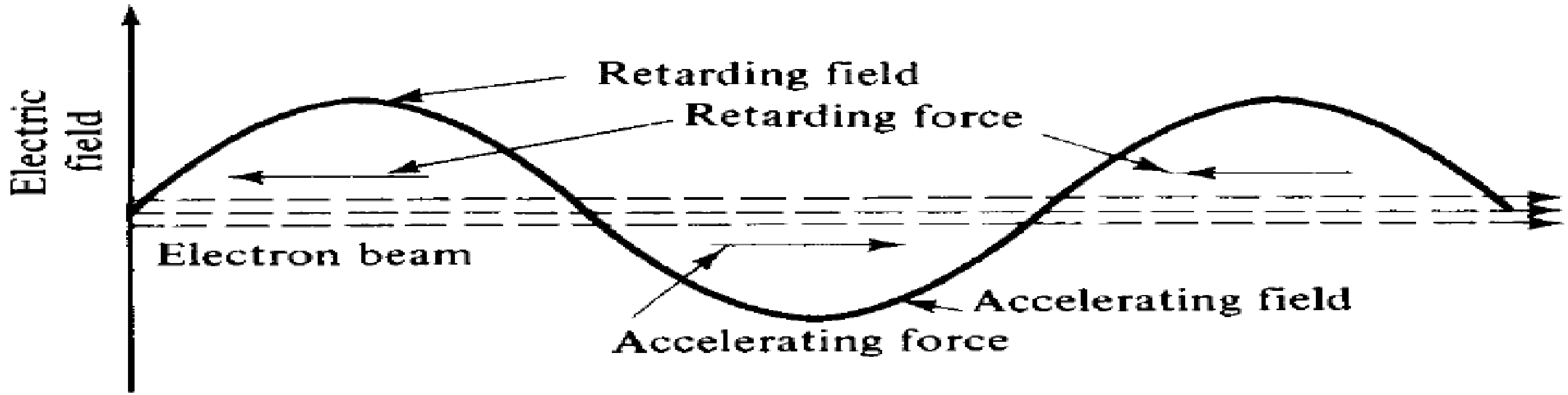

Figure 9-5-7 Interactions between electron beam and electric field.

Since the dc velocity of the electrons is slightly greater than the axial wave velocity, more electrons are in the retarding field than in the accelerating field, and a great amount of energy is transferred from the beam to the electromagnetic field. The microwave signal voltage is, in turn, amplified by the amplified field. The bunch continues to become more compact, and a larger amplification of the signal voltage occurs at the end of the helix.

The motion of electrons in the helix-type traveling-wave tube can be quantitatively analyzed in terms of the axial electric field. If the traveling wave is propagating in the z direction, the z component of the electric field can be expressed as

$$E_z = E_1 \sin(\omega t - \beta_p z) \tag{9-5-23}$$

where E_1 is the magnitude of the electric field in the z direction. If $t = t_0$ at $z = 0$, the electric field is assumed maximum. Note that $\beta_p = \omega / v_p$ is the axial phase constant of the microwave, and v_p is the axial phase velocity of the wave.

The equation of motion of the electron is given by

$$m \frac{dv}{dt} = -eE_1 \sin(\omega t - \beta_p z) \tag{9-5-24}$$

Assume that the velocity of the electron is

$$v = v_0 + v_e \cos(\omega_e t + \theta_e) \tag{9-5-25}$$

Then

$$\frac{dv}{dt} = -v_e \omega_e \sin(\omega_e t + \theta_e) \tag{9-5-26}$$

where v_0 = dc electron velocity
v_e = magnitude of velocity fluctuation in the velocity-modulated electron beam
ω_e = angular frequency of velocity fluctuation
θ_e = phase angle of the fluctuation

Substitution of Eq. (9-5-26) in Eq. (9-5-24) yields

$$m v_e \omega_e \sin(\omega_e t + \omega_e) = e E_1 \sin(\omega t - \beta_p z) \qquad (9\text{-}5\text{-}27)$$

For interactions between the electrons and the electric field, the velocity of the velocity-modulated electron beam must be approximately equal to the dc electron velocity. This is

$$v \approx v_0 \qquad (9\text{-}5\text{-}28)$$

$$\frac{dv}{dt} = -v_e \omega_e \sin(\omega_e t + \theta_e) \quad (9\text{-}5\text{-}26)$$

$$m\frac{dv}{dt} = -e E_1 \sin(\omega t - \beta_p z) \; 9\text{-}5\text{-}24)$$

Hence the distance z traveled by the electrons is

$$z = v_0(t - t_0) \qquad (9\text{-}5\text{-}29)$$

and

$$m v_e \omega_e \sin(\omega_e t + \theta_e) = e E_1 \sin[\omega t - \beta_p v_0(t - t_0)] \qquad (9\text{-}5\text{-}30)$$

Comparison of the left and right-hand sides of Eq. (9-5-30) shows that

$$v_e = \frac{eE_1}{m\omega_e} \qquad (9\text{-}5\text{-}31)$$

$$\omega_e = \beta_p(v_p - v_0)$$

$$\theta_e = \beta_p v_0 t_0$$

It can be seen that the magnitude of the velocity fluctuation of the electron beam is directly proportional to the magnitude of the axial electric field.

9-5-3 Convection Current

In order to determine the relationship between the circuit and electron beam quantities, the convection current induced in the electron beam by the axial electric field and the microwave axial field produced by the beam must first be developed. When the space-charge effect is considered, the electron velocity, the charge density, the current density, and the axial electric field will perturbate about their averages or dc values. Mathematically, these quantities can be expressed as

$$v = v_0 + v_1 e^{j\omega t - \gamma z} \tag{9-5-32}$$

$$\rho = \rho_0 + \rho_1 e^{j\omega t - \gamma z} \tag{9-5-33}$$

$$J = -J_0 + J_1 e^{j\omega t - \gamma z} \tag{9-5-34}$$

$$E_z = E_1 e^{j\omega t - \gamma z} \tag{9-5-35}$$

where $\gamma = \alpha_e + j\beta_e$ is the propagation constant of the axial waves. The minus sign is attached to J_0 so that J_0 may be a positive in the negative z direction. For a small signal, the electron beam-current density can be written

$$J = \rho v \approx -J_0 + J_1 e^{j\omega t - \gamma z} \tag{9-5-36}$$

ial electric field exists in the structure, it will perturbate the electron velocity according to the force equation. Hence the force equation can be written

$$\frac{dv}{dt} = -\frac{e}{m} E_1 e^{j\omega t - \gamma z} = \left(\frac{\partial}{\partial t} + \frac{dz}{dt}\frac{\partial}{\partial z}\right) v = (j\omega - \gamma v_0) v_1 e^{j\omega t - \gamma z} \tag{9-5-37}$$

where dz/dt has been replaced by v_0. Thus

$$v_1 = \frac{-e/m}{j\omega - \gamma v_0} E_1$$

In accordance with the law of conservation of electric charge, the continuity equation can be written

$$\nabla \cdot J + \frac{\partial \rho}{\partial t} = (-\gamma J_1 + j\omega\rho_1)e^{j\omega t - \gamma z} = 0 \qquad (9\text{-}5\text{-}39)$$

It follows that

$$\rho_1 = -\frac{j\gamma J_1}{\omega} \qquad (9\text{-}5\text{-}40)$$

Substitution Eqs. (9-5-38) and (9-5-40) in

$$J_1 = \rho_1 v_0 + \rho_0 v_1 \qquad (9\text{-}5\text{-}44)$$

gives

$$J_1 = J\frac{\omega}{v_0}\frac{e}{m}\frac{J_0}{(j\omega - \gamma v_0)^2}E_1 \qquad (9\text{-}5\text{-}42)$$

where $-J_0 = \rho_0 v_0$ has been replaced. If the magnitude of the axial electric field is uniform over the cross-sectional area of the electron beam, the spatial ac current i will be proportional to the dc current I_0 with the same proportionality constant for J_1 and J_0. Therefore the convection current in the electron beam is given by

$$i = j\frac{\beta_e I_0}{2V_0(j\beta_e - \gamma)^2}E_1 \qquad (9\text{-}5\text{-}43)$$

where $\beta_e \equiv \omega/v_0$ is defined as the phase constant of the velocity-modulated electron beam and $v_0 = \sqrt{(2e/m)V_0}$ has been used. This equation is called the *electronic equation*, for it determines the convection current induced by the axial electric field. If the axial field and all parameters are known, the convection current can be found by means of Eq. (9-5-43).

Furthermore, Eq. (9-5-11) shows that the field in a periodic structure can be expanded as an infinite series of waves, all at the same frequency but with different phase velocities v_{pn}. That is

$$v_{pn} = \frac{\omega}{\beta_n} \equiv \frac{\omega}{\beta_0 + (2\pi n/L)} \qquad (9\text{-}5\text{-}16)$$

The group velocity v_{gr}, defined by $v_{gr} = \partial\omega/\partial\beta$, is then given as

$$v_{gr} = \left[\frac{d(\beta_0 + 2\pi n/L)}{d\omega}\right]^{-1} = \frac{\partial\omega}{\partial\beta_0} \qquad (9\text{-}5\text{-}17)$$

Amplification Process

The slow-wave structure of the helix is characterized by the Brillouin diagram shown in Fig. 9-5-5. The phase shift per period of the fundamental wave on the structure is given by

$$\theta_1 = \beta_0 L \tag{9-5-18}$$

where $\beta_0 = \omega/v_0$ is the phase constant of the average beam velocity and L is the period or pitch.

Since the dc transit time of an electron is given by

$$T_0 = \frac{L}{v_o} \tag{9-5-19}$$

the phase constant of the nth space harmonic is

$$\beta_n = \frac{\omega}{v_0} = \frac{\theta_1 + 2\pi n}{v_0 T_0} = \beta_0 + \frac{2\pi n}{L}$$

When a signal voltage is coupled into the helix, axial electric field exerts a force on the electrons

$$\mathbf{F} = -e\mathbf{E} \quad \text{and} \quad \mathbf{E} = -\nabla V$$

the z component of the electric field can be expressed as

$$E_z = E_1 \sin(\omega t - \beta_p z) \tag{9-5-23}$$

The equation of motion of the electron is given by

$$m\frac{dv}{dt} = -eE_1 \sin(\omega t - \beta_p z) \tag{9-5-24}$$

the velocity of the electron is

$$v = v_0 + v_e \cos(\omega_e t + \theta_e) \qquad (9\text{-}5\text{-}25)$$

$$\frac{dv}{dt} = -v_e \omega_e \sin(\omega_e t + \theta_e) \qquad (9\text{-}5\text{-}26)$$

where v_0 = dc electron velocity
v_e = magnitude of velocity fluctuation in the velocity-modulated electron beam
ω_e = angular frequency of velocity fluctuation
θ_e = phase angle of the fluctuation

Substitution of Eq. (9-5-26) in Eq. (9-5-24) yields

$$m v_e \omega_e \sin(\omega_e t + \omega_e) = eE_1 \sin(\omega t - \beta_p z) \qquad (9\text{-}5\text{-}27)$$

Hence the distance z traveled by the electrons is

$$z = v_0(t - t_0) \tag{9-5-29}$$

$$m v_e \omega_e \sin(\omega_e t + \theta_e) = e E_1 \sin[\omega t - \beta_p v_0(t - t_0)] \tag{9-5-30}$$

$$v_e = \frac{e E_1}{m \omega_e} \tag{9-5-31}$$

$$\omega_e = \beta_p(v_p - v_0)$$

$$\theta_e = \beta_p v_0 t_0$$

It can be seen that the magnitude of the velocity fluctuation of the electron beam is directly proportional to the magnitude of the axial electric field.

Convection Current

the convection current induced in the electron beam by the axial electric field and the microwave axial field produced by the beam must first be developed.

Mathematically, these quantities can be expressed as

$$v = v_0 + v_1 e^{j\omega t - \gamma z} \tag{9-5-32}$$

$$\rho = \rho_0 + \rho_1 e^{j\omega t - \gamma z} \tag{9-5-33}$$

$$J = -J_0 + J_1 e^{j\omega t - \gamma z} \tag{9-5-34}$$

$$E_z = E_1 e^{j\omega t - \gamma z} \tag{9-5-35}$$

where $\gamma = \alpha_e + j\beta_e$ is the propagation constant of the axial waves.

the electron beam-current density can be written

$$J = \rho v \approx -J_0 + J_1 e^{j\omega t - \gamma z} \tag{9-5-36}$$

where $-J_0 = \rho_0 v_0$, $J_1 = \rho_1 v_0 + \rho_0 v_1$, and $\rho_1 v_1 \approx 0$ have been replaced. If an axial electric field exists in the structure, it will perturbate the electron velocity according to the force equation. Hence the force equation can be written

Hence the force equation can be written

$$\frac{dv}{dt} = -\frac{e}{m} E_1 e^{j\omega t - \gamma z} = \left(\frac{\partial}{\partial t} + \frac{dz}{dt}\frac{\partial}{\partial z}\right) v = (j\omega - \gamma v_0) v_1 e^{j\omega t - \gamma z} \tag{9-5-37}$$

where dz/dt has been replaced by v_0. Thus

$$v_1 = \frac{-e/m}{j\omega - \gamma v_0} E_1 \tag{9-5-38}$$

In accordance with the law of conservation of electric charge, the continuity equation can be written

$$\nabla \cdot J + \frac{\partial \rho}{\partial t} = (-\gamma J_1 + j\omega\rho_1)e^{j\omega t-\gamma z} = 0 \qquad (9\text{-}5\text{-}39)$$

$$\rho_1 = -\frac{j\gamma J_1}{\omega}$$

$$v_1 = \frac{-e/m}{j\omega - \gamma v_0}E_1 \qquad (9\text{-}5\text{-}38)$$

$$J_1 = \rho_1 v_0 + \rho_0 v_1$$

$$\rho_1 = -\frac{j\gamma J_1}{\omega}$$

$$J_1 = J\frac{\omega}{v_0}\frac{e}{m}\frac{J_0}{(j\omega - \gamma v_0)^2}E_1$$

where $-J_0 = \rho_0 v_0$ has been replaced. If the magnitude of the axial electric field is uniform over the cross-sectional area of the electron beam, the spatial ac current i will be proportional to the dc current I_0 with the same proportionality constant for J_1 and J_0. Therefore the convection current in the electron beam is given by

$$i = j\frac{\beta_e I_0}{2V_0(j\beta_e - \gamma)^2}E_1 \qquad (9\text{-}5\text{-}43)$$

where $\beta_e \equiv \omega/v_0$ is defined as the phase constant of the velocity-modulated electron beam and $v_0 = \sqrt{(2e/m)V_0}$ has been used. This equation is called the *electronic eauation*. for it determines the convection current induced by the axial electric field.

Axial Electric Field

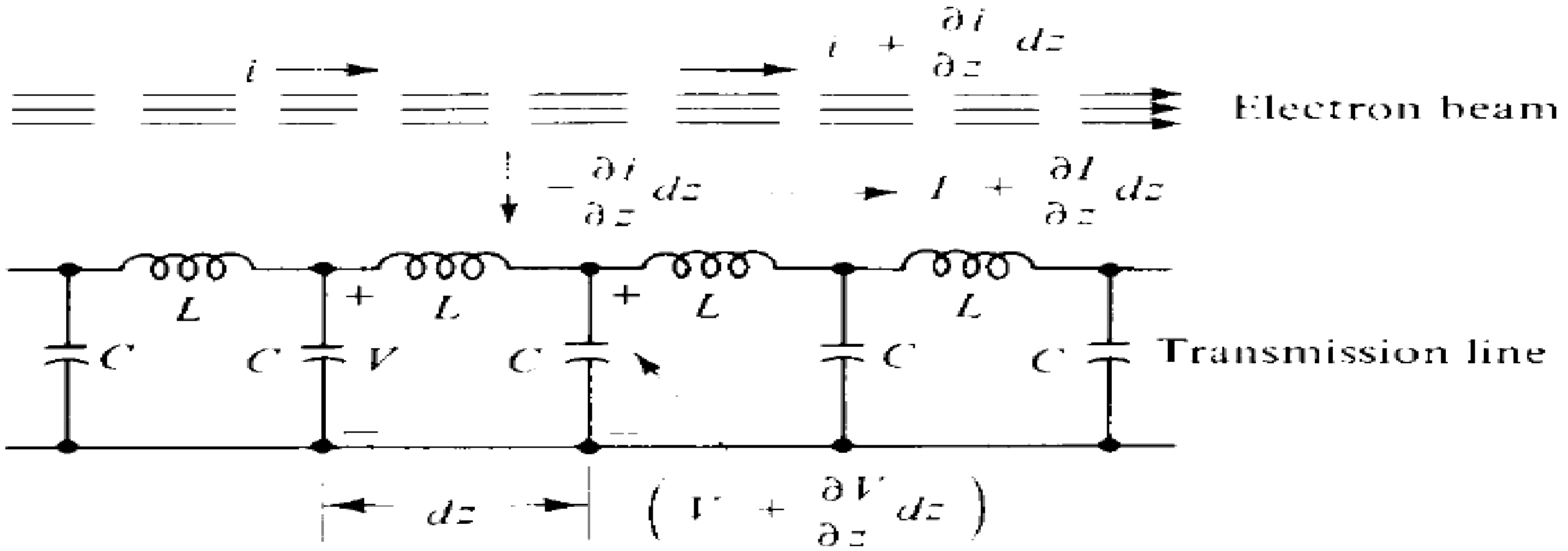

For simplicity, the slow-wave helix is represented by a distributed lossless transmission line. The parameters are defined as follows:

L = inductance per unit length
C = capacitance per unit length
I = alternating current in transmission line
V = alternating voltage in transmission line
i = convection current

Application of transmission-line theory and Kirchhoff's current law to the electron beam results,

$$\frac{\partial I}{\partial z} = -C\frac{\partial V}{\partial t} - \frac{\partial i}{\partial z}$$

$$-\gamma I = -j\omega CV + \gamma i \qquad (9\text{-}5\text{-}45)$$

From Kirchhoff's voltage law the voltage equation, after simplification, is

$$\frac{\partial V}{\partial z} = -L\frac{\partial I}{\partial t} \qquad (9\text{-}5\text{-}46)$$

$$-\gamma V = -j\omega LI$$

Elimination of the circuit current I from Eqs. (9-5-45) and (9-5-46) yields

$$\gamma^2 V = -V\omega^2 LC - \gamma ij\omega L \qquad (9\text{-}5\text{-}48)$$

$$\gamma_0 \equiv j\omega\sqrt{LC}$$

$$Z_0 = \sqrt{\frac{L}{C}}$$

Therefore $V = \dfrac{\gamma\gamma_0 Z_0}{\gamma^2 - \gamma_0^2} i$

Since $E_z = -\nabla V = -(\partial V/\partial z) = \gamma V$, the axial electric field is given by

$$E_1 = -\frac{\gamma^2 \gamma_0 Z_0}{\gamma^2 - \gamma_0^2} i \qquad (9\text{-}5\text{-}52)$$

This equation is called the *circuit equation* because it determines how the axial electric field of the slow-wave helix is affected by the spatial ac electron beam current.

Wave Modes

The wave modes of a helix-type traveling-wave tube can be determined by solving the electronic and circuit equations simultaneously for the propagation constants.

$$i = j\frac{\beta_e I_0}{2V_0(j\beta_e - \gamma)^2}E_1 \qquad (9\text{-}5\text{-}43)$$

$$E_1 = -\frac{\gamma^2 \gamma_0 Z_0}{\gamma^2 - \gamma_0^2} i \qquad (9\text{-}5\text{-}52)$$

The wave modes of a helix-type traveling-wave tube can be determined by solving the electronic and circuit equations simultaneously for the propagation constants. Each solution for the propagation constants represents a mode of traveling wave in the tube. It can be seen from Eqs. (9-5-43) and (9-5-52) that there are four distinct solutions for the propagation constants. This means that there are four modes of traveling wave in the O-type traveling-wave tube. Substitution of Eq. (9-5-43) in Eq. (9-5-52) yields

$$(\gamma^2 - \gamma_0^2)(j\beta_e - \gamma)^2 = -j\frac{\gamma^2 \gamma_0 Z_0 \beta_e I_0}{2V_o} \qquad (9\text{-}5\text{-}53)$$

Thus the values of the four propagation constants γ are given by

$$\gamma_1 = -\beta_e C\frac{\sqrt{3}}{2} + j\beta_e\left(1 + \frac{C}{2}\right) \qquad (9\text{-}5\text{-}66)$$

$$\gamma_2 = \beta_e C\frac{\sqrt{3}}{2} + j\beta_e\left(1 + \frac{C}{2}\right) \qquad (9\text{-}5\text{-}67)$$

$$\gamma_3 = j\beta_e(1 - C) \qquad (9\text{-}5\text{-}68)$$

$$\gamma_4 = -j\beta_e\left(1 - \frac{C^3}{4}\right) \qquad (9\text{-}5\text{-}69)$$

Gain Consideration

The output power gain in decibels is defined as

$$A_p \equiv 10 \log \left| \frac{V(\ell)}{V(0)} \right|^2 = -9.54 + 47.3NC \qquad \text{dB} \qquad (9\text{-}5\text{-}80)$$

where NC is a numerical number.

The output power gain shown in Eq. (9-5-80) indicates an initial loss at the circuit input of 9.54 dB. This loss results from the fact that the input voltage splits into three waves of equal magnitude and the growing wave voltage is only one-third the total input voltage. It can also be seen that the power gain is proportional to the length N in electronic wavelength of the slow-wave structure and the gain parameter C of the circuit. The amplitude of the output voltage is then given by

$$V(\ell) = \frac{V(0)}{3} \exp\left(\sqrt{3}\,\pi NC\right)$$

Magnetron oscillator

- Magnetrons provide microwave oscillations of very high frequency.

Types of magnetrons

1. Negative resistance type
2. Cyclotron frequency type
3. Cavity type

Description of types of magnetron

Negative resistance Magnetrons

- Make use of negative resistance between two anode segments but have low efficiency and are useful only at low frequencies (< 500 MHz).

Cyclotron frequency Magnetrons

- Depend upon synchronization between an alternating component of electric and periodic oscillation of electrons in a direction parallel to this field.
- Useful only for frequencies greater than 100 MHz.

Cavity Magnetrons

- Depend upon the interaction of electrons with a rotating electromagnetic field of constant angular velocity.
- Provide oscillations of very high peak power and hence are useful in radar applications

Cavity Magnetrons

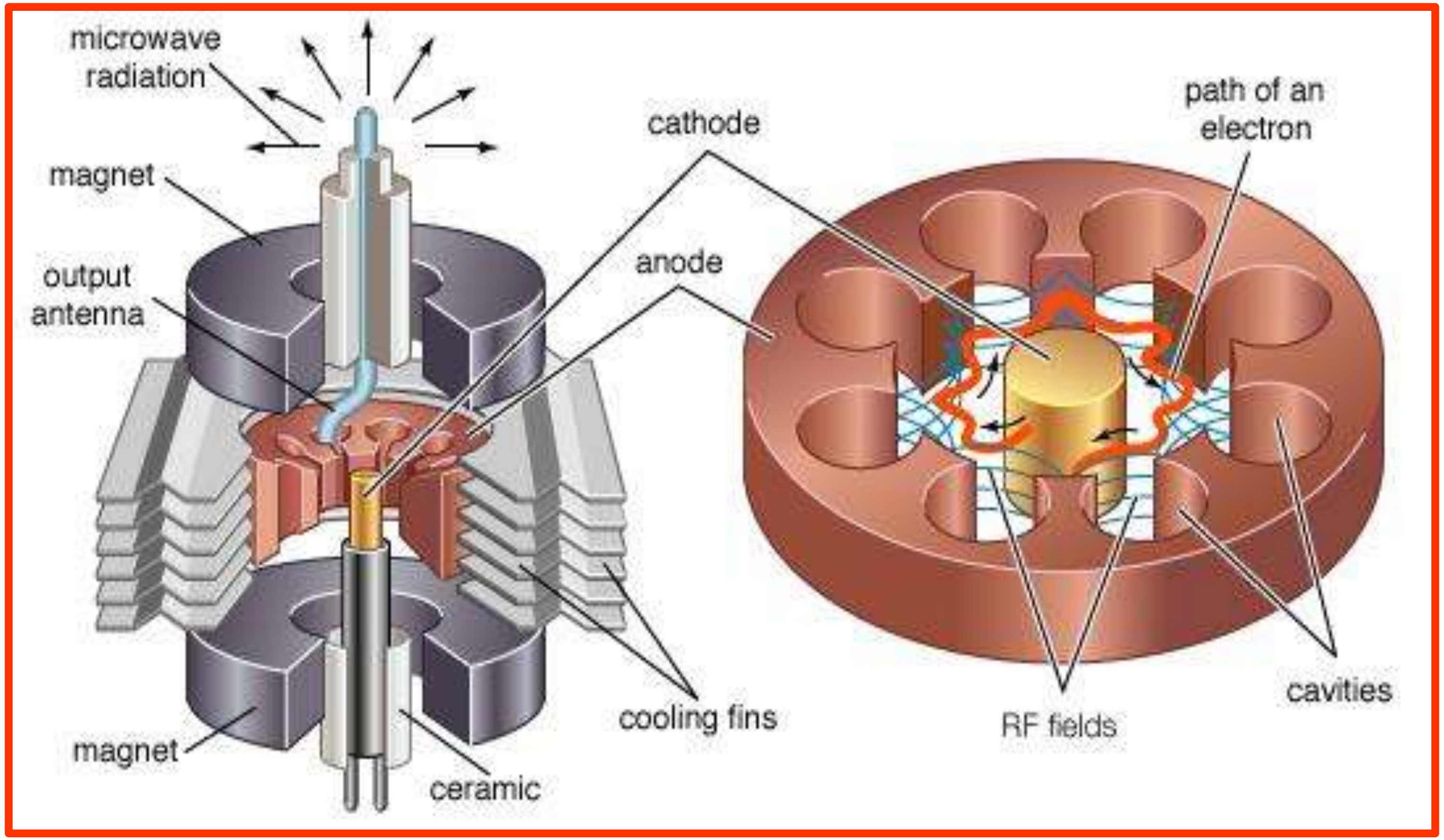

Cavity Magnetrons

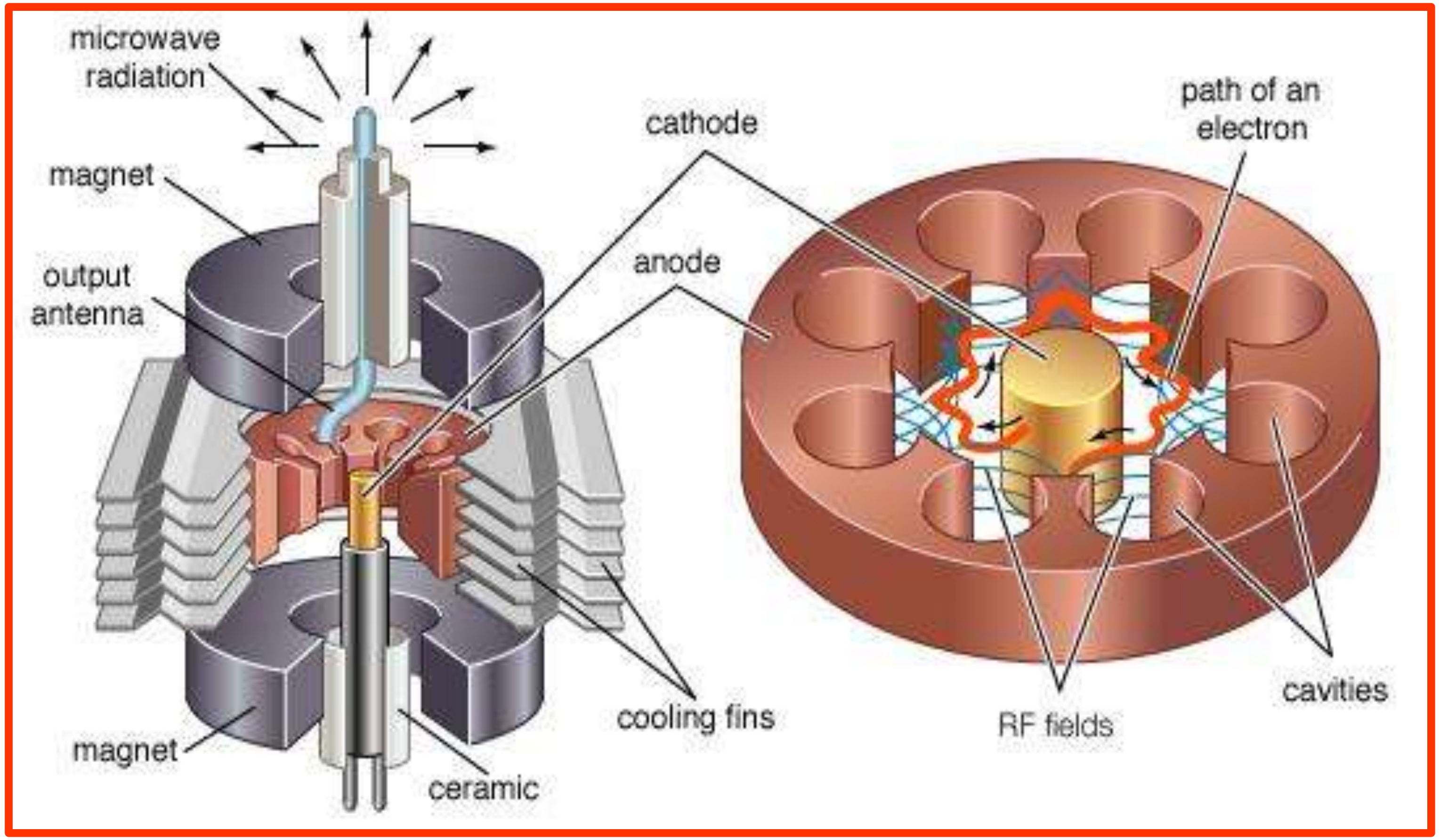

Cross sectional view of the anode assembly

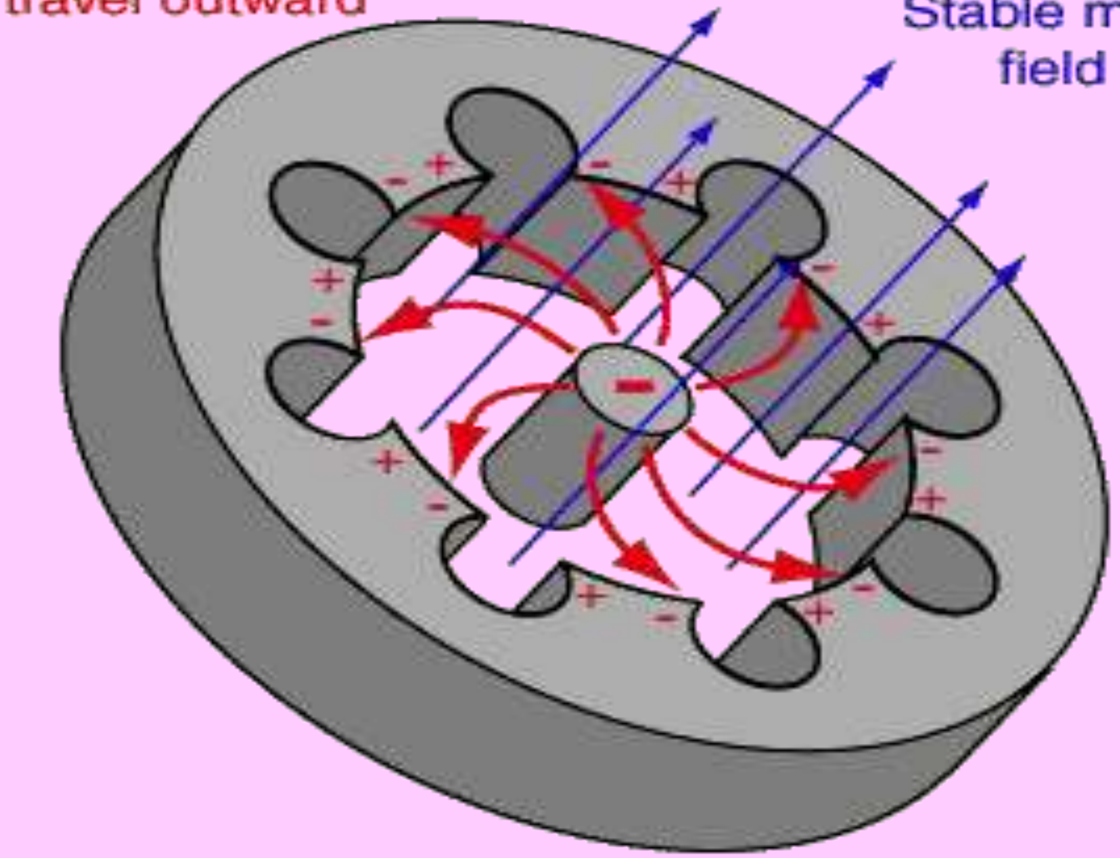

Electrons from a hot filament would travel radially to the outside ring if it were not for the magnetic field. The magnetic force deflects them in the sense shown and they tend to sweep around the circle. In so doing, they "pump" the natural resonant frequency of the cavities. The currents around the resonant cavities cause them to radiate electromagnetic energy at that resonant frequency.

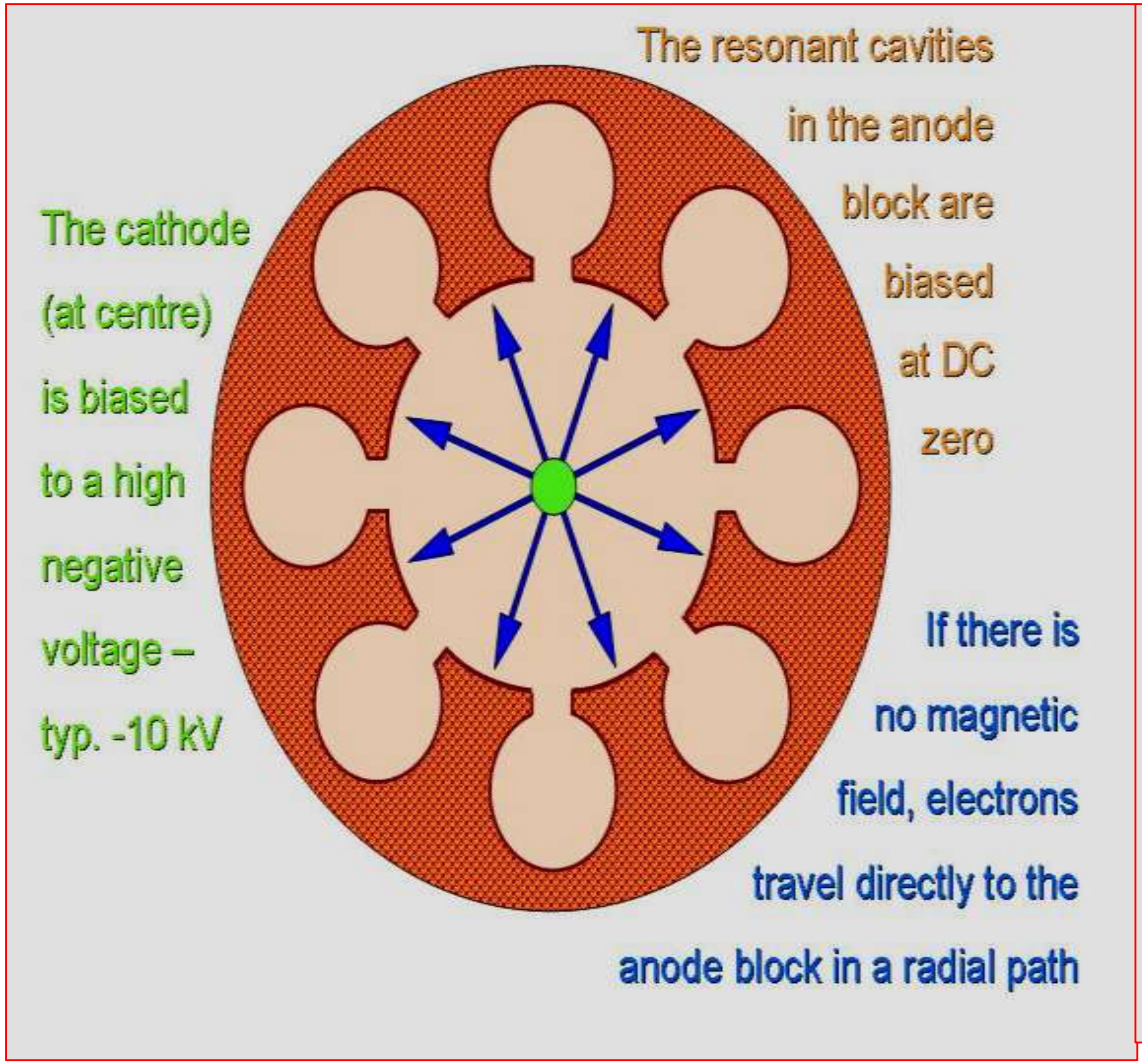

The resonant cavities in the anode block are biased at DC zero
The cathode (at centre) is biased to a high negative voltage – typ. -10 kV
If there is no magnetic field, electrons travel directly to the anode block in a radial path

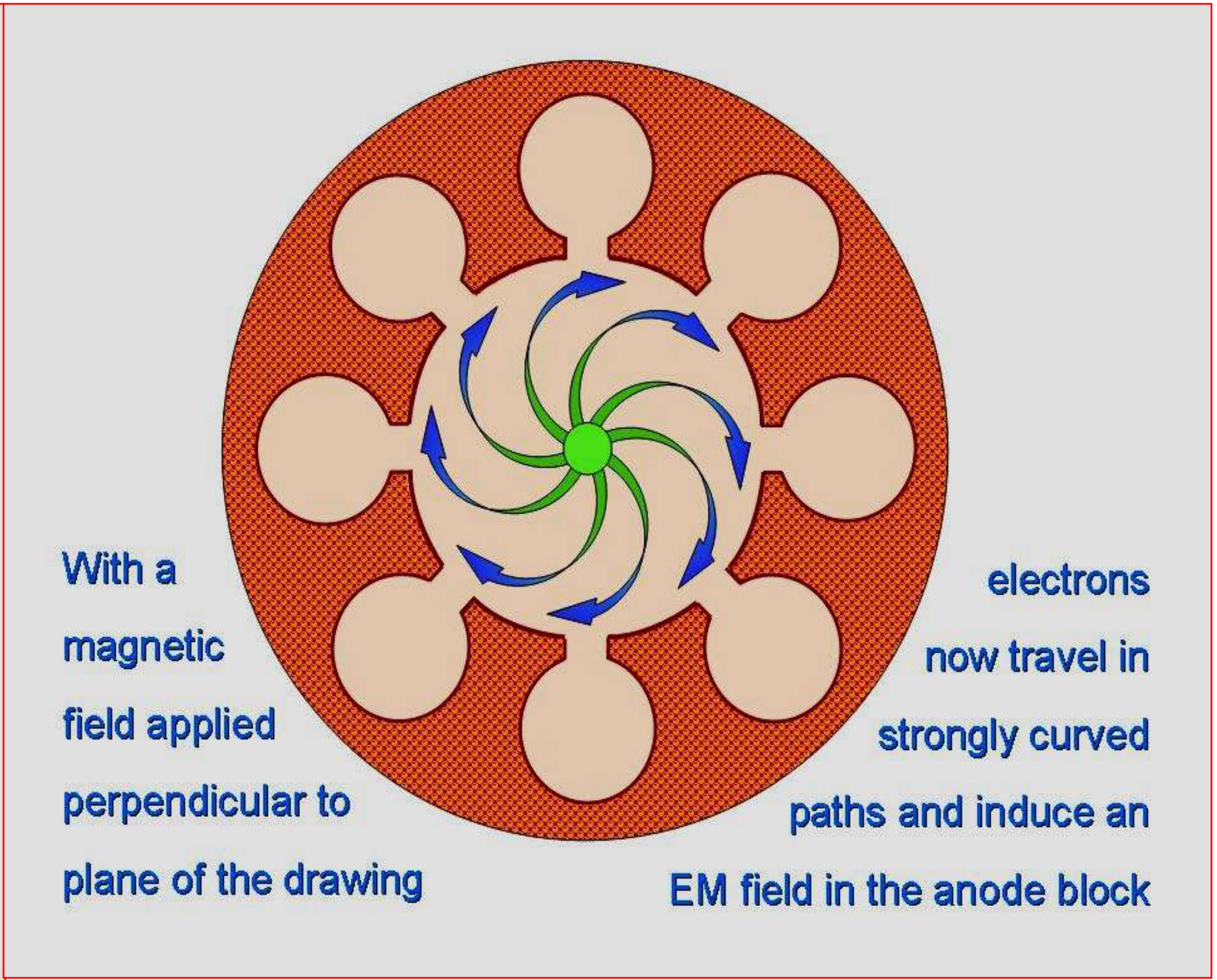

With a magnetic field applied perpendicular to plane of the drawing
electrons now travel in strongly curved paths and induce an EM field in the anode block

Fig (iii) Electron trajectories in the presence of crossed electric and magnetic fields

(a) no magnetic field

(b) small magnetic field

(c) Magnetic field = Bc

(d) Excessive magnetic field

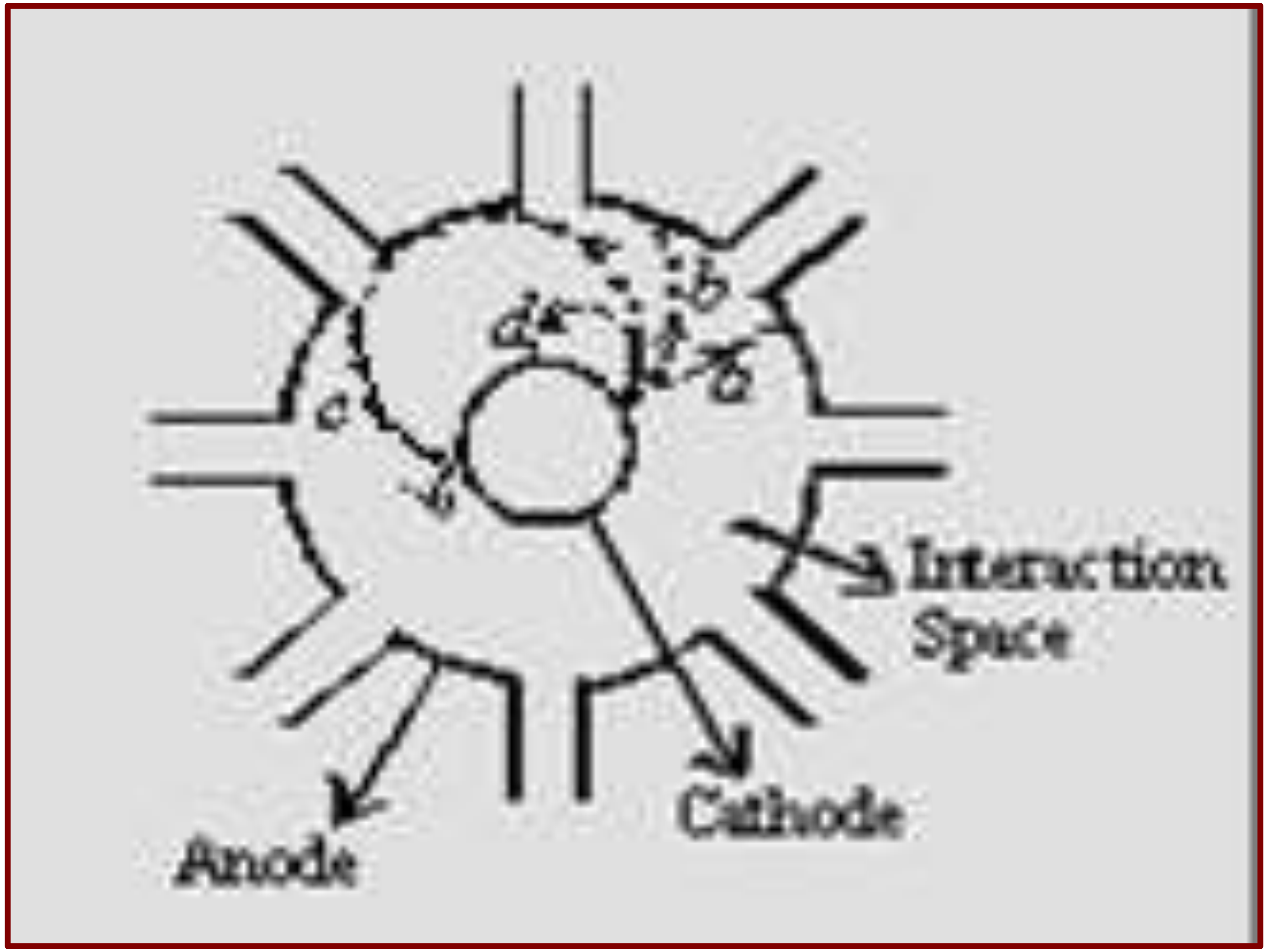

Working) Possible trajectory of electrons from cathode to anode in an eight cavity magnetron operating in π mode

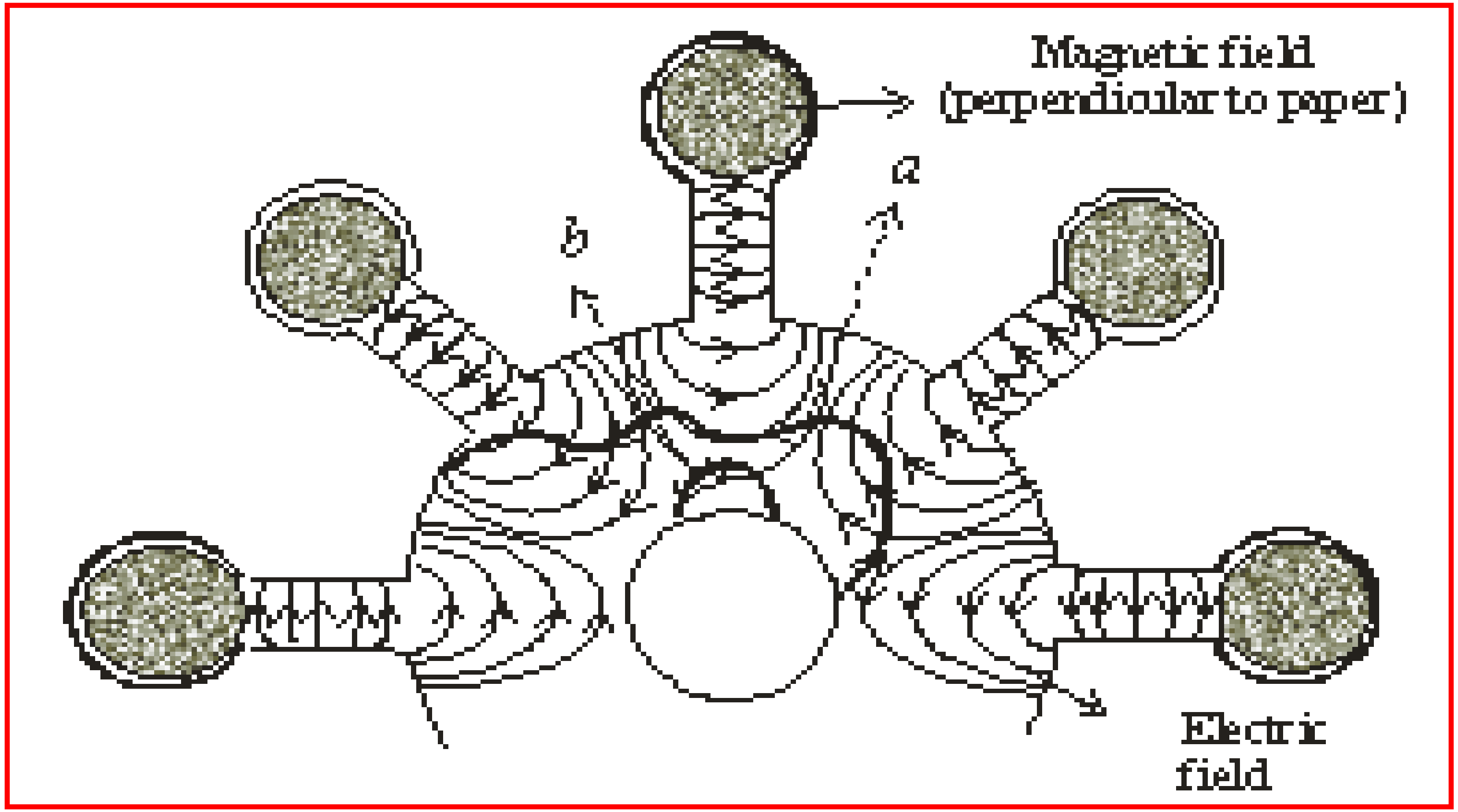

Hartree condition. The Hull cutoff condition determines the anode voltage or magnetic field necessary to obtain nonzero anode current as a function of the magnetic field or anode voltage in the absence of an electromagnetic field. The Hartree condition can be derived as follows and as shown in Fig. 10-1-9.

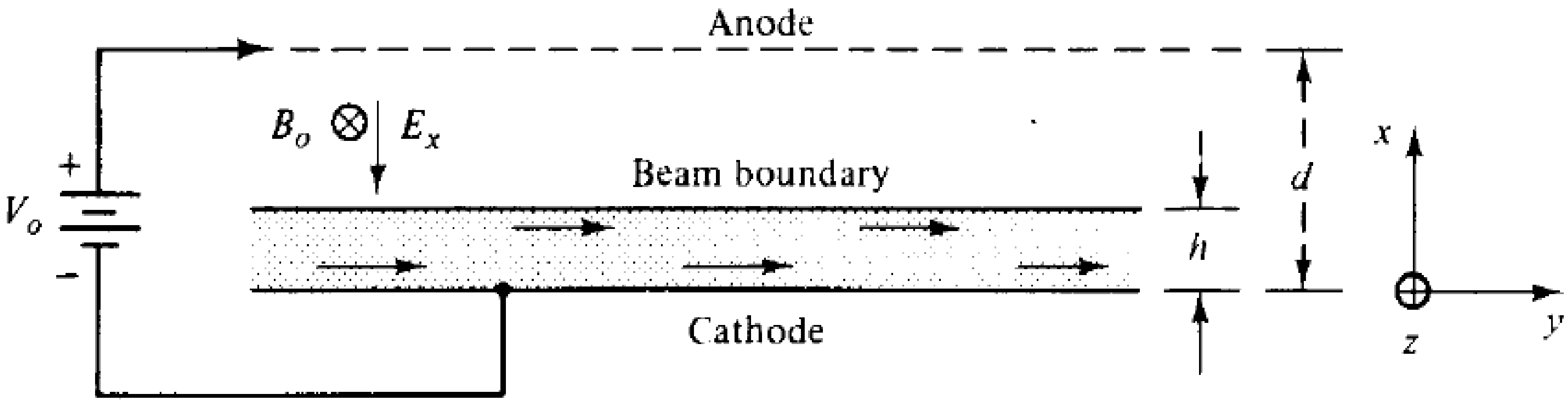

Figure 10-1-9 Linear model of a magnetron.

The electron beam lies within a region extending a distance h from the cathode, where h is known as the hub thickness. The spacing between the cathode and anode is d. The electron motion is assumed to be in the positive y direction with a velocity

$$\mathcal{V}_y = -\frac{E_x}{B_0} = \frac{1}{B_0}\frac{dV}{dx} \qquad (10\text{-}1\text{-}44)$$

where $B_0 = B_z$ is the magnetic flux density in the positive z direction
V = potential

From the principle of energy conservation, we have

$$\tfrac{1}{2} m \mathcal{V}_y^2 = eV$$

$$\mathcal{V}_y = -\frac{E_x}{B_0} = \frac{1}{B_0}\frac{dV}{dx}$$

$$\frac{1}{2} m \mathcal{V}_y^2 = eV$$

Therefore $$\left(\frac{dV}{dx}\right)^2 = \frac{2eV}{m} B_0^2$$

$$\left(\frac{m}{2eB_0}\right)^{1/2} \frac{dV}{\sqrt{V}} = dx$$

$$V = \frac{eB_0^2}{2m} x^2$$

where the constant of integration has been eliminated for $V = 0$ at $x = 0$. The p-
tential and electric field at the hub surface are given by

$$V(h) = \frac{e}{2m} B_0^2 h^2$$

$$E_x = -\frac{dV}{dx} = -\frac{\epsilon}{m} B_0^2 h$$

The potential at the anode is thus obtained from Eq. (10-

$$V_0 = -\int_0^d E_x \, dx$$

$$= -\int_0^h E_x \, dx - \int_h^d E_x \, dx$$

$$= V(h) + \frac{e}{m} B_0^2 h (d - h)$$

$$= \frac{e}{m} B_0^2 h (d - h/2)$$

The electron velocity at the hub surface $\mathcal{V}_y(h) = \frac{e}{m} B_0 h$

this electron velocity is equal to the phase velocity of the slow-wave structure

$$\frac{\omega}{\beta} = \frac{e}{m} B_0 h$$

For the π-mode operation, the anode potential is finally given by

$$V_{0h} = \frac{\omega B_0 d}{\beta} - \frac{m}{2e} \frac{\omega^2}{\beta^2} \qquad (10\text{-}1\text{-}54)$$

This is the Hartree anode voltage equation that is a function of the magnetic flux density and the spacing beween the cathode and anode.

B.Tech. (VII Sem.) 17EC27 - MICROWAVE ENGINEERING

UNIT-III

Microwave Solid State Devices: Introduction, Classification, Applications.

Transferred Electron Devices: Introduction, Gunn Diode – Principle, Two Valley Model Theory, RWH Theory, Characteristics, Modes of Operation.

Avalanche Transit Time Devices: Introduction, **IMPATT and TRAPATT** Diodes – Principle of Operation and Characteristics, related expressions.

for various microwave applications such as detection, frequency multiplication, attenuation, amplitude limiting, generation of oscillations, phase shifting, switching and for low noise amplifiers. These microwave solid state devices have a great advantage of smaller size, lighter weight, and higher reliability of operation, lower cost and higher capability of being incorporated into Microwave Integrated Circuits (MICs), as compared to electron transit time devices. This section will describe

These devices are broadly categorized in to four groups as shown in Fig. (7.1).

1. Transferred Electron Devices (TED)
2. Avalanche Transit Time Devices
3. Microwave Bipolar Junction Transistor (BJT)
4. Microwave Field Effect Transistor (FET's)

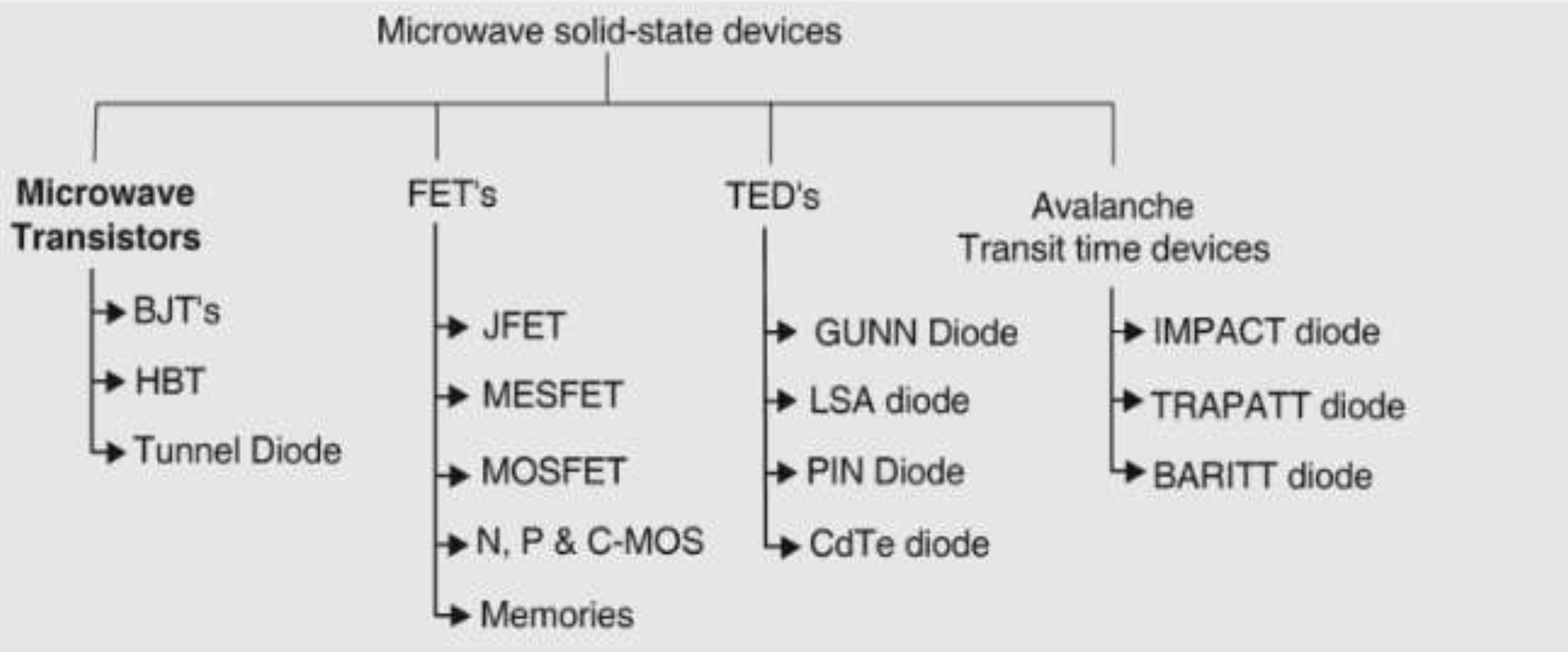

Fig. 7.1. Microwave solid-state devices.

9.4 APPLICATIONS OF SOLID-STATE DEVICES

Microwave solid-state devices are becoming more important. These devices have been invented for various applications in microwave frequency regions such as frequency multiplication, signal detection, attenuation, generation of oscillation, switching, phase shifting, amplitude limiting, and amplification. Some of their applications are as follows:

- As microwave generators
- As amplifiers in satellite communications and also in other space applications
- As transmitters for millimeter communication systems
- In radio transmitters, such as CW Doppler radar
- In broadband linear amplifiers and in low-power amplifiers
- As a pumping source for parametric amplifiers
- In transponders
- In both combinational and sequential logic circuits
- In microwave receivers

The differences between microwave transistors and transferred electron devices (TEDs) are fundamental.

1.Transistors operate with either junctions or gates

2.The majority of transistors are fabricated from elemental semiconductors, such as si or Ge

3.Transistors operate with "warm" electrons whose energy is not much greater than the thermal energy(0.026 eV at room temperature) of electrons in the semiconductor,

1.TEDs are bulk devices having no junctions or gates

2.TEDs are fabricated from compound semiconductors, such as gallium arsenide (GaAs), indium phosphide (InP), or cadmium telluride (CdTe).

3.TEDoperate with "hot" electrons whose energy is very much greater than the thermal energy

- The application of two-terminal semiconductor devices at microwave frequencies has been increased usage during the past decades
- The common characteristic of all active two-terminal solid-state devices is their negative resistance. The real part of their impedance is negative over a range of frequencies
- In a positive resistance the current through the resistance and the voltage across it are in phase. The voltage drop across a positive resistance is positive and a power of (I2 R) is dissipated in the resistance.
- In a negative resistance, however, the current and voltage are out of phase by180°. The voltage drop across a negative resistance is negative, and a power of (-I2 R) is generated by the power supply associated with the negative resistance
- In other words, positive resistances absorb power (passivedevices), whereas negative resistances generate power (active devices).

GUNN-EFFECT DIODES—GaAs DIODE

Gunn-effect diodes are named after J. B. Gunn, who in 1963 discovered a periodic fluctuations of current passing through the *n*-type gallium arsenide (GaAs) specimen when the applied voltage exceeded a certain critical value.

A schematic diagram of a uniform *n*-type GaAs diode with ohmic contacts at the end surfaces is shown in Fig. 7-1-1. J. B. Gunn observed the Gunn effect in the *n*-type GaAs bulk diode in 1963, an effect best explained by Gunn himself, who

Above some critical voltage, corresponding to an electric field of 2000–4000 volts/cm, the current in every specimen became a fluctuating function of time. In the GaAs specimens, this fluctuation took the form of a periodic oscillation superimposed upon the pulse current. . . . The frequency of oscillation was determined mainly by the specimen, and not by the external circuit. . . . The period of oscillation was usually inversely proportional to the specimen length and closely equal to the transit time of electrons between the electrodes, calculated from their estimated velocity of slightly over 10^7 cm/s. . . . The peak pulse microwave power delivered by the GaAs specimens to a matched load was measured. Value as high as 0.5 W at 1 Gc/s, and 0.15 W at 3 Gc/s, were found, corresponding to 1–2% of the pulse input power.*

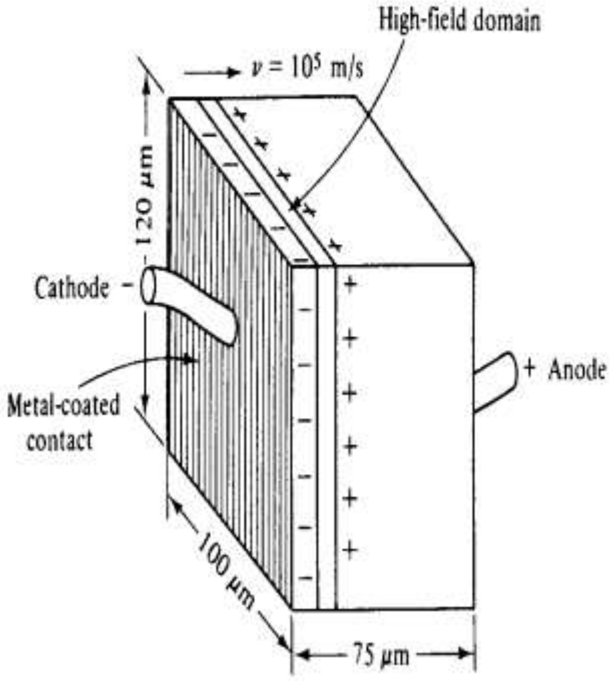

Figure 7-1-1 Schematic diagram for *n*-type GaAs diode.

From Gunn's observation the carrier drift velocity is linearly increased from zero to a maximum when the electric field is varied from zero to a threshold value. When the electric field is beyond the threshold value of 3000 V/cm for the *n*-type GaAs, the drift velocity is decreased and the diode exhibits negative resistance. This situation is shown in Fig. 7-1-2.

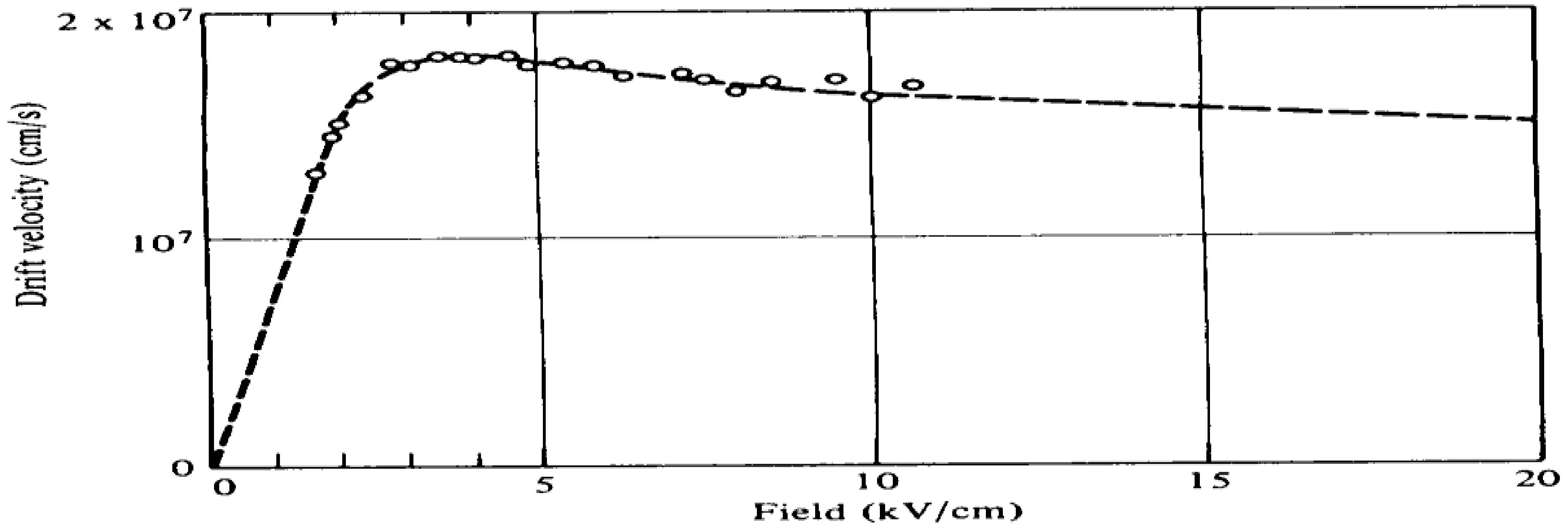

Figure 7-1-2 Drift velocity of electrons in *n*-type GaAs versus electric field.

The current fluctuations are shown in Fig. 7-1-3. The current waveform was produced by applying a voltage pulse of 16-V amplitude and 10-ns duration to a specimen of n-type GaAs 2.5×10^{-3} cm in length. The oscillation frequency was 4.5 GHz.

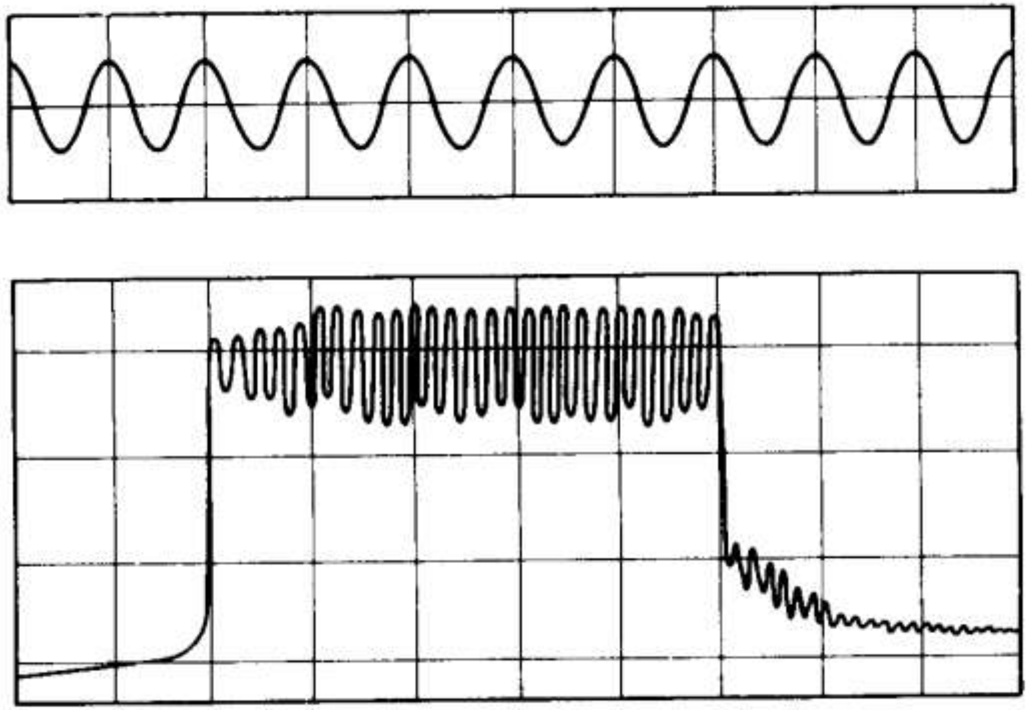

Figure 7-1-3 Current waveform of n-type GaAs reported by Gunn. (*After J. B. Gunn [8]; reprinted by permission of IBM, Inc.*)

Two-Valley Model Theory

A few years before the Gunn effect was discovered, Kroemer proposed a negative-mass microwave amplifier in 1958 [10] and 1959 [11]. According to the energy band theory of the *n*-type GaAs, a high-mobility lower valley is separated by an energy of 0.36 eV from a low-mobility upper valley as shown in Fig. 7-2-4. Table 7-2-1 lists

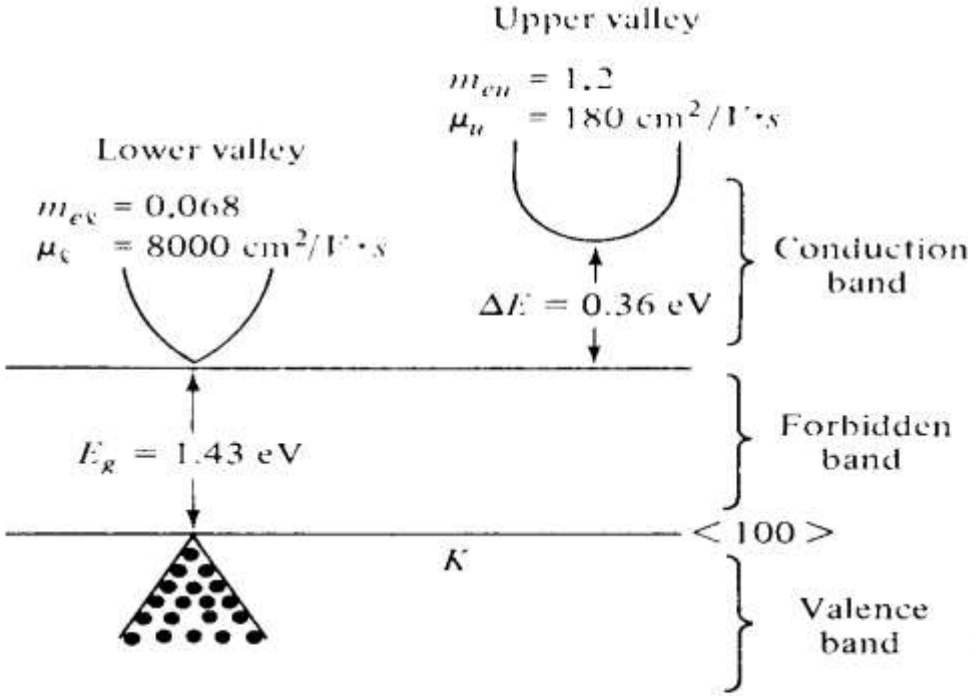

Figure 7-2-4 Two-valley model of electron energy versus wave number for *n*-type GaAs.

Electron densities in the lower and upper valleys remain the same under an equilibrium condition. When the applied electric field is lower than the electric field of the lower valley ($E < E_\ell$), no electrons will transfer to the upper valley as shown in Fig. 7-2-5(a). When the applied electric field is higher than that of the lower valley and lower than that of the upper valley ($E_\ell < E < E_u$), electrons will begin to transfer to the upper valley as shown in Fig. 7-2-5(b). And when the applied electric field is higher than that of the upper valley ($E_u < E$), all electrons will transfer to the upper valley as shown in Fig. 7-2-5(c).

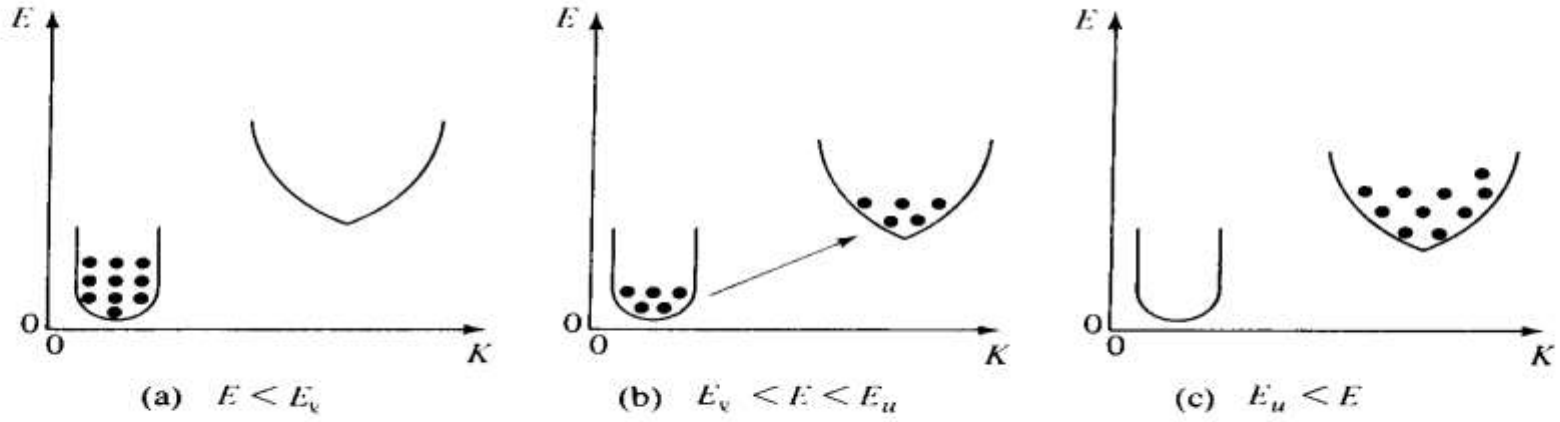

Figure 7-2-5 Transfer of electron densities.

If electron densities in the lower and upper valleys are n_ℓ and n_u, the conductivity of the n-type GaAs is

$$\sigma = e(\mu_\ell n_\ell + \mu_u n_u) \qquad (7\text{-}2\text{-}2)$$

where e = the electron charge
μ = the electron mobility
$n = n_\ell + n_u$ is the electron density

When a sufficiently high field E is applied to the specimen, electrons are accelerated and their effective temperature rises above the lattice temperature. Furthermore, the lattice temperature also increases. Thus electron density n and mobility μ are both functions of electric field E. Differentiation of Eq. (7-2-2) with respect to E yields

$$\frac{d\sigma}{dE} = e\left(\mu_\ell \frac{dn_\ell}{dE} + \mu_u \frac{dn_u}{dE}\right) + e\left(n_\ell \frac{d\mu_\ell}{dE} + n_u \frac{d\mu_u}{dE}\right) \qquad (7\text{-}2\text{-}3)$$

If the total electron density is given by $n = n_\ell + n_u$ and it is assumed that μ_ℓ and μ_u are proportional to E^p, where p is a constant, then

$$\frac{d}{dE}(n_\ell + n_u) = \frac{dn}{dE} = 0 \tag{7-2-4}$$

$$\frac{dn_\ell}{dE} = -\frac{dn_u}{dE} \tag{7-2-5}$$

$$\frac{d\mu}{dE} \propto \frac{dE^p}{dE} = pE^{p-1} = p\frac{E^p}{E} \propto p\frac{\mu}{E} = \mu\frac{p}{E} \tag{7-2-6}$$

Substitution of Eqs. (7-2-4) to (7-2-6) into Eq. (7-2-3) results in

$$\frac{d\sigma}{dE} = e(\mu_\ell - \mu_u)\frac{dn_\ell}{dE} + e(n_\ell\mu_\ell + n_u\mu_u)\frac{p}{E} \tag{7-2-7}$$

Then differentiation of Ohm's law $J = \sigma E$ with respect to E yields

$$\frac{dJ}{dE} = \sigma + \frac{d\sigma}{dE} E \qquad (7\text{-}2\text{-}8)$$

Equation (7-2-8) can be rewritten

$$\frac{1}{\sigma}\frac{dJ}{dE} = 1 + \frac{d\sigma/dE}{\sigma/E} \qquad (7\text{-}2\text{-}9)$$

Clearly, for negative resistance, the current density J must decrease with increasing field E or the ratio of dJ/dE must be negative. Such would be the case only if the right-hand term of Eq. (7-2-9) is less than zero. In other words, the condition for negative resistance is

$$-\frac{d\sigma/dE}{\sigma/E} > 1 \qquad (7\text{-}2\text{-}10)$$

RIDLEY–WATKINS–HILSUM (RWH) THEORY

Many explanations have been offered for the Gunn effect. In 1964 Kroemer [6] suggested that Gunn's observations were in complete agreement with the Ridley–Watkins–Hilsum (RWH) theory.

7·2·1 Differential Negative Resistance

The fundamental concept of the Ridley–Watkins–Hilsum (RWH) theory is the differential negative resistance developed in a bulk solid-state III-V compound when either a voltage (or electric field) or a current is applied to the terminals of the sample. There are two modes of negative-resistance devices: voltage-controlled and current-controlled modes as shown in Fig. 7-2-1(a) and (b), respectively [5].

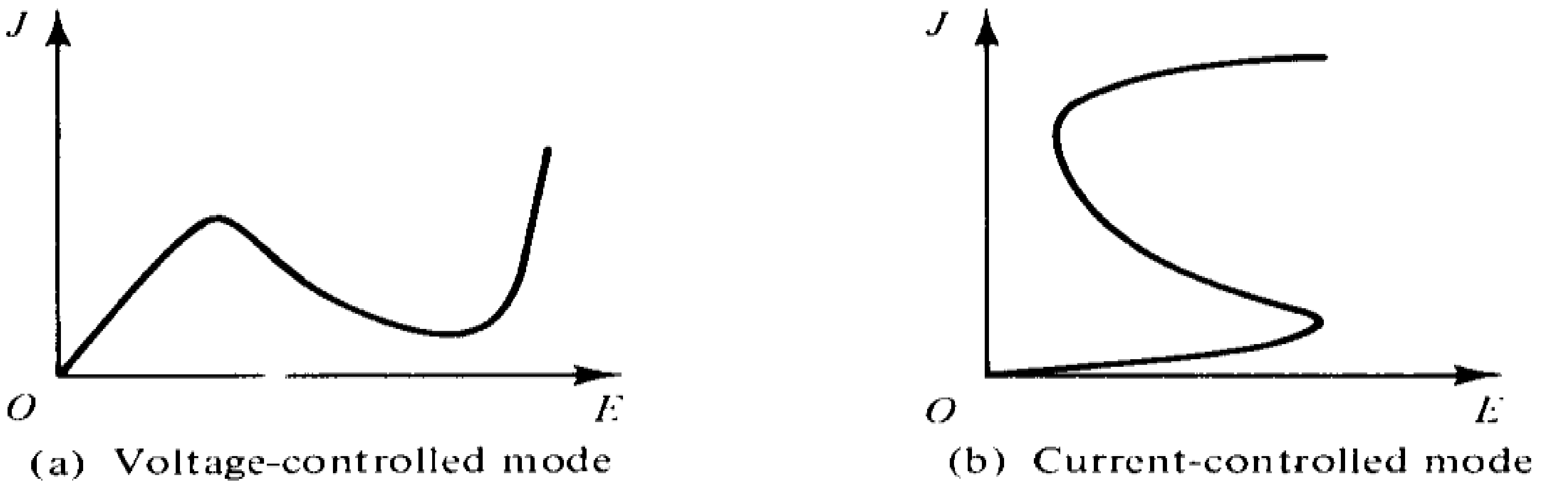

Figure 7-2-1 Diagram of negative resistance. (*From B. K. Ridley [5]; reprinted by permission of the Institute of Physics.*)

In the voltage-controlled mode the current density can be multivalued, whereas in the current-controlled mode the voltage can be multivalued. The major effect of the appearance of a differential negative-resistance region in the current-density-field curve is to render the sample electrically unstable.

On the basis of the Ridley–Watkins–Hilsum theory as described earlier, the band structure of a semiconductor must satisfy three criteria in order to exhibit negative resistance [12].

1. The separation energy between the bottom of the lower valley and the bottom of the upper valley must be several times larger than the thermal energy (about 0.026 eV) at room temperature. This means that $\Delta E > kT$ or $\Delta E > 0.026$ eV.
2. The separation energy between the valleys must be smaller than the gap energy between the conduction and valence bands. This means that $\Delta E < E_g$. Otherwise the semiconductor will break down and become highly conductive before the electrons begin to transfer to the upper valleys because hole-electron pair formation is created.
3. Electrons in the lower valley must have high mobility, small effective mass, and a low density of state, whereas those in the upper valley must have low mobility, large effective mass, and a high density of state. In other words, electron velocities (dE/dk) must be much larger in the lower valleys than in the upper valleys.

A mathematical analysis of differential negative resistance requires a detailed analysis of high-field carrier transports [13–14]. From electric field theory the magnitude of the current density in a semiconductor is given by

$$J = qnv \qquad (7\text{-}2\text{-}12)$$

where q = electric charge
n = electron density, and
v = average electron velocity.

Differentiation of Eq. (7-2-12) with respect to electric field E yields

$$\frac{dJ}{dE} = qn\frac{dv}{dE} \qquad (7\text{-}2\text{-}13)$$

The condition for negative differential conductance may then be written

$$\frac{dv_d}{dE} = \mu_n < 0 \qquad (7\text{-}2\text{-}14)$$

MODES OF OPERATION

1. Gunn oscillation mode: This mode is defined in the region where the product of frequency multiplied by length is about 10^7 cm/s and the product of doping multiplied by length is greater than $10^{12}/cm^2$. In this region the device is unstable because of the cyclic formation of either the accumulation layer or the high-field domain. In a circuit with relatively low impedance the device operates in the high-field domain mode and the frequency of oscillation is near the

2. Stable amplification mode: This mode is defined in the region where the product of frequency times length is about 10^7 cm/s and the product of doping times length is between 10^{11} and $10^{12}/cm^2$.

3. LSA oscillation mode: This mode is defined in the region where the product of frequency times length is above 10^7 cm/s and the quotient of doping divided by frequency is between 2×10^4 and 2×10^5.
4. Bias-circuit oscillation mode: This mode occurs only when there is either Gunn or LSA oscillation, and it is usually at the region where the product of frequency times length is too small to appear in the figure. When a bulk diode is biased to threshold, the average current suddenly drops as Gunn oscillation begins. The drop in current at the threshold can lead to oscillations in the bias circuit that are typically 1 kHz to 100 MHz [18].

7-3-2 Gunn Oscillation Modes ($10^{12}/cm^2 \leqslant (n_0 L) < 10^{14}/cm^2$)

Most Gunn-effect diodes have the product of doping and length ($n_0 L$) greater than $10^{12}/cm^2$. However, the mode that Gunn himself observed had a product $n_0 L$ that is much less. When the product of $n_0 L$ is greater than $10^{12}/cm^2$ in GaAs, the space-charge perturbations in the specimen increase exponentially in space and time in accordance with Eq. (7-3-1). Thus a high-field domain is formed and moves from the cathode to the anode as described earlier. The frequency of oscillation is given by the relation [19]

$$f = \frac{v_{dom}}{L_{eff}} \qquad (7\text{-}3\text{-}4)$$

where v_{dom} is the domain velocity and L_{eff} is the effective length that the domain travels from the time it is formed until the time that a new domain begins to form.

Transit-time domain mode ($fL \approx 10^7$ cm/s). When the electron drift velocity v_d is equal to the sustaining velocity v_s, the high-field domain is stable. In other words, the electron drift velocity is given by

$$v_d = v_s = fL \approx 10^7 \text{ cm/s} \quad (7\text{-}3\text{-}5)$$

Delayed domain mode (10^6 cm/s $< fL < 10^7$ cm/s). When the transit time is chosen so that the domain is collected while $E < E_{th}$ as shown in Fig. 7-3-4(b), a new domain cannot form until the field rises above threshold again. In this case, the oscillation period is greater than the transit time—that is, $\tau_0 > \tau_t$. This delayed

Quenched domain mode ($fL > 2 \times 10^7$ cm/s). If the bias field drops below the sustaining field E_s during the negative half-cycle as shown in Fig. 7-3-4(c), the domain collapses before it reaches the anode. When the bias field swings back above threshold, a new domain is nucleated and the process repeats. Therefore the oscillations occur at the frequency of the resonant circuit rather than at the transit-time fre-

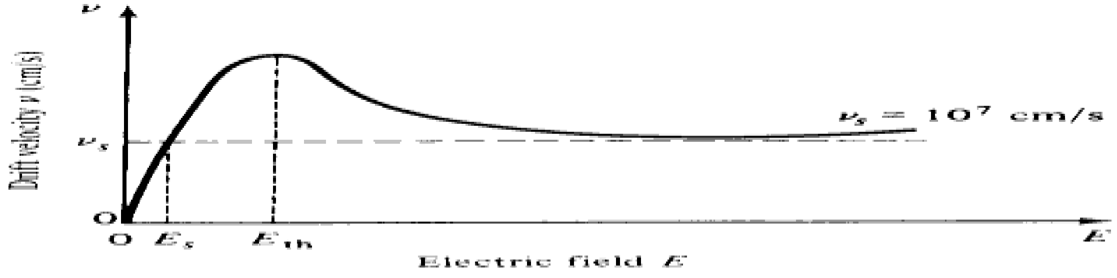

Figure 7-3-3 Electron drift velocity versus electric field.

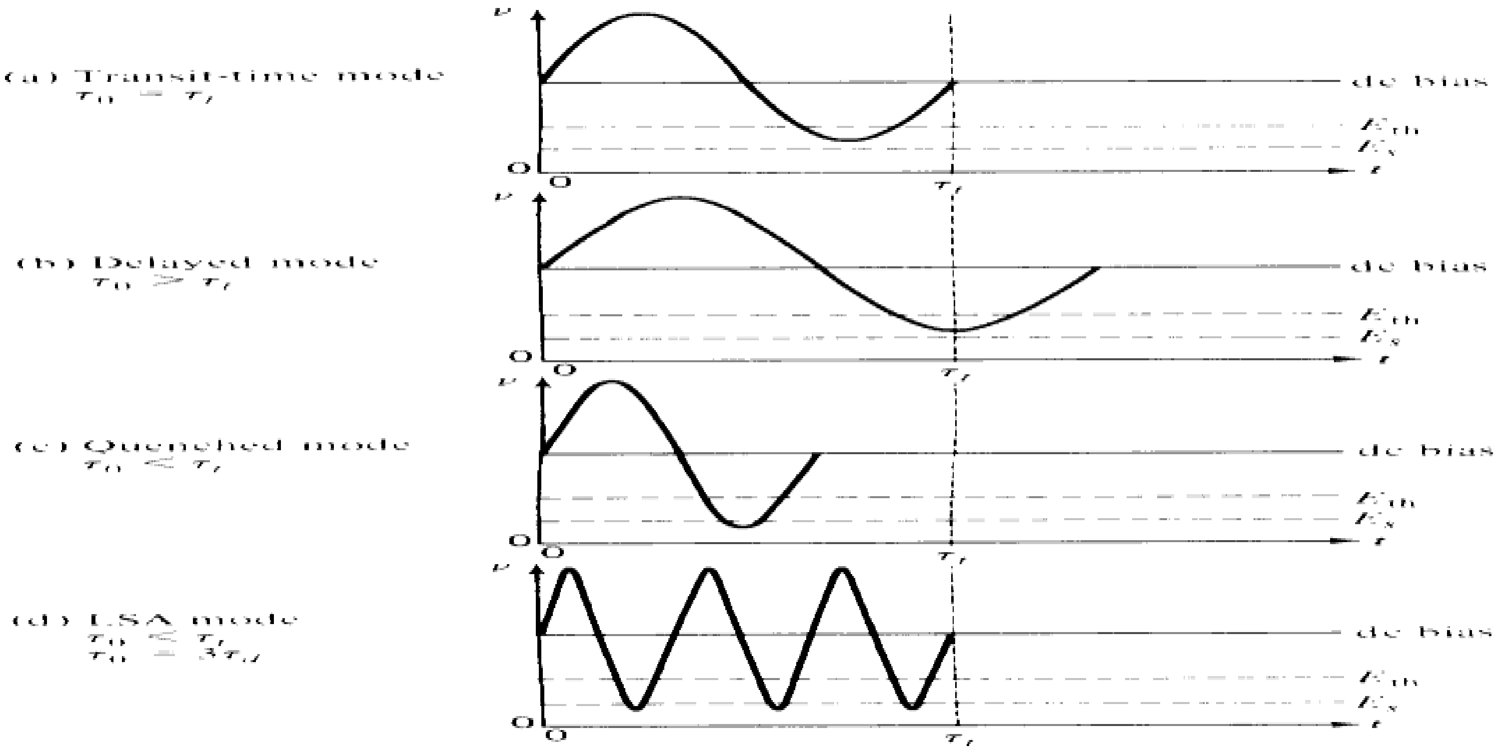

Figure 7-3-4 Gunn domain modes.

7-3-4 Stable Amplification Mode ($n_0 L < 10^{12}/\text{cm}^2$)

When the $n_0 L$ product of the device is less than about $10^{12}/\text{cm}^2$, the device exhibits amplification at the transit-time frequency rather than spontaneous oscillation. This situation occurs because the negative conductance is utilized without domain forma-

The various modes of operation of Gunn diodes can be classified on the basis of the times in which various processes occur. These times are defined as follows:

τ_t = domain transit time

τ_d = dielectric relaxation time at low field

τ_g = domain growth time

τ_0 = natural period of oscillation of a high-Q external electric circuit

Limited-Space-Charge Accumulation (LSA) Mode ($fL > 2 \times 10^7$ cm/s)

below threshold. Thus the LSA mode is the simplest mode of operation, and it consists of a uniformly doped semiconductor without any internal space charges. In this instance, the internal electric field would be uniform and proportional to the applied voltage. The current in the device is then proportional to the drift velocity at this field level. The efficiency of the LSA mode can reach 20%.

The oscillation period τ_0 should be no more than several times larger than the magnitude of the dielectric relaxation time in the negative conductance region τ_d. The oscillation indicated in Fig. 7-3-4(d) is $\tau_0 = 3\tau_d$. It is appropriate here to define the LSA boundaries. As described earlier, the sustaining drift velocity is 10^7 cm/s as

Avalanche Transit-Time Devices Avalanche transit-time diode oscillators rely on the effect of voltage breakdown across a reverse-biased *p-n* junction to produce a supply of holes and electrons. Ever

Two distinct modes of avalanche oscillator have been observed. One is the IMPATT mode, which stands for *impact ionization avalanche transit-time* operation. In this mode the typical dc-to-RF conversion efficiency is 5 to 10%, and frequencies are as high as 100 GHz with silicon diodes. The other mode is the TRAPATT mode, which represents *trapped plasma avalanche triggered transit* operation. Its typical conversion efficiency is from 20 to 60%.

The basic operating principle of IMPATT diodes can be most easily understood by reference to the first proposed avalanche diode, the Read diode [1]. The theory of this device was presented by Read in 1958, but the first experimental Read diode

The Read diode is an n^+-p-i-p^+ structure, where the superscript plus sign denotes very high doping and the *i* or *v* refers to intrinsic material. The device consists essentially of two regions. One is the thin *p* region at which avalanche multiplication occurs. This region is also called the high-field region or the avalanche region. The other is the *i* or *v* region through which the generated holes must drift in moving to the p^+ contact. This region is also called the intrinsic region or the drift region. The *p* region is very thin. The space between the n^+-p junction and the i-p^+ junction is called the space-charge region. Similar devices can be built in the p^+-n-i-n^+ structure, in which electrons generated from avalanche multiplication drift through the *i* region. The Read diode oscillator consists of an n^+-p-i-p^+ diode biased in reverse and mounted in a microwave cavity.

IMPATT DIODES

8-2-1 Physical Structures

A theoretical Read diode made of an n^+-p-i-p^+ or p^+-n-i-n^+ structure has been analyzed. Its basic physical mechanism is the interaction of the impact ionization avalanche and the transit time of charge carriers. Hence the Read-type diodes are called IMPATT diodes. These diodes exhibit a differential negative resistance by two effects:

1. The impact ionization avalanche effect, which causes the carrier current $I_0(t)$ and the ac voltage to be out of phase by 90°
2. The transit-time effect, which further delays the external current $I_e(t)$ relative to the ac voltage by 90°

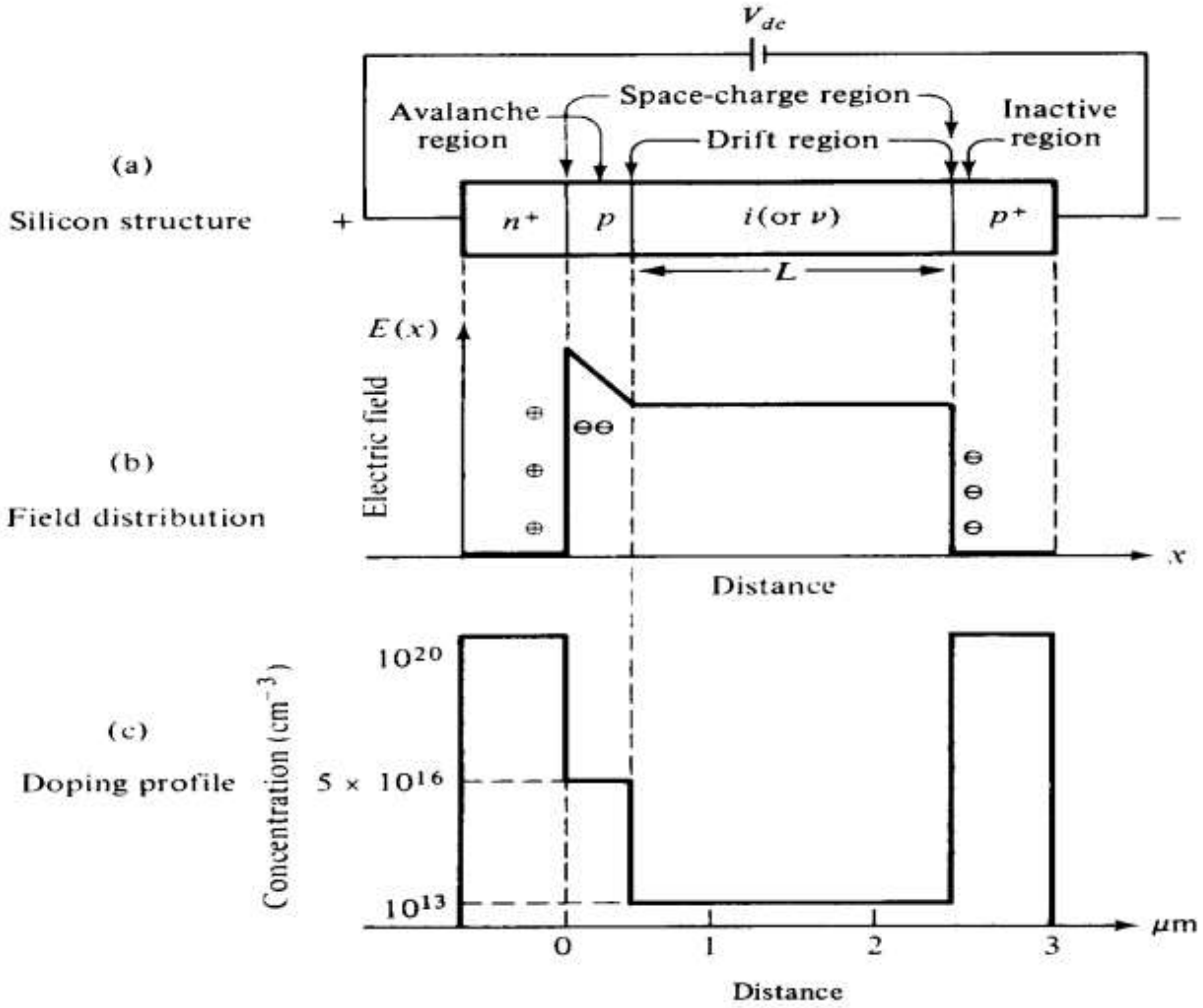

Figure 8-1-1 Read diode.

Avalanche Multiplication

When the reverse-biased voltage is well above the punchthrough or breakdown voltage, the space-charge region always extends from the n^+-p junction through the p and i regions to the i-p^+ junction. The fixed charges in the various regions are shown in Fig. 8-1-1(b). A positive charge gives a rising field in moving from left to right. The maximum field, which occurs at the n^+-p junction, is about several hundred kilovolts per centimeter. Carriers (holes) moving in the high field near the n^+-p junction acquire energy to knock valence electrons into the conduction band, thus producing hole-electron pairs. The rate of pair production, or avalanche multiplication, is a sensitive nonlinear function of the field. By proper doping, the field can be given a relatively sharp peak so that avalanche multiplication is confined to a very and the avalanche multiplication factor is

$$M = \frac{1}{1 - (V/V_b)^n} \qquad (8\text{-}1\text{-}1a)$$

where V = applied voltage
V_b = avalanche breakdown voltage
n = 3–6 for silicon is a numerical factor depending on the doping of p^+-n or n^+-p junction

Carrier Current $I_o(t)$ and External Current $I_e(t)$

As described previously, the Read diode is mounted in a microwave resonant circuit. An ac voltage can be maintained at a given frequency in the circuit, and the total field across the diode is the sum of the dc and ac fields. This total field causes breakdown at the n^+-p junction during the positive half of the ac voltage cycle if the field is above the breakdown voltage, and the carrier current (or the hole current in this case) $I_0(t)$ generated at the n^+-p junction by the avalanche multiplication grows exponentially with time while the field is above the critical value. During the negative half cycle, when the field is below the breakdown voltage, the carrier current $I_0(t)$ decays exponentially to a small steady-state value. The carrier current $I_0(t)$ is the current at the junction only and is in the form of a pulse of very short duration as shown in Fig. 8-1-3(d). Therefore the carrier current $I_0(t)$ reaches its maximum in the middle of the ac voltage cycle, or one-quarter of a cycle later than the voltage. Under the influence of the electric field the generated holes are injected into the space-charge region toward the negative terminal. As the injected holes traverse the drift space, they induce a current $I_e(t)$ in the external circuit as shown in Fig. 8-1-3(d).

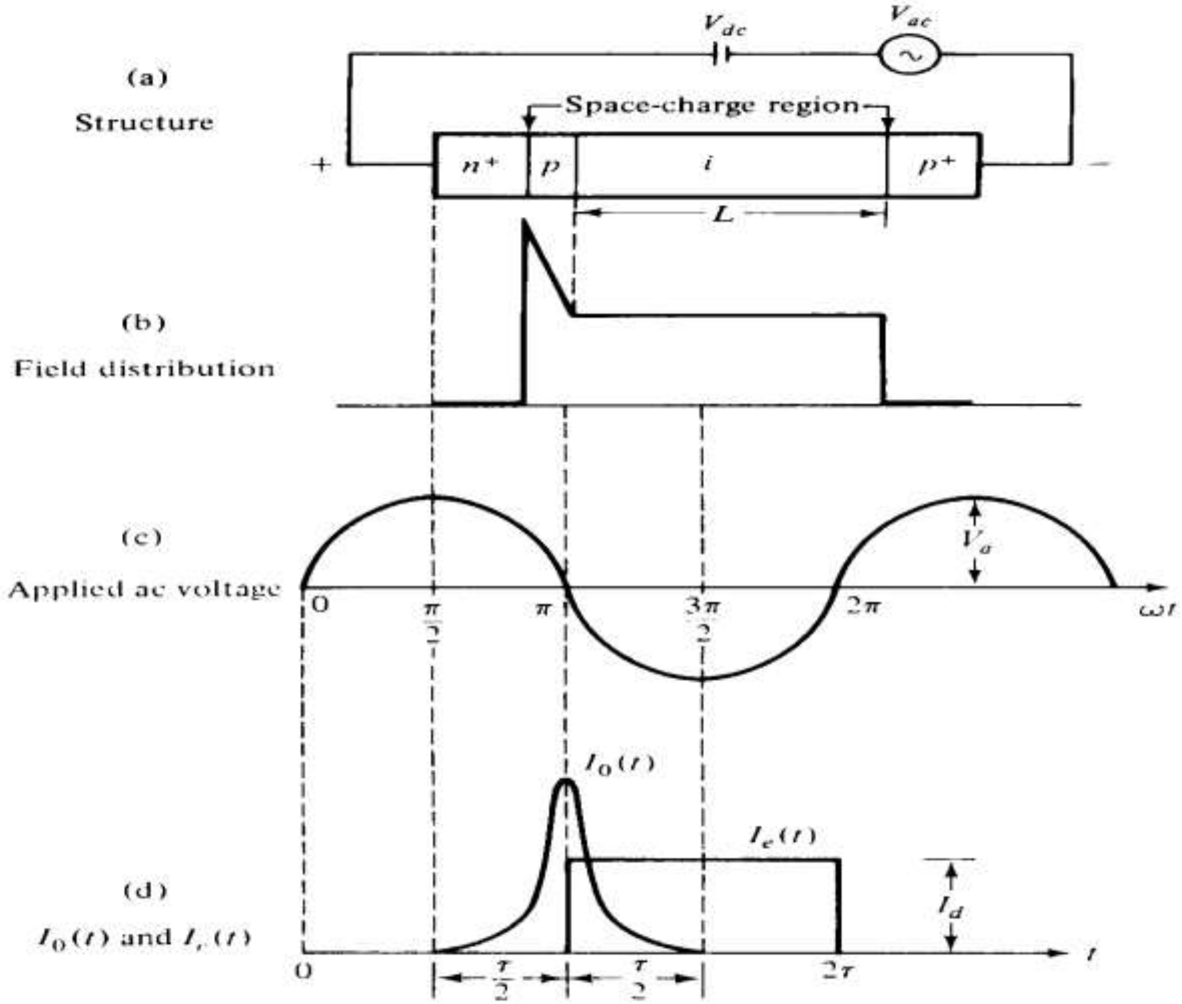

Figure 8-1-3 Field, voltage, and currents in Read diode. (*After Read [1];*

It can be seen that the induced current $I_e(t)$ in the external circuit is equal to the average current in the space-charge region. When the pulse of hole current $I_0(t)$ is suddenly generated at the n^+-p junction, a constant current $I_e(t)$ starts flowing in the external circuit and continues to flow during the time τ in which the holes are moving across the space-charge region. Thus, on the average, the external current $I_e(t)$ because of the moving holes is delayed by $\tau/2$ or 90° relative to the pulsed carrier current $I_0(t)$ generated at the n^+-p junction. Since the carrier $I_0(t)$ is delayed by one-quarter of a cycle or 90° relative to the ac voltage, the external current $I_e(t)$ is then delayed by 180° relative to the voltage as shown in Fig. 8-1-3(d). Therefore the cavity should be tuned to give a resonant frequency as

$$2\pi f = \frac{\pi}{\tau}$$

Then

$$f = \frac{1}{2\tau} = \frac{v_d}{2L} \qquad (8\text{-}1\text{-}4)$$

Since the applied ac voltage and the external current $I_e(t)$ are out of phase by 180°

IMPATT DIODES

8-2-1 Physical Structures

A theoretical Read diode made of an n^+-p-i-p^+ or p^+-n-i-n^+ structure has been analyzed. Its basic physical mechanism is the interaction of the impact ionization avalanche and the transit time of charge carriers. Hence the Read-type diodes are called IMPATT diodes. These diodes exhibit a differential negative resistance by two effects:

1. The impact ionization avalanche effect, which causes the carrier current $I_0(t)$ and the ac voltage to be out of phase by 90°
2. The transit-time effect, which further delays the external current $I_e(t)$ relative to the ac voltage by 90°

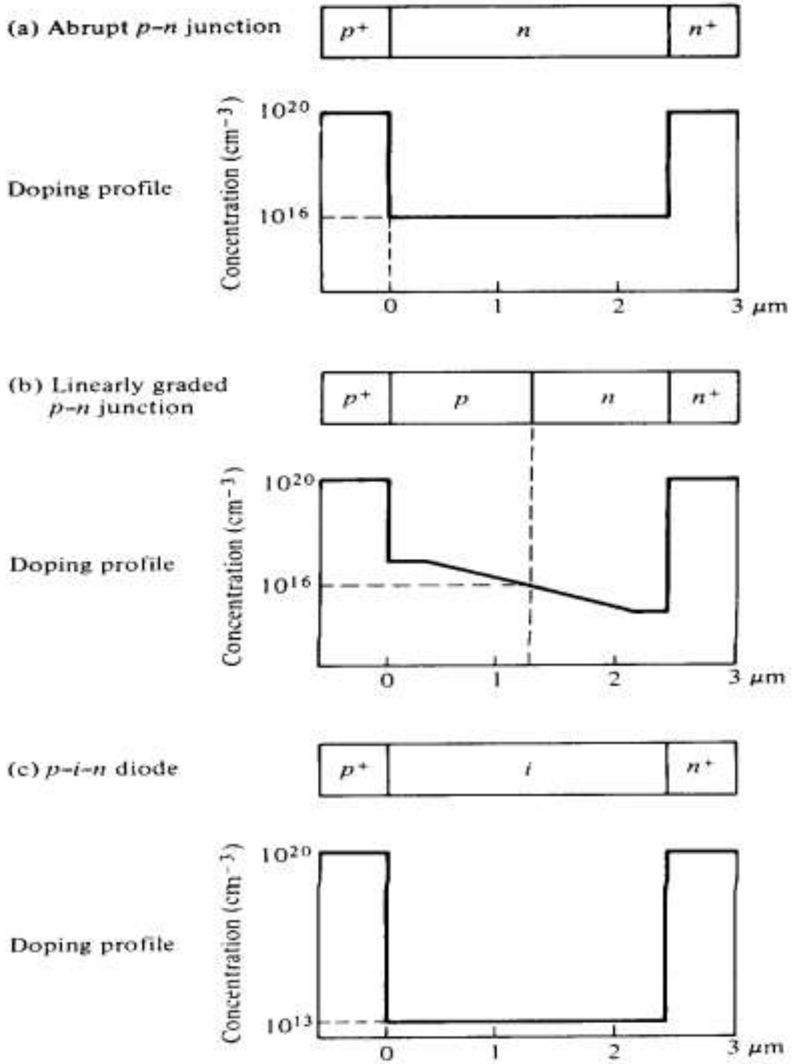

Figure 8-2-1 Three typical silicon IMPATT diodes. (*After R. L. Johnston e al. [4]; reprinted by permission of the Bell System, AT&T Co.*)

Moreover, θ is the transit angle, given by

$$\theta = \omega\tau = \omega\frac{L}{v_d} \tag{8-2-2}$$

and ω_r is the avalanche resonant frequency, defined by

$$\omega_r \equiv \left(\frac{2\alpha' v_d I_0}{\epsilon_s A}\right)^{1/2} \tag{8-2-3}$$

In Eq. (8-2-3) the quantity α' is the derivative of the ionization coefficient with respect to the electric field. This coefficient, the number of ionizations per centimeter produced by a single carrier, is a sharply increasing function of the electric field.

Power Output and Efficiency

For a uniform avalanche, the maximum voltage that can be applied across the diode is given by

$$V_m = E_m L \tag{8-2-5}$$

where L is the depletion length and E_m is the maximum electric field.

The maximum current is given by

$$I_m = J_m A = \sigma E_m A = \frac{\epsilon_s}{\tau} E_m A = \frac{v_d \epsilon_s E_m A}{L} \tag{8-2-6}$$

The capacitance across the space-charge region is defined as

$$C = \frac{\epsilon_s A}{L} \tag{8-2-8}$$

Substitution of Eq. (8-2-8) in Eq. (8-2-7) and application of $2\pi f \tau = 1$ yield

$$P_m f^2 = \frac{E_m^2 v_d^2}{4\pi^2 X_c} \tag{8-2-9}$$

The efficiency of the IMPATT diodes is given by

$$\eta = \frac{P_{ac}}{P_{dc}} = \left(\frac{V_a}{V_d}\right)\left(\frac{I_a}{I_d}\right)$$

An IMPATT diode has the following parameters:

Carrier drift velocity:	$v_d = 2 \times 10^7$ cm/s
Drift-region length:	$L = 6\ \mu$m
Maximum operating voltage:	$V_{0max} = 100$ V
Maximum operating current:	$I_{0max} = 200$ mA
Efficiency:	$\eta = 15\%$
Breakdown voltage:	$V_{bd} = 90$ V

Compute: (**a**) the maximum CW output power in watts; (**b**) the resonant frequency in gigahertz.

Solution

a. From Eq. (8-2-10) the CW output power is

$$P = \eta P_{dc} = 0.15 \times 100 \times 0.2 = 3\text{W}$$

b. From Eq. (8-2-4) the resonant frequency is

$$f = \frac{v_d}{2L} = \frac{2 \times 10^5}{2 \times 6 \times 10^{-6}} = 16.67 \text{ GHz}$$

TRAPATT DIODES

The abbreviation TRAPATT stands for *trapped plasma avalanche triggered transit* mode, a mode first reported by Prager et al. [7]. It is a high-efficiency microwave generator capable of operating from several hundred megahertz to several gigahertz.

Principles of Operation

The basic operation of the oscillator is a semiconductor *p-n* junction diode reverse-biased to current densities well in excess of those encountered in normal avalanche operation. Approximate analytic solutions for the TRAPATT mode in p^+-n-n^+ diodes

Approximate analytic solutions for the TRAPATT mode in p^+-n-n^+ diodes ses have shown that a high-field avalanche zone propagates through the diode and fills the depletion layer with a dense plasma of electrons and holes that become trapped in the low-field region behind the zone. A typical voltage waveform for the TRAPATT mode of an avalanche p^+-n-n^+ diode operating with an assumed square-wave current drive is shown in Fig. 8-3-1. At point A the electric field is uniform throughout the sample and its magnitude is large but less than the value required for avalanche breakdown. The current density is expressed by

$$J = \epsilon_s \frac{dE}{dt} \qquad (8\text{-}3\text{-}1)$$

where ϵ_s is the semiconductor dielectric permittivity of the diode.

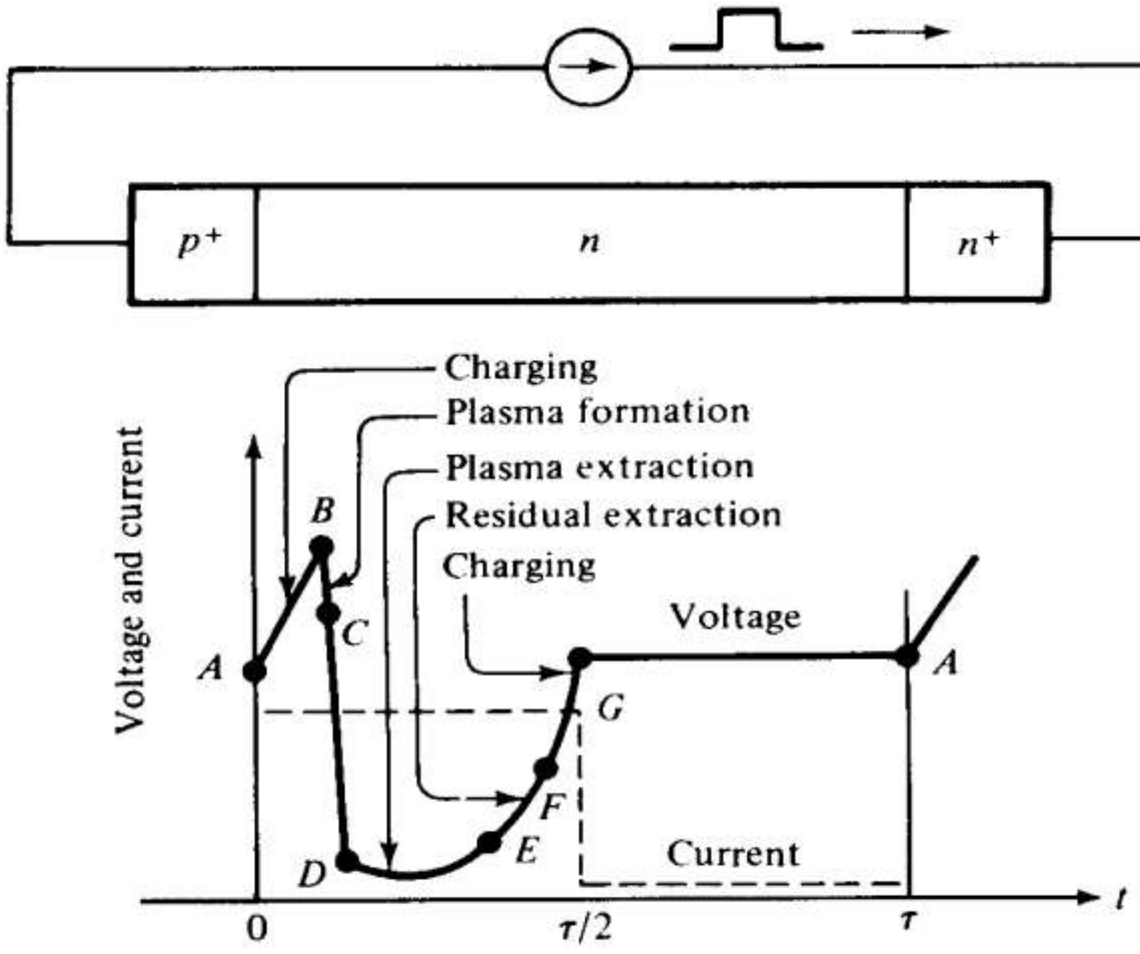

Figure 8-3-1 Voltage and current waveforms for TRAPATT diode. (*After A. S. Clorfeine et al. [8]; reprinted by*

At the instant of time at point *A*, the diode current is turned on. Since the only charge carriers present are those caused by the thermal generation, the diode initially charges up like a linear capacitor, driving the magnitude of the electric field above the breakdown voltage. When a sufficient number of carriers is generated, the particle current exceeds the external current and the electric field is depressed throughout the depletion region, causing the voltage to decrease. This portion of the cycle is shown by the curve from point *B* to point *C*. During this time interval the electric field is sufficiently large for the avalanche to continue, and a dense plasma of electrons and holes is created. As some of the electrons and holes drift out of the ends of the depletion layer, the field is further depressed and "traps" the remaining plasma. The voltage decreases to point *D*. A long time is required to remove the plasma because the total plasma charge is large compared to the charge per unit time

Thus the TRAPATT mode can operate at comparatively low frequencies, since the discharge time of the plasma—that is, the rate Q/I of its charge to its current—can be considerably greater than the nominal transit time τ_s of the diode at high field. Therefore the TRAPATT mode is still a transit-time mode in the real sense that the time delay of carriers in transit (that is, the time between injection and collection) is utilized to obtain a current phase shift favorable for oscillation.

Power Output and Efficiency

RF power is delivered by the diode to an external load when the diode is placed in a proper circuit with a load. The main function of this circuit is to match the diode effective negative resistance to the load at the output frequency while reactively terminating (trapping) frequencies above the oscillation frequency in order to ensure TRAPATT operation. To date, the highest pulse power of 1.2 kW has been obtained at 1.1 GHz (five diodes in series) [10], and the highest efficiency of 75% has been achieved at 0.6 GHz

UNIT-IV

Waveguide Components-I: Waveguide Multiport Junctions –E plane and H plane Tees, Magic Tee, Hybrid Ring; Directional Couplers –2 Hole, Bethe Hole types. Scattering Matrix–Significance, Formulation and Properties. S Matrix Calculations for E plane and H plane Tees, Magic Tee, Directional Coupler.

A waveguide Tee is formed when three waveguides are interconnected in the form of English alphabet T and thus waveguide tee is 3-port junction. The waveguide tees are used to connects a branch or section of waveguide in series or parallel with the main waveguide transmission line either for splitting or combining power in a waveguide system.

Types of Waveguide Tee Junctions:

• There are a number of different types of waveguide junction.

The major types are listed below:

1. H-type T Junction
2. E-Type T Junction
3. Magic T waveguide junction
4. Hybrid Ring Waveguide Junction

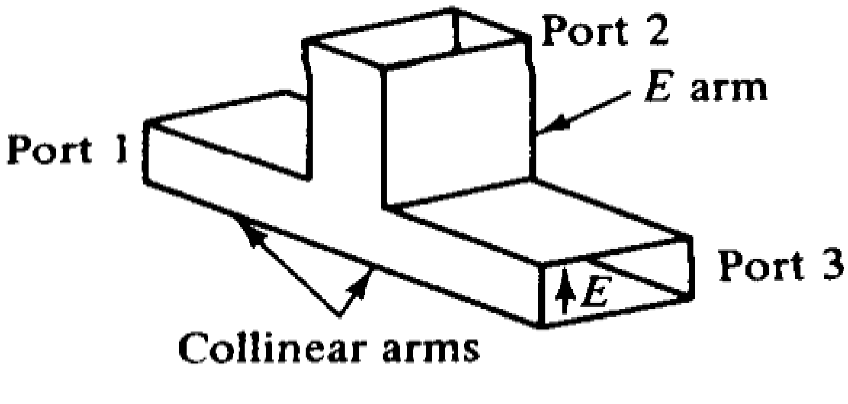

(a) E-plane tee

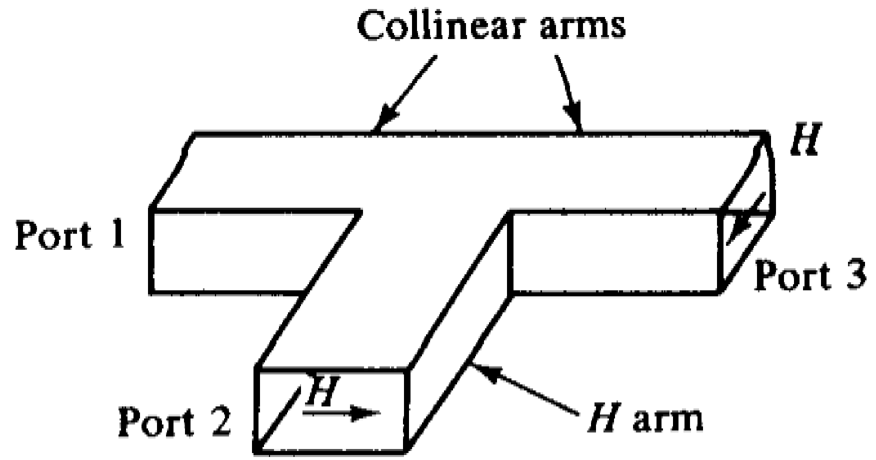

(b) H-plane tee

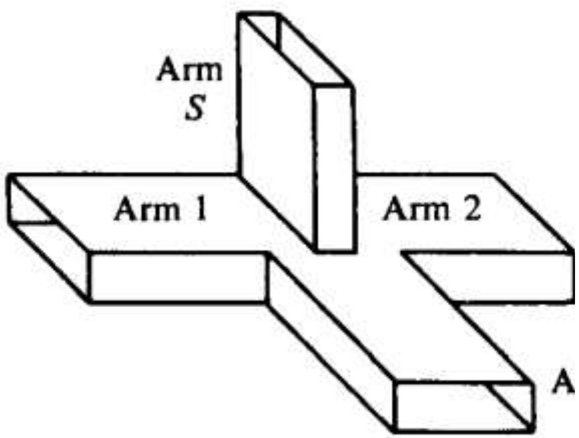

(c) Magic tee

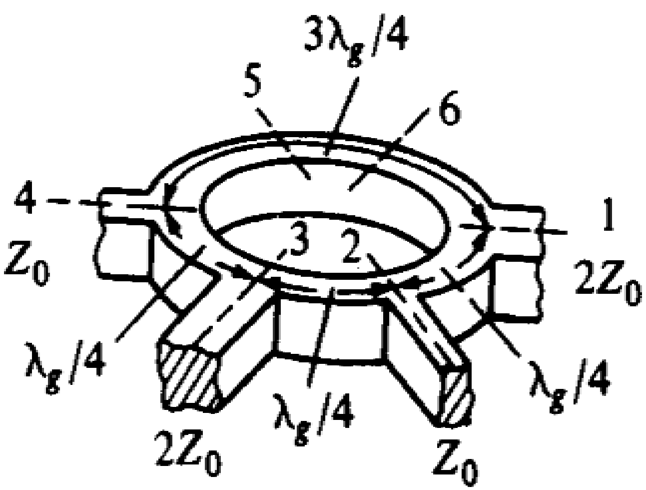

(d) Hybrid ring

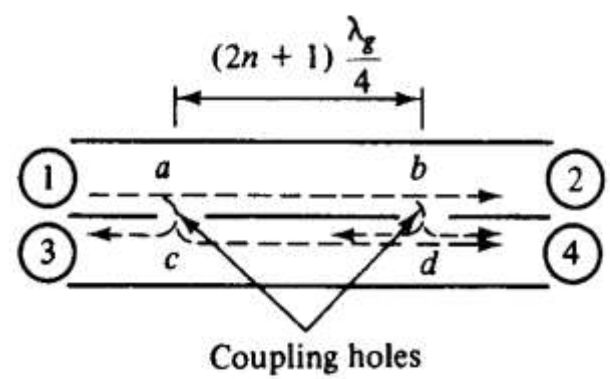

(e) Directional coupler

Microwave circuits consists of several microwave devices connected in some way to achieve the desired transmission of a microwave signal

The interconnection of two or more microwave devices may be regarded as a **microwave junction**. Waveguide Tees as the E-plane tee, H-plane tee, Magic tee, hybrid ring tee(rat-race circuit), directional coupler and the circulator

E-plane Tee(series tee):

An E-plane tee is a waveguide tee in which the axis of its side arm is parallel to the E field of the main guide . if the collinear arms are symmetric about the side arm. If the E-plane tee is perfectly matched with the aid of screw tuners at the junction, the diagonal components of the scattering matrix are zero because there will be no reflection . When the waves are fed into side arm, the waves appearing at port 1 and port 2 of the collinear arm will be in opposite phase and in same magnitude.

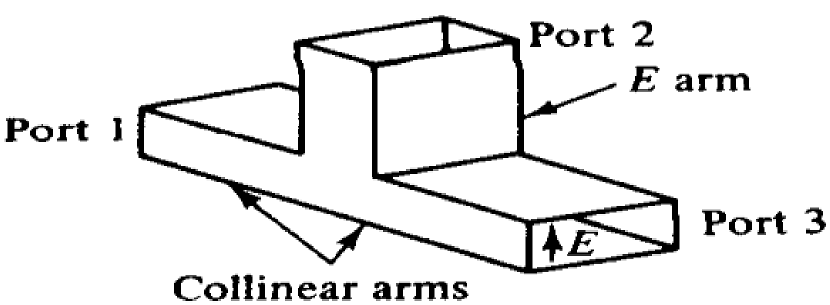

(a) E-plane tee

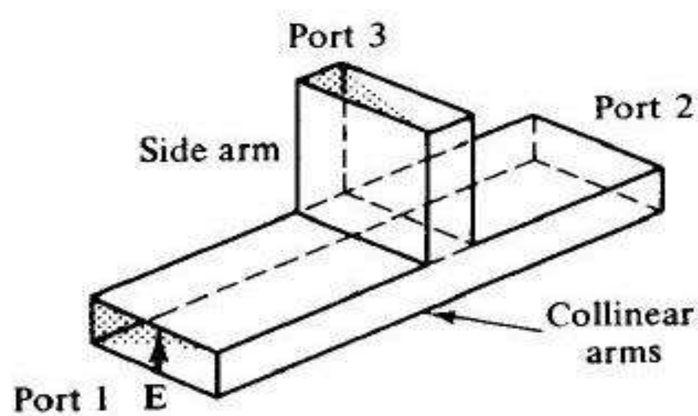

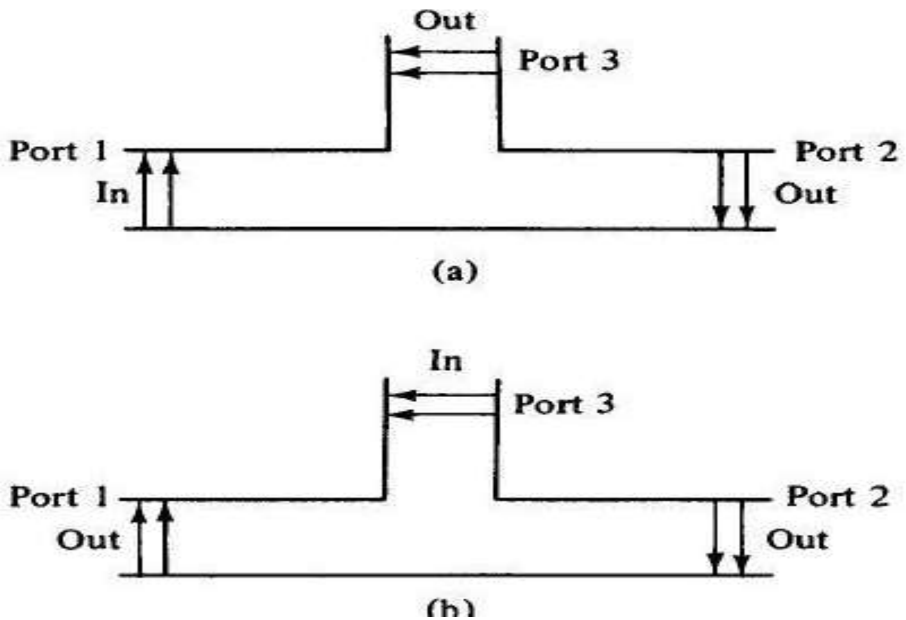

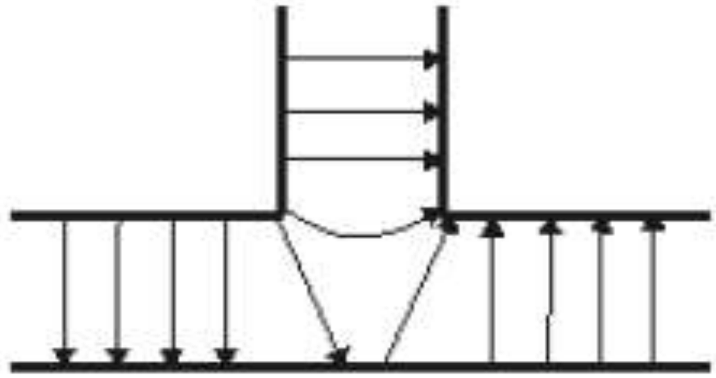

Waveguide E-type junction E fields

It is called an E-type T junction because the junction arm, i.e. the top of the "T" extends from the main waveguide in the same direction as the E field.

• It is characterized by the fact that the outputs of this form of waveguide junction are 180° out of phase with each other.

The basic construction of the waveguide junction shows the three port waveguide device. • Although it may be assumed that the input is the single port and the two outputs are those on the top section of the "T", actually any port can be used as the input, the other two being outputs.

• WORKNG:– To see how the waveguide junction operates, and how the 180° phase shift occurs, it is necessary to look at the electric field. The magnetic field is omitted from the diagram for simplicity.

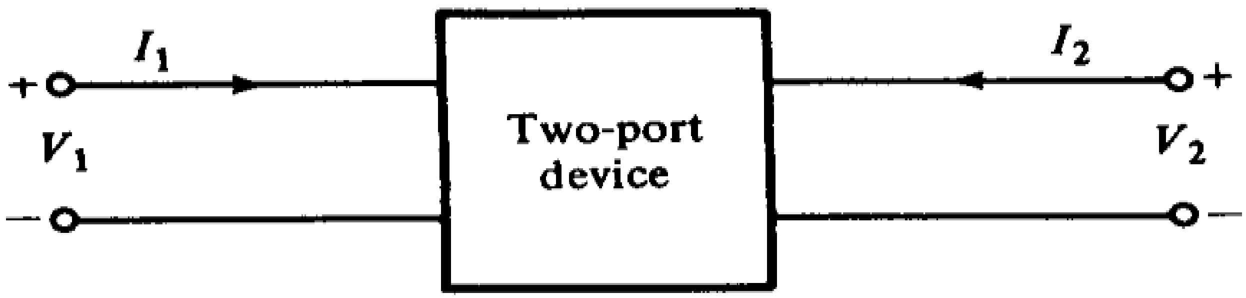

Two-port network.

H parameters: $\begin{bmatrix} V_1 \\ I_2 \end{bmatrix} = \begin{bmatrix} h_{11} & h_{12} \\ h_{21} & h_{22} \end{bmatrix} \begin{bmatrix} I_1 \\ V_2 \end{bmatrix}$

$$V_1 = h_{11}I_1 + h_{12}V_2$$
$$I_2 = h_{21}I_1 + h_{22}V_2$$

Z parameters: $\begin{bmatrix} V_1 \\ V_2 \end{bmatrix} = \begin{bmatrix} z_{11} & z_{12} \\ z_{21} & z_{22} \end{bmatrix} \begin{bmatrix} I_1 \\ I_2 \end{bmatrix}$

$$V_1 = z_{11}I_1 + z_{12}I_2$$
$$V_2 = z_{21}I_1 + z_{22}I_2$$

ABCD parameters: $\begin{bmatrix} V_1 \\ I_1 \end{bmatrix} = \begin{bmatrix} A & B \\ C & D \end{bmatrix} \begin{bmatrix} V_2 \\ -I_2 \end{bmatrix}$

$$V_1 = AV_2 - BI_2$$
$$I_1 = CV_2 - DI_2$$

All these network parameters relate total voltages and total currents at each of the two ports

If the frequencies are in the microwave range, however

The H,Y and Z parameters cannot be measured
for the following reasons:

1. Equipment is not readily available to measure total voltage and total current at the ports of the network.
2. Short and Open circuits are difficult to achieve over a broad band of frequencies.

3. Active devices, such as power transistors and tunnel diodes, frequently will not have stability for a short or open circuit.

New method of characterization is needed:
The logical variables to use at the microwave frequencies are travelling waves rather than total voltages and total currents. These are the S parameters,

S - PARAMETERS : Scattering matrix parameters:

Definition: The scattering matrix of an m-port junction is a square matrix of a set of elements which relate incident and reflected waves at the port of the junction. The diagonal elements of the s-matrix represents reflection coefficients and off diagonal elements represent transmission coefficients.

Characteristics of s-matrix:

1. It describes any passive microwave component.
2. It exists for linear passive and time invariant networks.
3. It gives complete information on reflection and transmission coefficients.

A scattering matrix represents the relationship between the parameters an's(incident wave amplitude) , bn's(reflected wave amplitude).

Properties of S-matrix

1. Scattering matrix is always a square matrix of order n x n.

2. $[S][S]^* = [I]$.
   i.e. S matrix is unit matrix,
   I=identity matrix of same order as that of S,
   S^* = Complex conjugate.

3. Scattering matrix posses property of symmetry,
   i.e. $S_{ij} = S_{ji}$

4. $\sum_{i=1}^{n} S_{ij} S_{ik}^* = 0, for\ j \neq k, \quad j,k = 1,2,3, \ldots \ldots n.$
   i.e. sum of products between any row and column with complex conjugate of any other row or column is zero.

5. If any port, moved away from the junction by a distance of βd , then the coefficients of S_{ij} involving that particular port will be multiplied by the factor $e^{-j\beta d}$.

Tee Junction

A waveguide or coaxial-line junction with three independent ports Matrix of third order, containing nine elements, six of which should be independent. The characteristics of a three port junction can be explained by three theorems of the tee junction. These theorems are derived from the equivalent Circuit representation of the tee junction

1. A short circuit may always be placed in one of the arms of a three-port junction in such a way that no power can be transferred through the other two arms.

2. If the junction is symmetric about one of its arms, a short circuit can always be placed in that arm so that no reflections occur in power transmission between the other two arms.(i.e the arms present matched impedances.)

3. It is impossible for a general three-port junction of arbitrary symmetry to present matched impedances at all three arms.

E-plane Tee

Series Tee

A waveguide tee in which the **axis** of its side arm is **parallel to the E-field** of the main guide

If the collinear arms are symmetric about the side arm, there are two different transmission characteristics

Two way Transmission of E-plane tee

a) i/p-main arm

b) i/p-side arm

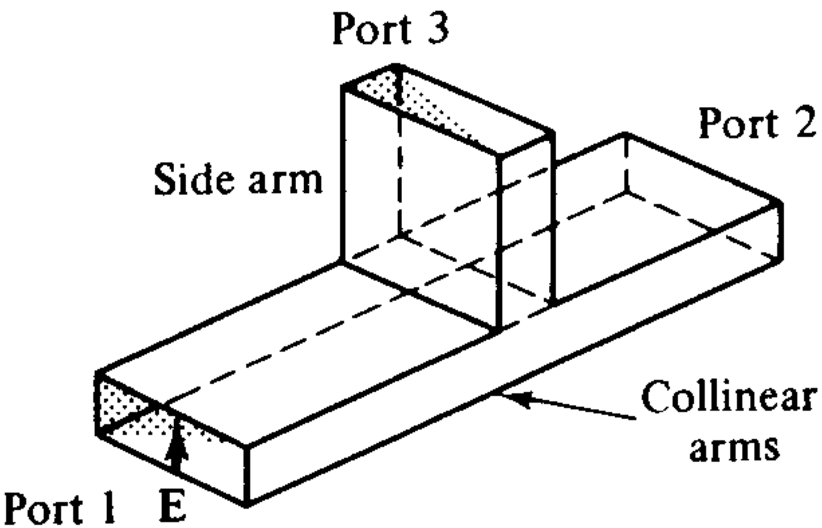

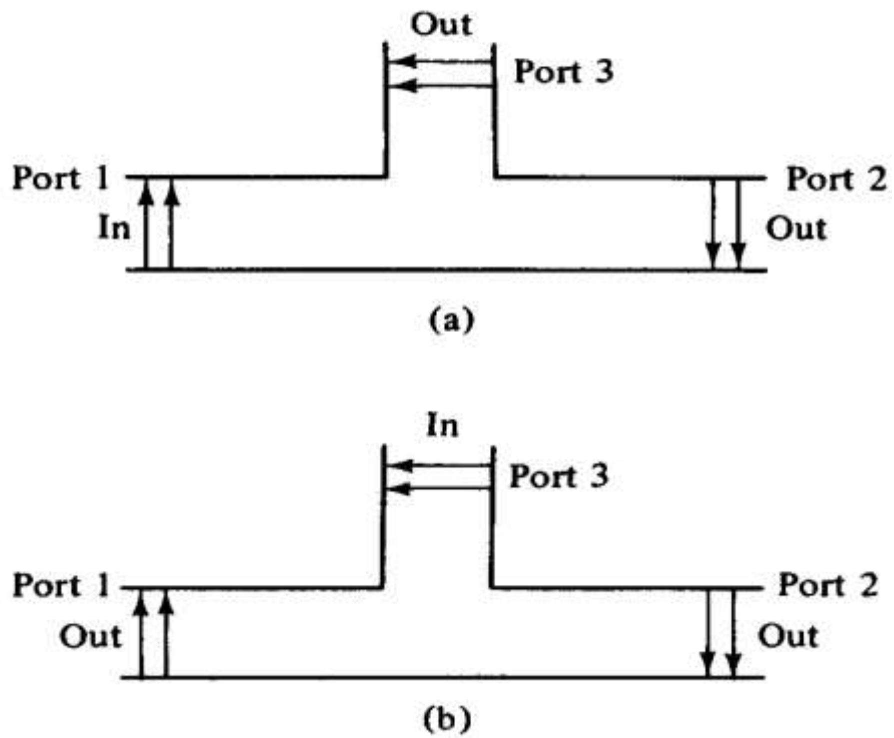

Scattering matrix for E plane Tee:

In E-plane tee junction, power in port 3 is the difference of the two signals entering at 1 and 2 simultaneously. It is a three port junction and its S MATRIX is given by

1. The diagonal components of the S matrix, S11, S22 and S33 are zero because there will be no reflection.
2. When the waves are fed into the side arm (port 3), the waves appearing at port1 and port2 of the collinear arm will be in the opposite phase and in the same magnitude.

Therefore, S13 = -S23 (both have opposite signs) -ve sign indicates that S13 and S23 have opposite signs

An E-Plane Tee junction is formed by attaching a simple waveguide to the broader dimension of a rectangular waveguide, which already has two ports. The arms of rectangular waveguides make two ports called **collinear ports** i.e., Port1 and Port2, while the new one, Port3 is called as Side arm or **E-arm**. This E-plane Tee is also called as **Series Tee**.

As the axis of the side arm is parallel to the electric field, this junction is called E-Plane Tee junction. This is also called as **Voltage** or **Series junction**. The ports 1 and 2 are 180° out of phase with each other. The cross-sectional details of E-plane tee can be understood by the following figure.

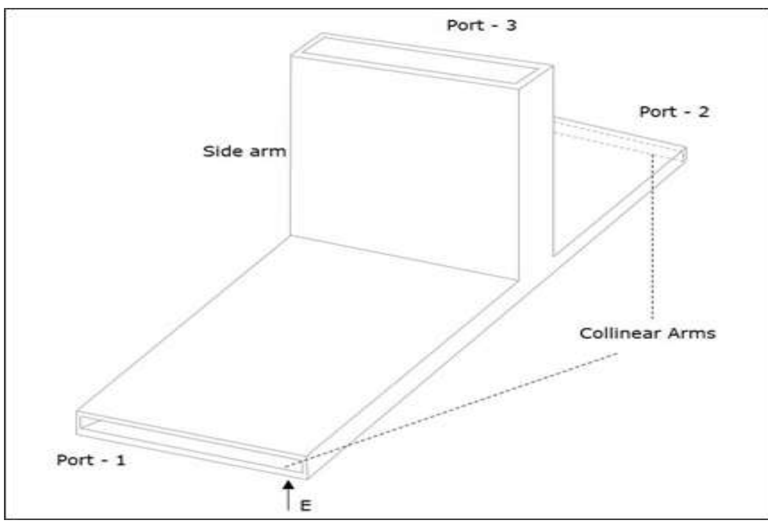

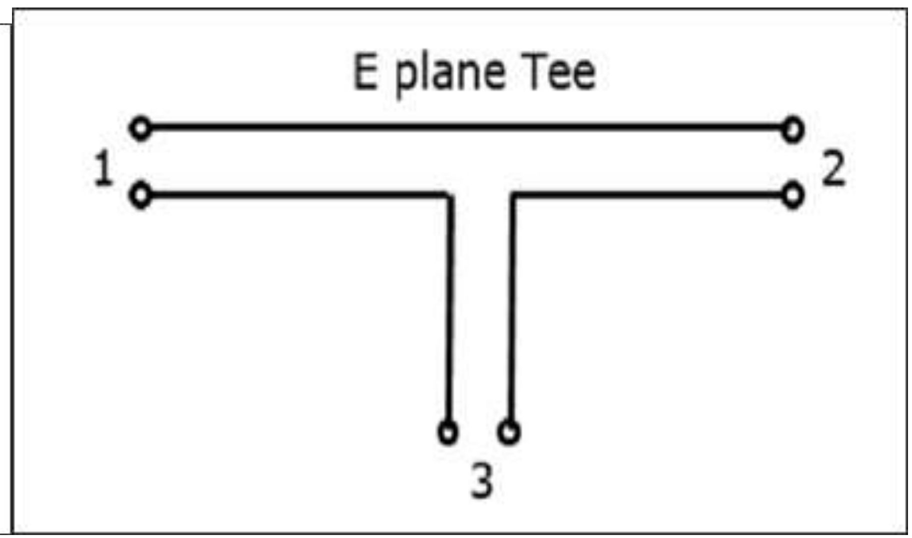

Properties of E-Plane Tee

The properties of E-Plane Tee can be defined by its $[S]_{3x3}$ matrix.

It is a 3×3 matrix as there are 3 possible inputs and 3 possible outputs.

$$[S] = \begin{bmatrix} S_{11} & S_{12} & S_{13} \\ S_{21} & S_{22} & S_{23} \\ S_{31} & S_{32} & S_{33} \end{bmatrix} \quad \text{........ Equation 1}$$

Scattering coefficients S_{13} and S_{23} are out of phase by 180° with an input at port 3.

$$S_{23} = -S_{13} \quad \text{........ Equation 2}$$

The port is perfectly matched to the junction.

$$S_{33} = 0 \quad \text{........ Equation 3}$$

From the symmetric property,

$$S_{ij} = S_{ji}$$

$$S_{12} = S_{21} \;\; S_{23} = S_{32} \;\; S_{13} = S_{31} \quad \text{........ Equation 4}$$

Considering equations 3 & 4, the $[S]$ matrix can be written as,

Considering equations 3 & 4, the $[S]$ matrix can be written as,

$$[S] = \begin{bmatrix} S_{11} & S_{12} & S_{13} \\ S_{12} & S_{22} & -S_{13} \\ S_{13} & -S_{13} & 0 \end{bmatrix} \quad \text{........ Equation 5}$$

We can say that we have four unknowns, considering the symmetry property.

From the Unitary property

$$[S][S]* = [I]$$

$$\begin{bmatrix} S_{11} & S_{12} & S_{13} \\ S_{12} & S_{22} & -S_{13} \\ S_{13} & -S_{13} & 0 \end{bmatrix} \begin{bmatrix} S_{11}^* & S_{12}^* & S_{13}^* \\ S_{12}^* & S_{22}^* & -S_{13}^* \\ S_{13}^* & -S_{13}^* & 0 \end{bmatrix} = \begin{bmatrix} 1 & 0 & 0 \\ 0 & 1 & 0 \\ 0 & 0 & 1 \end{bmatrix}$$

Multiplying we get,

$$Noting R as row and C as column$$

$$R_1C_1 : S_{11}S_{11}^* + S_{12}S_{12}^* + S_{13}S_{13}^* = 1$$

$$|S_{11}|^2 + |S_{11}|^2 + |S_{11}|^2 = 1 \quad \text{........ Equation 6}$$

$$|S_{11}|^2 + |S_{11}|^2 + |S_{11}|^2 = 1$$ .... **Equation 6**

|S11| ² + |S12| ² + |S13| ²

$$R_2C_2 : |S_{12}|^2 + |S_{22}|^2 + |S_{13}|^2 = 1$$ .... **Equation 7**

$$R_3C_3 : |S_{13}|^2 + |S_{13}|^2 = 1$$ .... **Equation 8**

$$R_3C_1 : S_{13}S_{11}^* - S_{13}S_{12}^* = 1$$ .... **Equation 9**

Equating the equations 6 & 7, we get

$$S_{11} = S_{22}$$ .... **Equation 10**

From Equation 8,

$$2|S_{13}|^2 \quad or \quad S_{13} = \frac{1}{\sqrt{2}}$$ .... **Equation 11**

From Equation 9,

$$S_{13}\left(S_{11}^* - S_{12}^*\right)$$

Or $S_{11} = S_{12} = S_{22}$ .... **Equation 12**

Using the equations 10, 11, and 12 in the equation 6,

$$|S_{11}|^2 + |S_{11}|^2 + \tfrac{1}{2} = 1$$

$$2|S_{11}|^2 = \tfrac{1}{2}$$

Or $S_{11} = \frac{1}{2}$ .... **Equation 13**

Substituting the values from the above equations in $[S]$ matrix,

We get,

$$[S] = \begin{bmatrix} \frac{1}{2} & \frac{1}{2} & \frac{1}{\sqrt{2}} \\ \frac{1}{2} & \frac{1}{2} & -\frac{1}{\sqrt{2}} \\ \frac{1}{\sqrt{2}} & -\frac{1}{\sqrt{2}} & 0 \end{bmatrix}$$

We know that $[b] = [S][a]$

$$\begin{bmatrix} b_1 \\ b_2 \\ b_3 \end{bmatrix} = \begin{bmatrix} \frac{1}{2} & \frac{1}{2} & \frac{1}{\sqrt{2}} \\ \frac{1}{2} & \frac{1}{2} & -\frac{1}{\sqrt{2}} \\ \frac{1}{\sqrt{2}} & -\frac{1}{\sqrt{2}} & 0 \end{bmatrix} \begin{bmatrix} a_1 \\ a_2 \\ a_3 \end{bmatrix}$$

Where b is output port and a is input port.

$$\therefore \quad \begin{bmatrix} b_1 \\ b_2 \\ b_3 \end{bmatrix} = \begin{bmatrix} \frac{1}{2} & \frac{1}{2} & \frac{1}{\sqrt{2}} \\ \frac{1}{2} & \frac{1}{2} & -\frac{1}{\sqrt{2}} \\ \frac{1}{\sqrt{2}} & -\frac{1}{\sqrt{2}} & 0 \end{bmatrix} \begin{bmatrix} a_1 \\ a_2 \\ a_3 \end{bmatrix} \quad \ldots(2.3.20)$$

$$\therefore \quad b_1 = \frac{1}{2} a_1 + \frac{1}{2} a_2 + \frac{1}{\sqrt{2}} a_3 \quad \ldots(2.3.21)$$

$$b_2 = \frac{1}{2} a_1 + \frac{1}{2} a_2 - \frac{1}{\sqrt{2}} a_3 \quad \ldots(2.3.22)$$

$$b_3 = \frac{1}{\sqrt{2}} a_1 - \frac{1}{\sqrt{2}} a_2 \qquad \text{...(2.3.23)}$$

There are three cases arises in E-plane tee :

Case 1 :

- When an input at port-3 equally divides between port-1 and port-2 but introduces a phase shift of 180° between two output. Hence E-plane tee acts as a 3 dB splitter.

$$a_1 = a_2 = 0, \quad a_3 \neq 0$$

From equation (2.3.21) to (2.3.23), output is :

$$b_1 = \frac{1}{\sqrt{2}} a_3, \quad b_2 = \frac{-1}{\sqrt{2}} a_3, \quad b_3 = 0$$

Case 2 :

Equal inputs at port-1 and 2 result in no output.

$$a_1 = a_2 = a$$

$$a_3 = 0$$

From equation (2.3.21) to (2.3.23),

$$b_1 = \frac{a}{2} + \frac{a}{2}$$

$$b_2 = \frac{a}{2} + \frac{a}{2}$$

$$b_3 = \frac{1}{\sqrt{2}} a - \frac{1}{\sqrt{2}} a = 0 \quad \text{i.e. } b_3 = 0$$

Case 3 :

- When input at port-1 is non zero and at ports-2 and 3, it is zero, then output is

$a_1 \neq 0, \ a_2 = 0, a_3 = 0$

$$b_1 = \frac{a_1}{2}$$

$$b_2 = \frac{a_1}{2}$$

H-plane Tee waveguide junction

This type of waveguide junction is called an H-plane Tee junction because the long axis of the main top of the "T" arm is parallel to the plane of the magnetic lines of force in the waveguide.

- It is characterized by the fact that the two outputs from the top of the "T" section in the waveguide are in phase with each other.

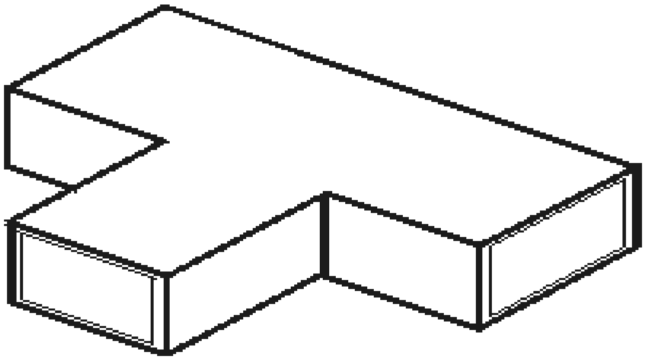

Waveguide H-type junction

To see how the waveguide junction operates, the diagram below shows the electric field lines.

The electric field lines are shown using the traditional notation - a cross indicates a line coming out of the screen, whereas a dot indicates an electric field line going into the screen.

- It can be seen from the diagram that the signals at all ports are in phase.
- Although it is easiest to consider signals entering from the lower section of the "T", any port can actually be used the phase relationships are preserved whatever entry port is used.

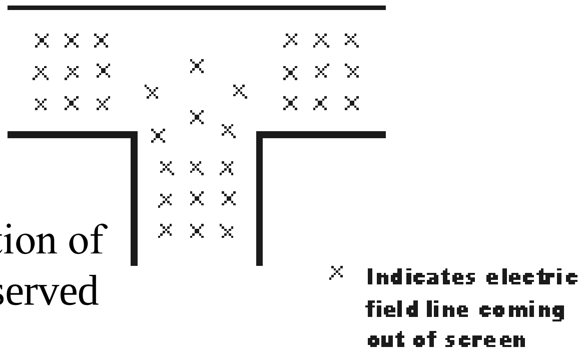

Waveguide H-type junction electric fields

An H-Plane Tee junction is formed by attaching a simple waveguide to a rectangular waveguide which already has two ports. The arms of rectangular waveguides make two ports called **collinear ports** i.e., Port1 and Port2, while the new one, Port3 is called as Side arm or **H-arm**. This H-plane Tee is also called as **Shunt Tee**.

As the axis of the side arm is parallel to the magnetic field, this junction is called H-Plane Tee junction. This is also called as **Current junction**, as the magnetic field divides itself into arms.

The cross-sectional details of H-plane tee can be understood by the following figure.

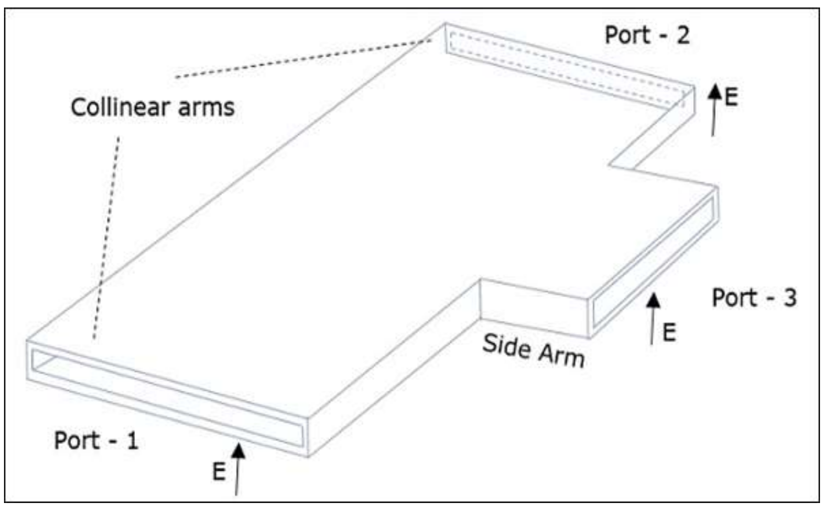

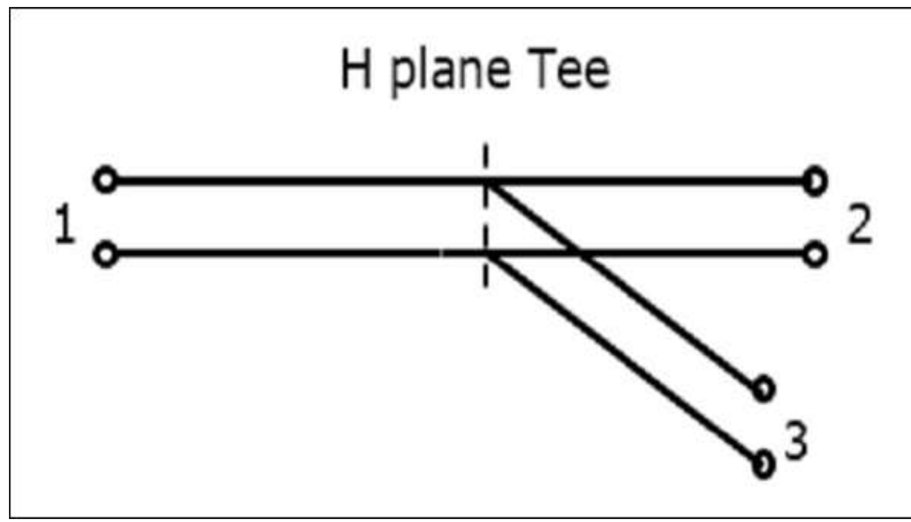

Properties of H-Plane Tee

The properties of H-Plane Tee can be defined by its $[S]_{3\times3}$ matrix.

It is a 3×3 matrix as there are 3 possible inputs and 3 possible outputs.

$$[S] = \begin{bmatrix} S_{11} & S_{12} & S_{13} \\ S_{21} & S_{22} & S_{23} \\ S_{31} & S_{32} & S_{33} \end{bmatrix} \quad \text{........ Equation 1}$$

Scattering coefficients S_{13} and S_{23} are equal here as the junction is symmetrical in plane.

From the symmetric property,

$$S_{ij} = S_{ji}$$

$$S_{12} = S_{21} \;\; S_{23} = S_{32} = S_{13} \;\; S_{13} = S_{31}$$

The port is perfectly matched

$$S_{33} = 0$$

Now, the $[S]$ matrix can be written as,

Now, the $[S]$ matrix can be written as,

$$[S] = \begin{bmatrix} S_{11} & S_{12} & S_{13} \\ S_{12} & S_{22} & S_{13} \\ S_{13} & S_{13} & 0 \end{bmatrix} \quad \text{........ Equation 2}$$

We can say that we have four unknowns, considering the symmetry property.

From the Unitary property

$$[S][S]* = [I]$$

$$\begin{bmatrix} S_{11} & S_{12} & S_{13} \\ S_{12} & S_{22} & S_{13} \\ S_{13} & S_{13} & 0 \end{bmatrix} \begin{bmatrix} S_{11}^* & S_{12}^* & S_{13}^* \\ S_{12}^* & S_{22}^* & S_{13}^* \\ S_{13}^* & S_{13}^* & 0 \end{bmatrix} = \begin{bmatrix} 1 & 0 & 0 \\ 0 & 1 & 0 \\ 0 & 0 & 1 \end{bmatrix}$$

Multiplying we get,

$$NotingRasrowandCascolumn$$

$$R_1C_1 : S_{11}S_{11}^* + S_{12}S_{12}^* + S_{13}S_{13}^* = 1$$

$$|S_{11}|^2 + |S_{12}|^2 + |S_{13}|^2 = 1 \quad \text{........ Equation 3}$$

$$R_2C_2 : |S_{12}|^2 + |S_{22}|^2 + |S_{13}|^2 = 1$$ .... **Equation 4**

$$R_3C_3 : |S_{13}|^2 + |S_{13}|^2 = 1$$ .... **Equation 5**

$$R_3C_1 : S_{13}S_{11}^* - S_{13}S_{12}^* = 0$$ .... **Equation 6**

$$2|S_{13}|^2 = 1 \quad or \quad S_{13} = \frac{1}{\sqrt{2}}$$ .... **Equation 7**

$$|S_{11}|^2 = |S_{22}|^2$$

$$S_{11} = S_{22}$$ .... **Equation 8**

From the Equation 6, $S_{13}\left(S_{11}^* + S_{12}^*\right) = 0$

Since, $S_{13} \neq 0, S_{11}^* + S_{12}^* = 0, \; or \; S_{11}^* = -S_{12}^*$

Or $S_{11} = -S_{12} \; or \; S_{12} = -S_{11}$ .... **Equation 9**

Using these in equation 3,

Since, $S_{13} \neq 0, S_{11}^* + S_{12}^* = 0, \; or \; S_{11}^* = -S_{12}^*$

$$|S_{11}|^2 + |S_{11}|^2 + \frac{1}{2} = 1 \quad or \quad 2|S_{11}|^2 = \frac{1}{2} \quad or \quad S_{11} = \frac{1}{2}$$ ..... **Equation 10**

From equation 8 and 9,

$$S_{12} = -\frac{1}{2}$$ .... **Equation 11**

$$S_{22} = \frac{1}{2}$$ .... **Equation 12**

Substituting for S_{13}, S_{11}, S_{12} and S_{22} from equation 7 and 10, 11 and 12 in equation 2,

We get,

$$[S] = \begin{bmatrix} \frac{1}{2} & -\frac{1}{2} & \frac{1}{\sqrt{2}} \\ -\frac{1}{2} & \frac{1}{2} & \frac{1}{\sqrt{2}} \\ \frac{1}{\sqrt{2}} & \frac{1}{\sqrt{2}} & 0 \end{bmatrix}$$

We know that $[b] = [s][a]$

$$\begin{bmatrix} b_1 \\ b_2 \\ b_3 \end{bmatrix} = \begin{bmatrix} \frac{1}{2} & -\frac{1}{2} & \frac{1}{\sqrt{2}} \\ -\frac{1}{2} & \frac{1}{2} & \frac{1}{\sqrt{2}} \\ \frac{1}{\sqrt{2}} & \frac{1}{\sqrt{2}} & 0 \end{bmatrix} \begin{bmatrix} a_1 \\ a_2 \\ a_3 \end{bmatrix}$$

This is the scattering matrix for H-Plane Tee, which explains its scattering properties

4. H-Plane TEE JUNCTION (Shunt Tee):

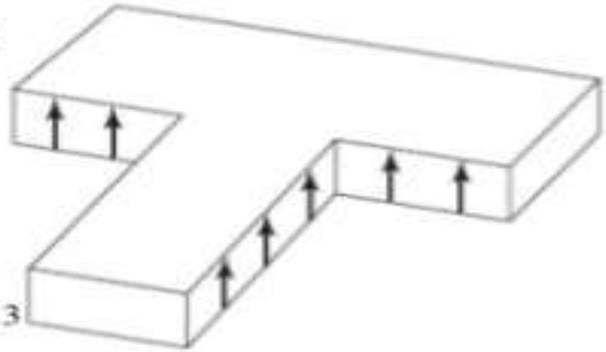

- H-plane Tee junction is formed by cutting a rectangular slot along the width of a main waveguide and attaching another waveguide – the side arm – called as H-arm as shown in above figure 3.
- The port 1 and 2 of the main waveguide are called as collinear ports and port 3 is the H-arm or side arm.
- H-Plane Tee is so-called because the axis of the side arm is parallel to the planes of the H-field of the main transmission line. As all three arms of H-plane tee lie in the plane of magnetic field, the magnetic field divides itself into the arms; this is thus a **current junction.**
- If the H-plane junction is completely symmetrical and waves enter through the side arm, the waves that leave through the mains arms are **equal in magnitude and phase.** Since the electric field is not bent as the wave passes through a H-plane junction, but merely divides between two arms; fields of same polarity approaching the junction from the two main arms produce components of electric field that add in side arm. The effective value of field leaving through the side arm is proportional to the phasor sum of entering fields.

- Maximum energy delivery to side arm occurs when waves entering the junction through main arms are in phase. The standing wave in the main line then has an anti-node of electric field at the junction, and a current-node at the same junction. High energy delivery to a branch line connected to a transmission line at a point of high voltage and low current takes place if branch lin is connected in shunt with the main line.
- Since it is a three port junction the scattering matrix can be derived as follows:
  1. [S] Matrix of order 3 x 3.

$$[S] = \begin{bmatrix} S_{11} & S_{12} & S_{13} \\ S_{21} & S_{22} & S_{23} \\ S_{31} & S_{32} & S_{33} \end{bmatrix} \quad \ldots\ldots\ldots\ldots\ldots\ldots\ldots(9)$$

  2. Because of plane of symmetry of the junction, the Scattering coefficients are

$$S_{23} = S_{13} \ldots\ldots\ldots\ldots(26)$$

  As the waves coming out of the port 1 and 2 of the collinear arm will be opposite phase and in same magnitude. Negative sign indicates phase difference.

  3. If the port 3 is perfectly matched to the junction $S_{33} = 0 \ldots\ldots\ldots\ldots(27)$

  4. For symmetric property $S_{ij} = S_{ji}$

$$\therefore S_{12} = S_{21}\,; \qquad S_{13} = S_{31}; \qquad S_{23} = S_{32} = S_{13} \ldots\ldots\ldots\ldots(28)$$

5. From unitary property, $[S][S]^* = [I]$

$$\begin{bmatrix} S_{11} & S_{12} & S_{13} \\ S_{12} & S_{22} & S_{13} \\ S_{13} & S_{13} & 0 \end{bmatrix} \begin{bmatrix} S_{11}^* & S_{12}^* & S_{13}^* \\ S_{12}^* & S_{22}^* & S_{13}^* \\ S_{13}^* & S_{13}^* & 0 \end{bmatrix} = \begin{bmatrix} 1 & 0 & 0 \\ 0 & 1 & 0 \\ 0 & 0 & 1 \end{bmatrix}$$

R_1C_1: $|S_{11}|^2 + |S_{12}|^2 + |S_{13}|^2 = 1 \ldots\ldots (29)$

R_2C_2: $|S_{12}|^2 + |S_{22}|^2 + |S_{13}|^2 = 1 \ldots\ldots (30)$

R_3C_3: $0 + |S_{13}|^2 + |S_{13}|^2 = 1 \ldots\ldots (31)$

R_3C_1: $S_{13}.S_{11}^* + S_{13}.S_{12}^* = 1 \ldots\ldots (32)$

From equations (29), and (30), we get

$$S_{11} = S_{22} \ldots\ldots\ldots (33)$$

From equation (31), $S_{13} = \frac{1}{\sqrt{2}} \ldots\ldots\ldots (34)$

From equation (32), $S_{13}(S_{11}^* + S_{12}^*) = 0$

$$but\ S_{13} \neq 0 \ \therefore (S_{11}^* + S_{12}^*) = 0$$

$$\therefore S_{11}^* = -S_{22}^*$$

$$\therefore S_{11} = -S_{22} \quad and \quad \therefore S_{12} = -S_{11} \ldots\ldots\ldots ($$

Using these values from equation 33, 34 and 35 in equation 29,

$$|S_{11}|^2 + |S_{11}|^2 + \frac{1}{2} = 1$$

$$\therefore S_{11} = \frac{1}{2} \ldots\ldots\ldots (36)$$

$$\therefore S_{22} = -\frac{1}{2} \ldots\ldots\ldots (38) from\ eq.35$$

Substituting the values of $S_{11}, S_{12}, S_{13}, S_{22}$, the [S] matrix of equation 29 becomes

$$[S] = \begin{bmatrix} \frac{1}{2} & -\frac{1}{2} & \frac{1}{\sqrt{2}} \\ -\frac{1}{2} & \frac{1}{2} & \frac{1}{\sqrt{2}} \\ \frac{1}{\sqrt{2}} & -\frac{1}{\sqrt{2}} & 0 \end{bmatrix} \ldots\ldots\ldots (9)$$

We know that, $[b] = [S][a]$

$$\begin{bmatrix} b_1 \\ b_2 \\ b_3 \end{bmatrix} = \begin{bmatrix} \frac{1}{2} & -\frac{1}{2} & \frac{1}{\sqrt{2}} \\ -\frac{1}{2} & \frac{1}{2} & \frac{1}{\sqrt{2}} \\ \frac{1}{\sqrt{2}} & -\frac{1}{\sqrt{2}} & 0 \end{bmatrix} \begin{bmatrix} a_1 \\ a_2 \\ a_3 \end{bmatrix}$$

$$\therefore b_1 = \frac{1}{2}a_1 - \frac{1}{2}a_2 + \frac{1}{\sqrt{2}}a_3 \ldots\ldots\ldots (40)$$

$$\therefore b_2 = -\frac{1}{2}a_1 - \frac{1}{2}a_2 + \frac{1}{\sqrt{2}}a_3 \ldots\ldots\ldots (41)$$

$$\therefore b_3 = \frac{1}{\sqrt{2}}a_1 + \frac{1}{\sqrt{2}}a_2 \ldots\ldots\ldots (42)$$

<u>Case 1:</u> Input is given at port 3 and no inputs at port 1 and 2, $a_3 \neq 0, a_1 = a_2 = 0$.

From equation 40, $b_1 = \frac{1}{\sqrt{2}}a_3$

From equation 41, $b_2 = \frac{1}{\sqrt{2}}a_3$

From equation 42, $b_3 = 0$

Case 2: Input is given at port 1 and port 2, and no input at port 3, $a_3 = 0, \boldsymbol{a_1} = \boldsymbol{a_2} = \boldsymbol{a}$.

From equation 40, $\boldsymbol{b_1} = \frac{a}{2} - \frac{a}{2} = \mathbf{0}$

From equation 41, $\boldsymbol{b_2} = \frac{a}{2} - \frac{a}{2} = \mathbf{0}$

From equation 42, $\boldsymbol{b_3} = \frac{a}{\sqrt{2}} + \frac{a}{\sqrt{2}}$

Input at port 3 is the addition of the two inputs at port 1 and port 2 and these are added in phase.

5. E-H Plane TEE OR MAGIC TEE:

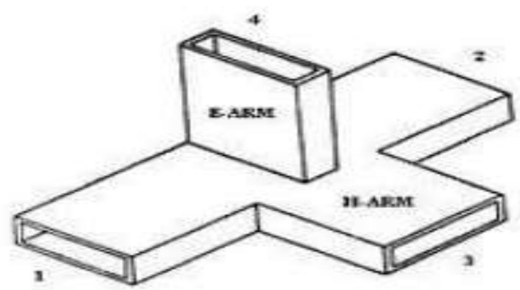

- A magic tee is a combination of E-plane and H-plane Tee.
- Magic tee, combines the power dividing properties of both H-plane and E-plane tee, and has the advantages of being completely matched at all the ports.
- If two signals of same magnitude and phase are fed into port 1 and port 2, then outpur will be zero at port 3 and additive at port 4.
- If signal is fed from port 4 (H-arm) then signals divides equally in magnitude and phase between port 1 and 2 and no signal appears at port 3 (E-arm).
- If signal is fed into port 3, then signal divides equally in magnitude, but opposite in phase at port 1 and 2, and no signal comes out from port 4, i.e. output at port 4 is zero.
- This magic occurs, because E-arm causes a phase delay while H-arm causes a phase advance, resulting into is $S_{12} = S_{21} = 0$.
- Using the properties of E and H-plane tee, its scattering matrix can be obtained as follows:
  1. [S] Matrix is a 4 x 4 matrix since there are 4 ports.

Magic T waveguide junction

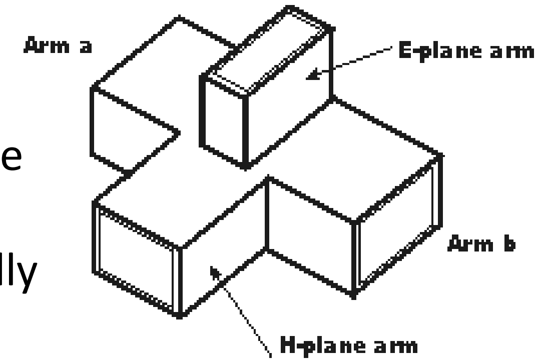

Magic T waveguide junction

E-plane:
– To look at the operation of the Magic T waveguide junction, take the example of when a signal is applied into the "E plane" arm.
– A signal injected into the E-plane port will also be divided equally between ports 1 and 2, but will be 180 degrees out of phase.

• H-plane:
A signal injected into the H-plane port will be divided equally between ports 1and 2, and will be in phase.

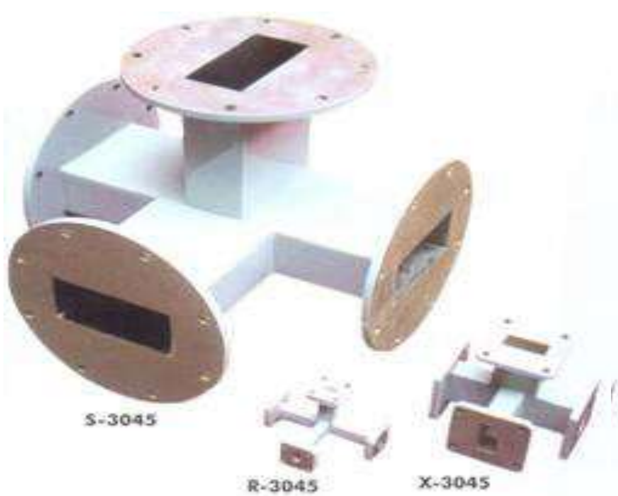

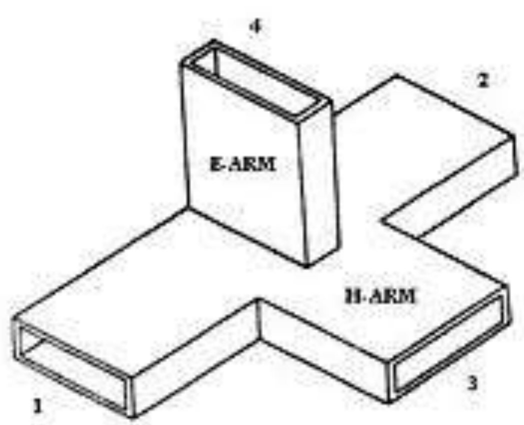

An E-H Plane Tee junction is formed by attaching two simple waveguides one parallel and the other series, to a rectangular waveguide which already has two ports. This is also called as **Magic Tee**, or **Hybrid** or **3dB coupler**.

The arms of rectangular waveguides make two ports called **collinear ports** i.e., Port 1 and Port 2, while the Port 3 is called as **H-Arm** or **Sum port** or **Parallel port**. Port 4 is called as **E-Arm** or **Difference port** or **Series port**.

The cross-sectional details of Magic Tee can be understood by the following figure.

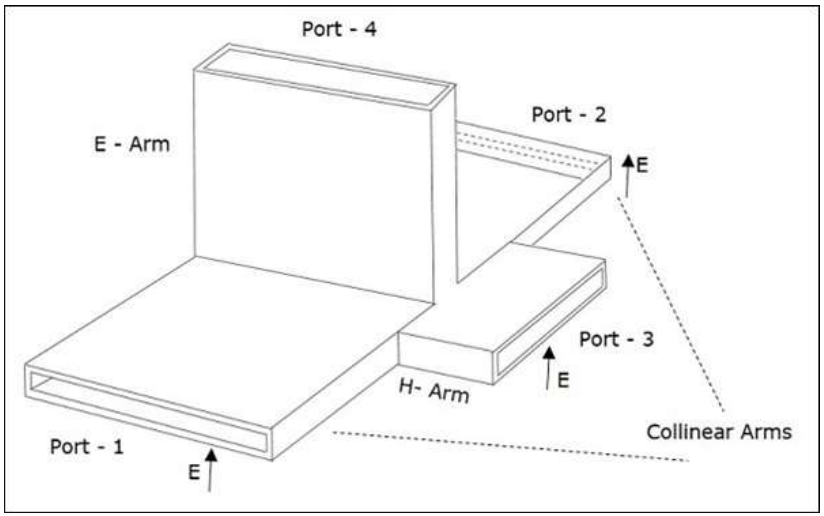

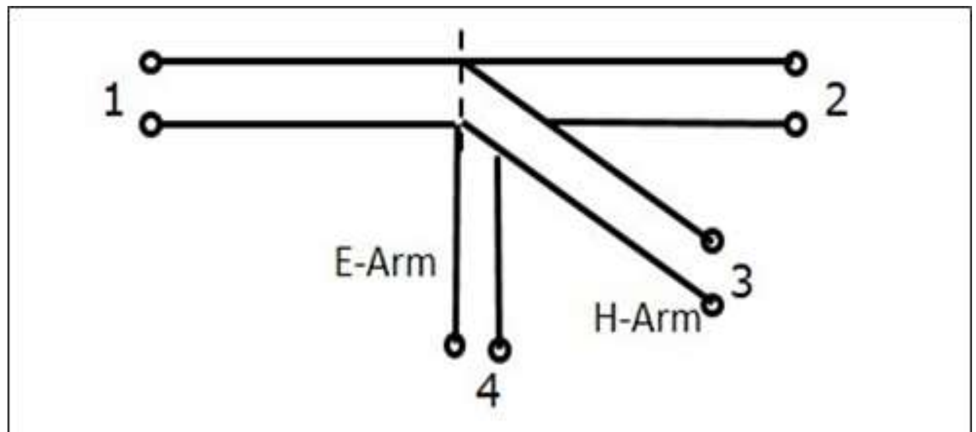

Magic Tee junction

$$[S] = \begin{bmatrix} S_{11} & S_{12} & S_{13} & S_{14} \\ S_{21} & S_{22} & S_{23} & S_{24} \\ S_{31} & S_{32} & S_{33} & S_{34} \\ S_{41} & S_{42} & S_{43} & S_{44} \end{bmatrix} \ldots\ldots (43)$$

2. Because of H-plane Tee junction,

$$S_{23} = S_{13} \ldots\ldots (44)$$

3. Because of E-plane Tee junction

$$S_{24} = -S_{14} \ldots\ldots (45)$$

4. Because of the geometry, an input to port 3 cannot come out of port 4 and vice versa. Hence they are called as isolated ports.

$$S_{34} = S_{43} = 0 \ldots\ldots. (46)$$

5. From symmetry property, $S_{ij} = S_{ji}$

$$S_{12} = S_{21}\ ;\ S_{31} = S_{13}\ ;\ S_{41} = S_{14}\ ;$$
$$S_{23} = S_{32}\ ;\ S_{34} = S_{43}\ ;\ S_{42} = S_{24} \ \ldots\ldots. (47)$$

6. If ports 3 and 4 are perfectly matched to the junction.

$$S_{33} = S_{44} = 0$$

Substituting all the above results, S-matrix is

$$[S] = \begin{bmatrix} S_{11} & S_{12} & S_{13} & S_{14} \\ S_{12} & S_{22} & S_{13} & -S_{14} \\ S_{13} & S_{13} & 0 & 0 \\ S_{14} & -S_{14} & 0 & 0 \end{bmatrix} \ldots\ldots\ldots (48)$$

7. From unitary property, $[S][S]^* = [I]$

$$\begin{bmatrix} S_{11} & S_{12} & S_{13} & S_{14} \\ S_{12} & S_{22} & S_{13} & -S_{14} \\ S_{13} & S_{13} & 0 & 0 \\ S_{14} & -S_{14} & 0 & 0 \end{bmatrix} \begin{bmatrix} S_{11}^* & S_{12}^* & S_{13}^* & S_{14}^* \\ S_{12}^* & S_{22}^* & S_{13}^* & -S_{14}^* \\ S_{13}^* & S_{13}^* & 0 & 0 \\ S_{14}^* & -S_{14}^* & 0 & 0 \end{bmatrix} = \begin{bmatrix} 1 & 0 & 0 & 0 \\ 0 & 1 & 0 & 0 \\ 0 & 0 & 1 & 0 \\ 0 & 0 & 0 & 1 \end{bmatrix}$$

$$R_1C_1: \quad |S_{11}|^2 + |S_{12}|^2 + |S_{13}|^2 + |S_{14}|^2 = 1 \ldots\ldots\ldots (49)$$
$$R_2C_2: \quad |S_{12}|^2 + |S_{22}|^2 + |S_{13}|^2 + |S_{14}|^2 = 1 \ldots\ldots\ldots (50)$$
$$R_3C_3: \quad |S_{13}|^2 + |S_{13}|^2 = 1 \ldots\ldots\ldots (51)$$
$$R_4C_4: \quad |S_{14}|^2 + |S_{14}|^2 = 1 \ldots\ldots\ldots (52)$$

From equation 51 and 52,

$$S_{13} = \frac{1}{\sqrt{2}} \ and \ S_{14} = \frac{1}{\sqrt{2}} \ldots\ldots\ldots\ldots\ldots\ldots (53)$$

Using the values of equation 53 into equation 49, we get,

$$|S_{11}|^2 + |S_{12}|^2 + \frac{1}{2} + \frac{1}{2} = 1$$
$$|S_{11}|^2 + |S_{12}|^2 = 0$$
$$|S_{11}|^2 = -|S_{12}|^2 \ldots\ldots (54)$$

Comparing equations 49 and 50, we found that $S_{11} = S_{22}$......(55)

As seen earlier $S_{12} = S_{21} = 0$

$$S_{11} = S_{12} = S_{22} = 0$$

This shows that port 1 and 2 are perfectly matched to the junction. Hence in any four port junction, if any tow ports are perfectly matched to the junction, then the remaining two ports are automatically matched to the junction. Such a junction where in all the four ports are perfectly matched to the junction is called as MAGIC TEE.

Thus by substituting the values we get,

$$[S] = \frac{1}{\sqrt{2}}\begin{bmatrix} 0 & 0 & 1 & 1 \\ 0 & 0 & 1 & -1 \\ 1 & 1 & 0 & 0 \\ 1 & -1 & 0 & 0 \end{bmatrix} \ldots\ldots\ldots (56)$$

8. We know that [b]=[S][a].

$$\begin{bmatrix} b_1 \\ b_2 \\ b_3 \\ b_4 \end{bmatrix} = \frac{1}{\sqrt{2}}\begin{bmatrix} 0 & 0 & 1 & 1 \\ 0 & 0 & 1 & -1 \\ 1 & 1 & 0 & 0 \\ 1 & -1 & 0 & 0 \end{bmatrix}\begin{bmatrix} a_1 \\ a_2 \\ a_3 \\ a_4 \end{bmatrix}$$

$$\therefore b_1 = \frac{1}{\sqrt{2}}(a_3 + a_4) \ldots\ldots\ldots\ldots\ldots\ldots (57)$$

$$\therefore b_2 = \frac{1}{\sqrt{2}}(a_3 - a_4) \ldots\ldots\ldots\ldots\ldots\ldots (58)$$

$$\therefore b_3 = \frac{1}{\sqrt{2}}(a_1 + a_2) \ldots\ldots\ldots\ldots\ldots\ldots\ldots (59)$$

$$\therefore b_4 = \frac{1}{\sqrt{2}}(a_1 - a_2) \ldots\ldots\ldots\ldots\ldots\ldots\ldots (60)$$

<u>Case 1:</u> Input is given at port 3 and no inputs at port 1, 2 and 4, $a_3 \neq 0, a_1 = a_2 = a_4 = 0$.

From equation 57, $b_1 = \frac{1}{\sqrt{2}} a_3$

From equation 58, $b_2 = \frac{1}{\sqrt{2}} a_3$

From equation 59 and 60, $b_3 = b_4 = 0$

This is the property of H-plane Tee.

<u>Case 2:</u> Input is given at port 4 and no inputs at port 1, 2 and 3, $a_4 \neq 0, a_1 = a_2 = a_3 = 0$.

From equation 57, $b_1 = \frac{1}{\sqrt{2}} a_4$

From equation 58, $b_2 = -\frac{1}{\sqrt{2}} a_4$

From equation 59 and 60, $b_3 = b_4 = 0$

This is the property of E-plane Tee.

<u>Case 3:</u> Input is given at port 1 and no inputs at port 4, 2 and 3, $a_1 \neq 0, a_4 = a_2 = a_3 = 0$.

From equation 57 and 58 $\boldsymbol{b_1 = 0}$, $\boldsymbol{b_2 = 0}$

From equation 59 $\boldsymbol{b_3 = \frac{1}{\sqrt{2}} a_1}$

From equation 60, $\boldsymbol{b_4 = -\frac{1}{\sqrt{2}} a_1}$

When power is fed to port 1, nothing comes out of port 2 even though they are collinear ports (Magic!!). Hence ports 1 and 2 are called as **isolated ports.**
Similarly an input at port 2 cannot come out at port 1.
Similarly E and H-ports are **isolated ports.**

<u>Case 4:</u> Equal input is given at port 3 and 4; no inputs at port 1 and 2, $a_3 = a_4$; $a_1 = a_2 = 0$.

From equation 57,$\boldsymbol{b_1 = \frac{1}{\sqrt{2}}(2a_3)}$,

From equation 58, 59 and 60, $\boldsymbol{b_2 = b_3 = b_4 = 0}$

This is called as an additive property.

<u>Case 5:</u> Equal input is given at port 1 and 2; no inputs at port 3 and 4, $a_1 = a_2$; $a_3 = a_4 = 0$.

From equation 57, 58, and 60, $\boldsymbol{b_1 = b_2 = b_4 = 0}$

From equation 59, $\boldsymbol{b_3 = \frac{1}{\sqrt{2}}(2a_1)}$

Equal inputs at ports 1 and 2 results in an output port 3 (additive port)and no output at port 1, 2 and 4. This is similar to case 4.

Applications of magic tee

1. As an isolator.
2. As a matching device
3. As a phase shifter.
4. As duplexer.
5. As mixer.

Hybrid Ring

It is 180° hybrid having 4 ports as shown in the figure. It is also called as hybrid ring coupler. It is used as 3 dB coupler. It is used in various RF and microwave systems as alternative to magic tee device. But unlike magic tee, it does not require any matching structure in order to obtain similar functionalities. It is available in various designs such as microstrip, stripline and waveguide structures.

It is used in wide variety of applications such as balanced mixers, balanced amplifiers, antenna feeding networks, power multipliers or power dividers etc.

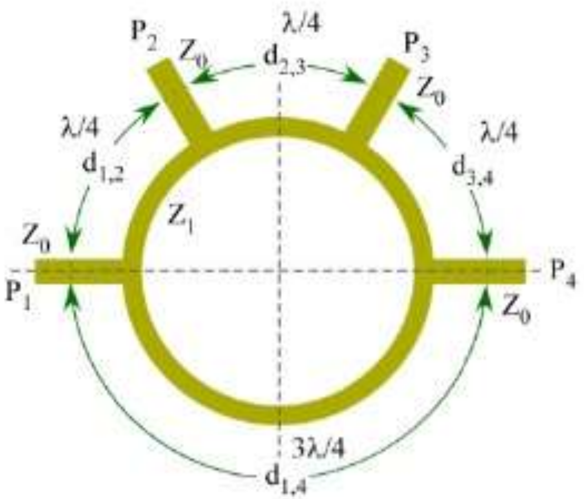

Hybrid Ring

As shown it has four ports which are λ/4 away from the other in the top half of the hybrid ring (i.e. between P1 and P2, P2 and P3, P3 and P4). In the bottom half of the hybrid ring P1 and P4 ports are 3*λ/4 wavelengths away from each other. It is also called rat race coupler.

Hybrid Rings (Rat-Race Circuits)

Hybrid Ring S-Matrix

$$\begin{bmatrix} 0 & S_{12} & 0 & S_{14} \\ S_{21} & 0 & S_{23} & 0 \\ 0 & S_{32} & 0 & S_{34} \\ S_{41} & 0 & S_{43} & 0 \end{bmatrix}$$

⇩

$$\frac{-i}{\sqrt{2}}\begin{pmatrix} 0 & 1 & 0 & -1 \\ 1 & 0 & 1 & 0 \\ 0 & 1 & 0 & 1 \\ -1 & 0 & 1 & 0 \end{pmatrix}$$

Rat Race Coupler S-Matrix

Annular line of proper electrical length to sustain standing waves, to which four arms are connected at proper intervals by means of series or parallel junctions.

Hybrid ring
With series
junctions

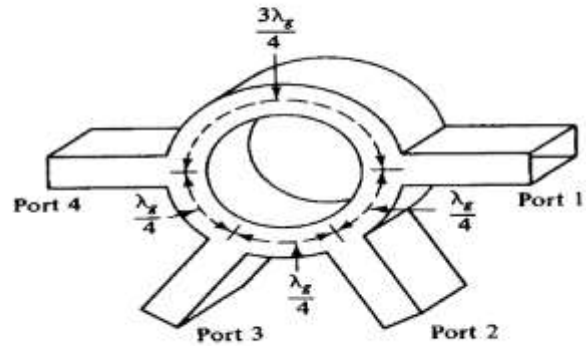

Characteristics similar to hybrid tee.

When a wave is fed into port 1, it will not appear at port 3 because the difference of phase shifts for the waves travelling in the clockwise and anticlockwise directions is 180.

Thus the waves are cancelled at port 3.

Similarly the waves fed into port 2 will not emerge at port 4 and so on.

Directional Coupler

Directional Coupler is a 4 port device which has primary and secondary waveguides. The primary wave guide is from port 1 to port 2 and secondary waveguide is from port 3 to port 4.

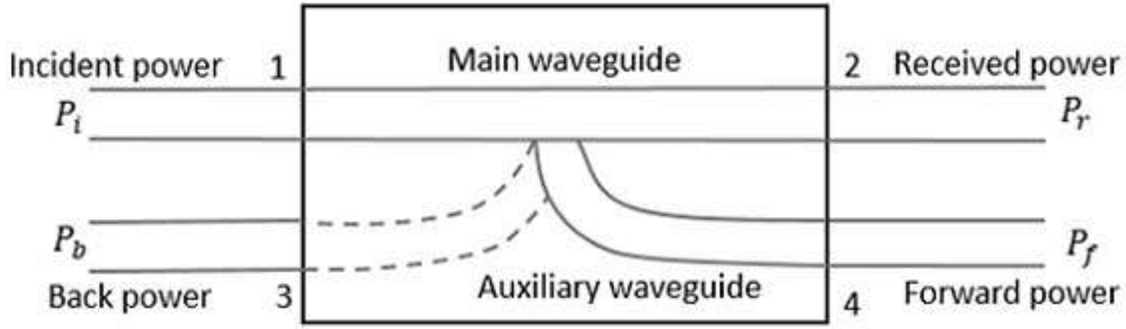

- Directional coupler is used to couple microwave power, which is unidirectional in most of the cases. The properties of a directional coupler are,

1. All the ports are matched.
2. When the power moves from port 1 to port 2, little portion of it would gets coupled to port 4 and not to port 3.
3. When the power moves from port 2 to port 1, little portion of it would gets coupled to port 3 and not to port 4.
4. The coupling factor of a directional coupler is the ratio of incident power to forward power.

Coupling factor = $10 \log(P_i/P_f) = 10 \log(P_1/P_4)$

- Directivity of the directional coupler is the ratio of forward power to back power.

Directivity = $10 \log(P_f/P_b) = 10 \log(P_4/P_3)$

- Isolation of a directional coupler is the ratio of incident power to back power.

$I = 10 \log(P_i/P_b)$= . $I = 10 \log(P_1/P_3)$

- Isolation = Coupling factor + Directivity.

Two hole directional coupler is same as conventional directional coupler, but with two holes in common between primary and secondary waveguides.
The spacing between these two holes is given by,
$L = (2n+1)\lambda_g/4$ Where, n = an integer λ_g = wavelength

- A fraction of energy entering into port 1 passes through holes and is radiated into port 2. The forward waves in port 4 are in the same phase and are added.
- The backward waves in port 3 are out of phase and are cancelled.

The general S matrix of a directional coupler is,

$$S = \begin{bmatrix} S_{11} & S_{12} & S_{13} & S_{14} \\ S_{21} & S_{22} & S_{23} & S_{24} \\ S_{31} & S_{32} & S_{33} & S_{34} \\ S_{41} & S_{42} & S_{43} & S_{44} \end{bmatrix} ------(1)$$

Since all ports in a directional coupler are matched.
$S_{11} = S_{22} = S_{33} = S_{44} = 0$ ----------------- (2)

- Since there is no coupling between ports 1 & 3 and ports 2 & 4

$S_{13} = S_{31} = S_{24} = S_{42} = 0$ ------------- (3)

Apply equation (2) & (3) in (1)

$$S = \begin{bmatrix} 0 & S_{12} & 0 & S_{14} \\ S_{12} & 0 & S_{23} & 0 \\ 0 & S_{23} & 0 & S_{34} \\ S_{14} & 0 & S_{34} & 0 \end{bmatrix}$$

By unitary property, [S][S]* = I

$$\begin{bmatrix} 0 & S_{12} & 0 & S_{14} \\ S_{12} & 0 & S_{23} & 0 \\ 0 & S_{23} & 0 & S_{34} \\ S_{14} & 0 & S_{34} & 0 \end{bmatrix} \begin{bmatrix} 0 & S_{12}^* & 0 & S_{14}^* \\ S_{12}^* & 0 & S_{23}^* & 0 \\ 0 & S_{23}^* & 0 & S_{34}^* \\ S_{14}^* & 0 & S_{34}^* & 0 \end{bmatrix} = \begin{bmatrix} 1 & 0 & 0 & 0 \\ 0 & 1 & 0 & 0 \\ 0 & 0 & 1 & 0 \\ 0 & 0 & 0 & 1 \end{bmatrix}$$

R_1C_1 => $|S_{12}|^2 + |S_{14}|^2 = 1$ ------------ (4)
R_2C_2 => $|S_{12}|^2 + |S_{23}|^2 = 1$ ------------ (5)
R_3C_3 => $|S_{23}|^2 + |S_{34}|^2 = 1$ ------------ (6)
R_1C_3 => $S_{12} S_{23}^* + S_{14} S_{34}^* = 0$ ----------- (7)
Comparing eq (4) and (5)

$|S_{12}|^2 + |S_{14}|^2 = |S_{12}|^2 + |S_{23}|^2$
$S_{14} = S_{23}$ --------------- (8)
Comparing eq (5) and (6)
$|S_{12}|^2 + |S_{23}|^2 = |S_{34}|^2 + |S_{23}|^2$
$S_{12} = S_{34}$ --------------- (9)

Let, S_{12} be real and positive,

ie, $S_{12} = S_{34} = p$ --------------- (10)
applying equation (10) in (7)

Therefore,
$p\, S_{23}^* + S_{14}\, p = 0$

$p\,[S_{23}^* + S_{14}] = 0$
$p\,[S_{23}^* + S_{23}] = 0$
$S_{23}^* + S_{23} = 0$

To satisfy the above condition, S_{23} should be a complex value.
Let $S_{23} = jq$

Therefore, the S matrix of directional coupler is

$$S = \begin{bmatrix} 0 & p & 0 & jq \\ p & 0 & jq & 0 \\ 0 & jq & 0 & p \\ jq & 0 & p & 0 \end{bmatrix}$$

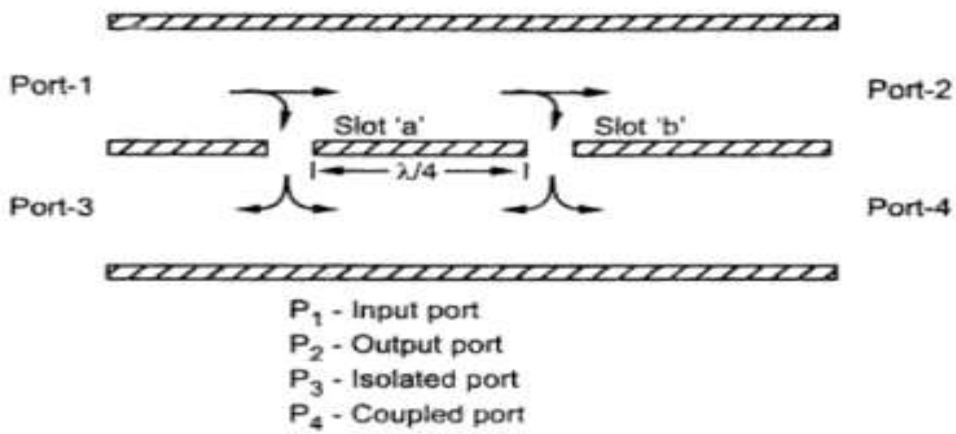

Fig. 3.8.5 Two hole directional coupler

- Two hole directional coupler consists of two guides with two (holes) common between them. These two apertures holes are at a distance of $\lambda_g/4$.
- Energy is coupled through the slots from the main to the coupled guide. Because the slots are a quarter-wavelength a part, the energy in the coupled guide will cancel in one direction and reinforce in the other direction.
- Consider a wave propagating from port-1 to port-2. When the wave passes slot a energy is radiated into the coupled guide, where it radiates in both directions. The main guide wave continues to propagate toward slot b. Part of the wave couples through slot b into the other guide. As before the coupled wave propagates in both directions in the other guide. The portion that propagates towards port-4 is in phase with slot a energy and thus reinforces the signal. But the prtion that propagates from slot b back towards slot a is phase shifted 180°. Thus the port-3 signals from slots a and b are out

of phase by 180° and cancel each other. We can label port 1 the input, port-2 the output, port-3 the isolated port and port-4 the coupled port.

- The spacing between slots a and b is critical because it is necessary to effect a 180° phase shift in the a-b-b-a path.

3.8.4 Bathe Hole Directional Coupler

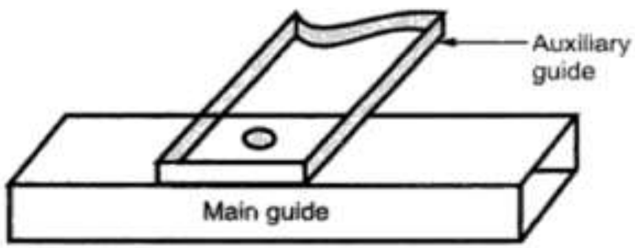

Fig. 3.8.7 Bathe hole directional coupler

- Bathe hole directional coupler consists of two rectangular waveguides coupled by means of circular aperture located at the center of common broad edge.

•coupling process through a single hole in directional coupler improves directivity the power entering port1 is coupled through coaxial probe output and the power entering port2 is absorbed by the matched load

•The auxiliary guide is placed at such an angle that magnitude of the magnetically excited wave is made equal to the that of electrically excited wave for improved directivity

UNIT-V

Waveguide Components-II: Waveguide Discontinuities – Waveguide irises, Tuning Screws and Posts, Matched Loads; Waveguide Attenuators – Resistive Card, Rotary Vane types; Waveguide Phase Shifters – Dielectric, Rotary Vane types; Ferrites– Composition and Characteristics, Faraday Rotation; Ferrite Components – Gyrator, Isolator, Circulator. Microwave Measurements: Description of Microwave Bench – Different Blocks and their Features, Precautions; Measurement of Attenuation, Frequency, VSWR, Cavity Q, Impedance, Power.

Waveguide irises, tuning screws and posts.

Waveguide irises: In any waveguide system, when there is a mismatch there will be reflections. In transmission lines, in order to overcome this mismatch lumped impedances or stubs of required value are placed at pre calculated points. In waveguides too, some discontinuities are made use for matching purposes. Any susceptances appearing across the guide, causing mismatch (production of standing waves) needs to be cancelled by introducing another susceptance of the same magnitude but of opposite nature.

Irises (also called windows, apertures or diaphragms) are made use of for the purpose impedance matching.

An inductive iris allows a current to flow where none flowed before. The iris is placed in a position where the magnetic field is strong (or where electric field is relatively weak). Since the plane of polarization of electric field is parallel to the plane of iris, the current flow due to iris causes a magnetic field to be set up.

In capacitive iris, it is seen that the potential which existed between the top and bottom walls of the waveguide now exists between surfaces which are closer. The capacitive iris is placed in a position where the electric field is strong.

In parallel resonant iris, the inductive and capacitive irises are combined. For the dominant mode, the iris presents a high impedance and the shunting effect for this mode will be negligible. Parallel resonant **iris** acts as a band pass filter to suppress unwanted modes.

- A series resonant iris which supported by a non metallic material and it is transparent to the flow of microwave energy.

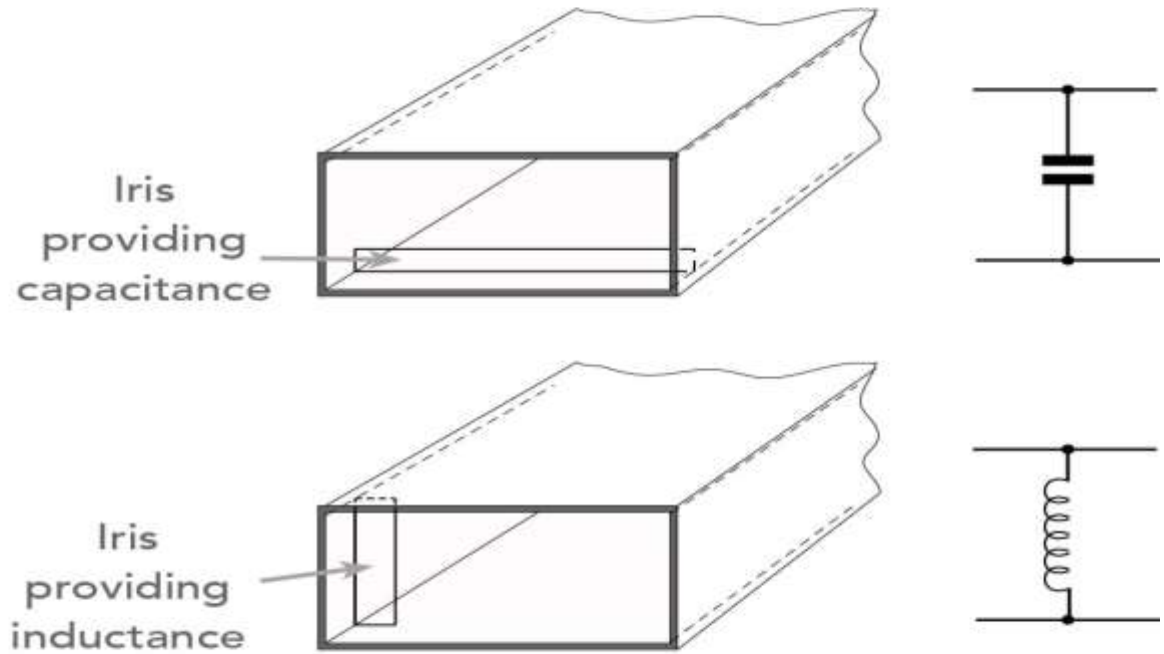

Matching Elements in Waveguide

Rectangular Waveguide
(end view)

Note:
Planar discontinuities are modeled as purely shunt elements.

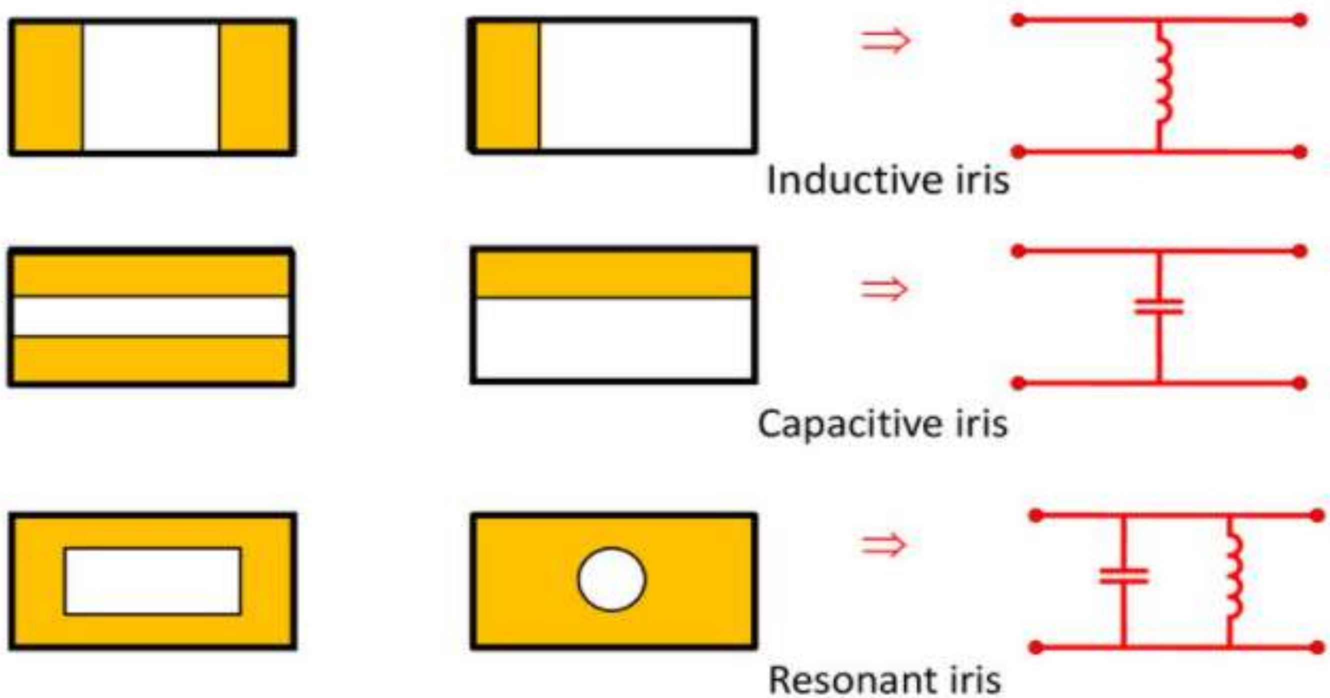

quivalent circuit gives us the correct reflection and transmission of the TE_{10} mode.

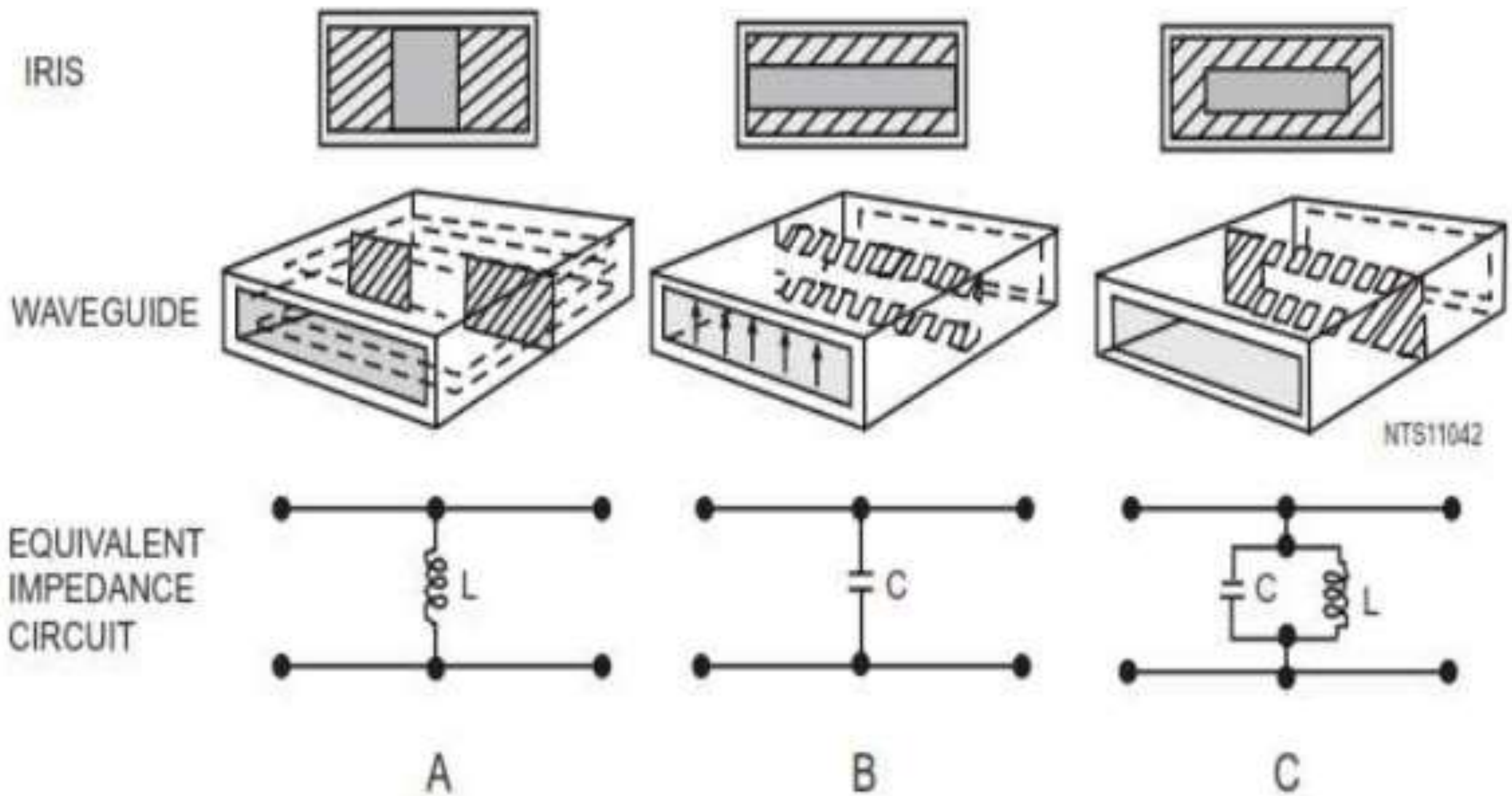
IRIS
WAVEGUIDE
NTS11042
EQUIVALENT
IMPEDANCE
CIRCUIT
L
C
C
L
A
B
C

- An inductive iris and its equivalent circuit are illustrated in figure view (A). The iris places a shunt inductive reactance across the waveguide that is directly proportional to the size of the opening.
- Notice that the edges of the inductive iris are perpendicular to the magnetic plane.
- `The shunt capacitive reactance, illustrated in view (B), basically acts the same way. Again, the reactance is directly proportional to the size of the opening, but the edges of the iris are perpendicular to the electric plane.
- The iris, illustrated in view (C), has portions across both the magnetic and electric planes and forms an equivalent parallel-LC circuit across the waveguide.
- At the resonant frequency, the iris acts as a high shunt resistance. Above or below resonance, the iris acts as a capacitive or inductive reactance.

Waveguide Impedance Matching

- Waveguide transmission systems are not always perfectly impedance matched to their load devices.
- The standing waves that result from a mismatch cause a power loss, a reduction in power-handling capability, and an increase in frequency sensitivity.
- Impedance-changing devices are therefore placed in the waveguide to match the waveguide to the load. These devices are placed near the source of the standing waves.
- Figure illustrates three devices, called irises, that are used to introduce inductance or capacitance into a waveguide.
- An iris is nothing more than a metal plate that contains an opening through which the waves may pass. The iris is located in the transverse plane.

Irises (also called windows, apertures or diaphragms) are made use of for the purpose impedance matching.

Waveguide Window

- Waveguide windows, also known as Diaphragms, Apertures or Irises, are used to provide impedance matching in the waveguide in the same way as we used stubs in case of transmission lines. Three common types of windows include:
- Inductive Windows
- Capacitive Windows
- Resonant Windows

Inductive Window

- Conducting diaphragms extending in a waveguide from side walls as shown in figure have the effect of adding an inductive susceptance across the waveguide at the point at which diaphragms are placed.
- This is because, the iris in figure allows current to flow where none flowed before.
- The electric field that advanced before now has conducting surface in its plane, which permits current flow.
- Thus some energy is stored in the magnetic field which leads to an increased inductance at that point of the waveguide.
- Such an element is therefore, called an inductive window.
- The amount of normalised inductive susceptance added is a function of the window insertion distance l.

Capacitive Window

- Conducting diaphragms extending into the waveguide from top and bottom walls constitute what is known as a capacitive window as shown in figure.
- These windows produce the effect of ac capacitive susceptance shunted across the waveguide at that point.
- It is obvious that the potential which earlier had existed between top and bottom walls of waveguide now exists between surfaces that are closer.
- This results in an increased capacitance at that point.
- Capacitive windows are not used extensively because of the danger of voltage breakdown which ultimately places a limit on the power that can be transmitted through the waveguide.

Resonant Window

- A conducting diaphragm of the form shown in figure gives the effect of a parallel tuned LC circuit connected across the guide at the point where diaphragm is placed.
- An equivalent circuit is shown in figure. As a first approximation, a resonant window may be considered to be a combination of an inductive and a capacitive window, at the same point in the guide.
- If the inner dimensions of aperture are properly chosen, the frequency range covered is large. However, a limit of minimum aperture size prevents any further changes.
- The value of Q that can be obtained is of the order of 10 and decreases as the size of aperture is increased. Since impedance offered by the resonant window is very high for the dominant mode, and the shunting effect is negligible for the same mode, other modes will be significantly attenuated. Windows are usually employed only to correct a permanent mismatch, rather than to provide adjustable matching.

POSTS and SCREWS

- POSTS and SCREWS made from conductive material can be used for impedance-changing devices in waveguides.
- Figure A and B, illustrate two basic methods of using posts and screws.
- A post or screw which only partially penetrates into the waveguide acts as a shunt capacitive reactance.
- When the post or screw extends completely through the waveguide, making contact with the top and bottom walls, it acts as an inductive reactance. Note that when screws are used the amount of reactance can be varied.
- When the depth of the penetration is $\lambda/4$, a series resonance occurs .

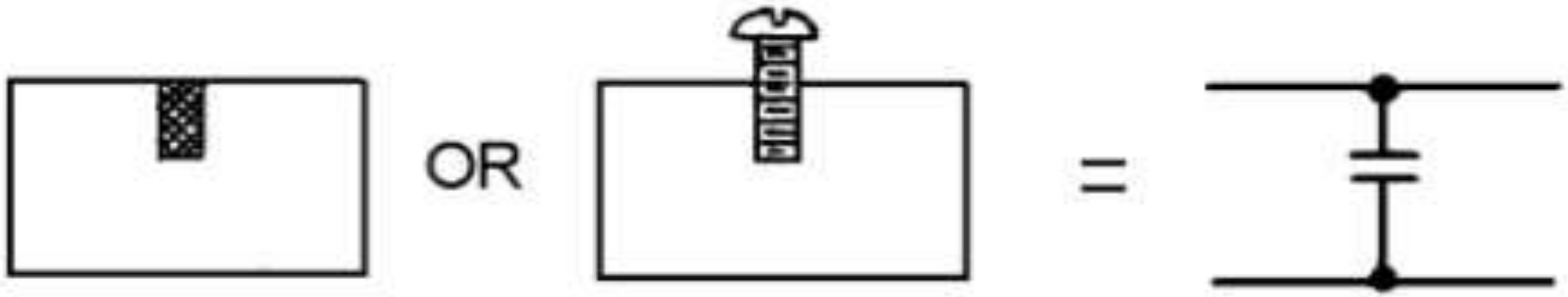

Figure A: Conducting POSTS and SCREWS Penetrating

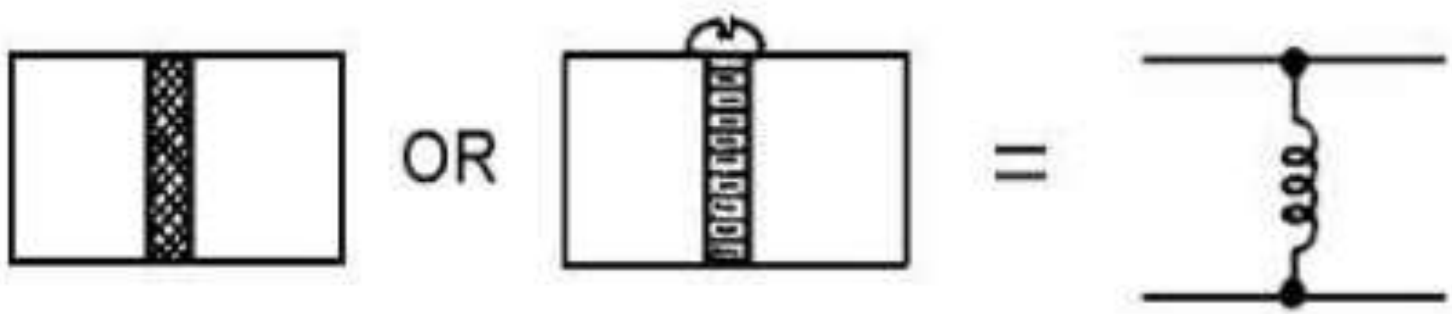

Figure B: Conducting POSTS and SCREWS Extending through

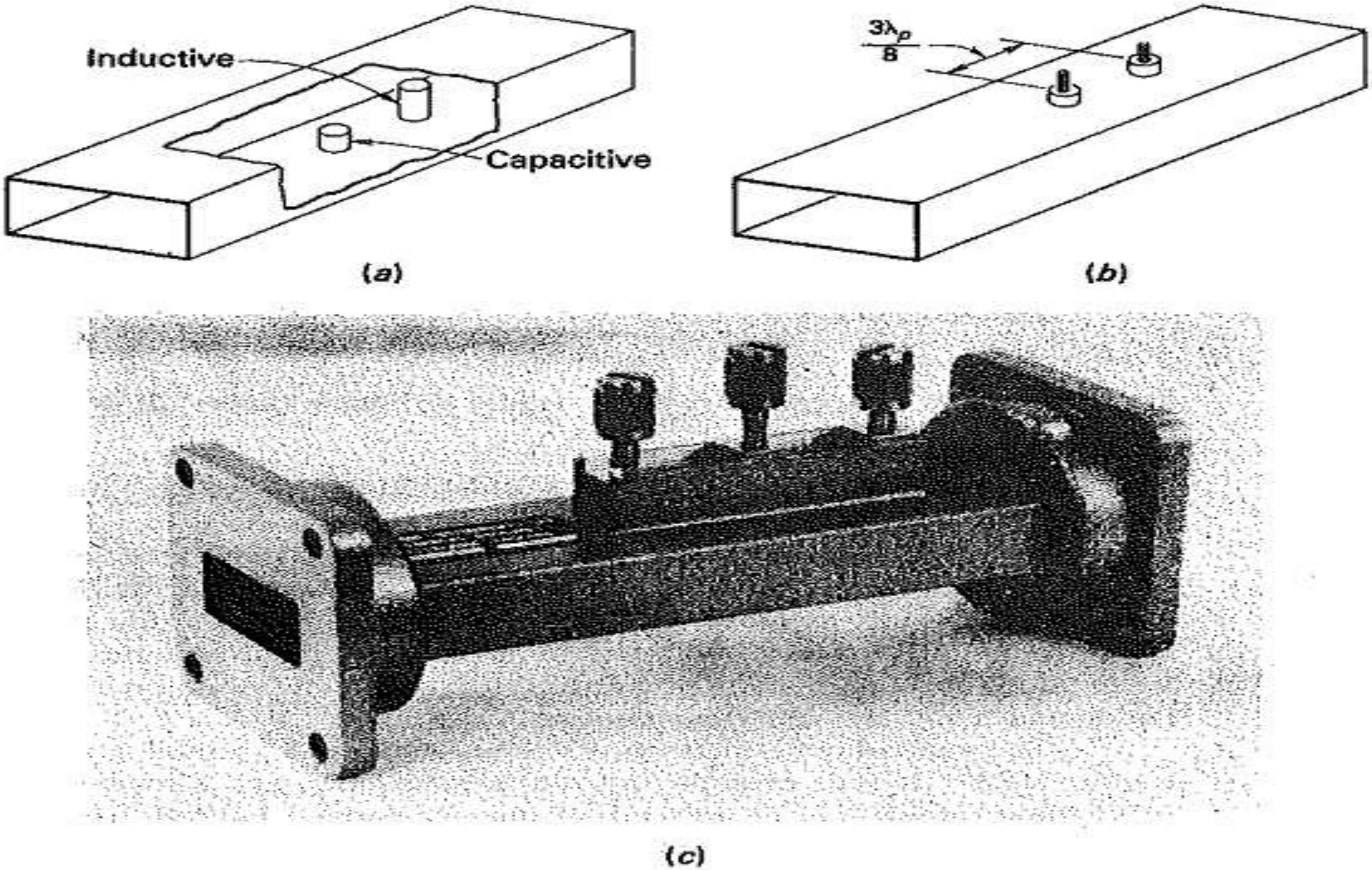

FIGURE 10-31 (*a*) Waveguide posts; (*b*) two-screw matcher; (*c*) three-screw tuner.

cylindrical post, extending into the waveguide from one of the broad sides, has the same effect as an iris in providing lumped reactance at that point. A post may also be capacitive or inductive, depending on how far it extends into the waveguide, and each type is shown in Figure 10-31a.

When such a post extends slightly into the waveguide, a capacitive susceptance is provided at that point and increases until the penetration is approximately a quarter-wavelength, at which point series resonance occurs. Further insertion of the post results in the providing of an inductive susceptance, which decreases as insertion is more complete. The resonance at the midpoint insertion has a sharpness that is inversely proportional to the diameter of the post, which can once again be employed as a filter, However, this time it is used as a band-stop filter, perhaps to allow the propagation of a higher mode in a purer form.

A combination of two such posts in close proximity, now called screws and shown in Figure 10-3 b, is often used as a very effective waveguide matcher, similar to the double-stub tuner . A three-screw tuner, as shown in Figure10.3c may also be used, to provide even greater versatility.

MATCHED TERMINATION

Clip slide

- Terminators are used in coaxial lines, strip lines and waveguides to absorb the incident power without appreciable reflection and radiation
- It is equivalent to terminating the line in its characteristic impedance

➢ A termination is a **one-port device which absorbs all the incident power, never radiate and reflect.**

➢ Its only purpose is to **ABSORB all the incident energy** without causing standing waves.

➢ The basic characteristics of terminations are:
  - VSWR , Power handling capability , Frequency range

Matched Load

- **Types of Terminations**
  - **Matched Load**
  - **Variable Short circuit**

- It provides termination and absorbs all the incident power. It is also equivalent in terminating the line by its characteristic impedance.
- A simple form of matched load in a waveguide is a piece of resistive card placed in guide parallel to the dielectric field.
- The card must be long enough to absorb all the power.
- The front end of the card is tapered, so that it presents no sudden discontinuity to the signal.

Waveguide Attenuators- Resistive card, Rotary Vane types.

Attenuator

- An attenuator is a passive microwave component which, when inserted in the signal path of a system, reduces the signal by a specified amount.
- They normally possess a low VSWR which makes them ideal for reducing load VSWR in order to reduce measurement uncertainties.
- They are sometimes used simply to absorb power, either to reduce it to a measurable level

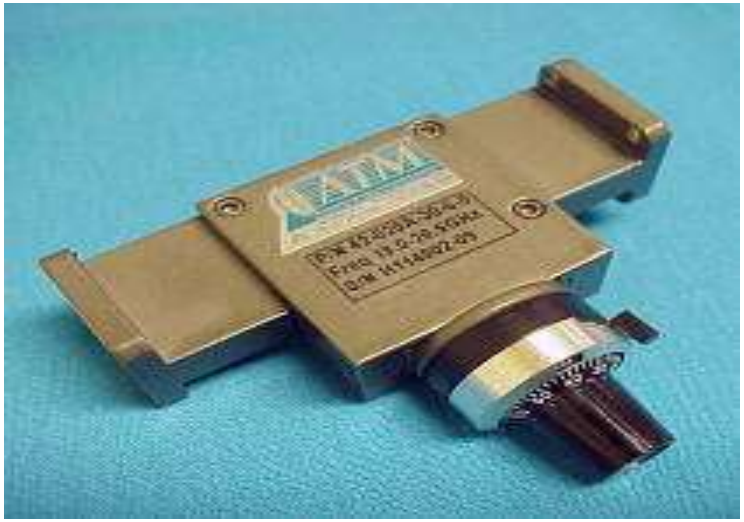

Resistive-card attenuator. The resistive-card attenuator (Fig. 7–24) may be either fixed or variable. In the fixed version, the card is bonded in place as indicated in part *a* of the figure. The card is tapered at both ends in order to maintain a

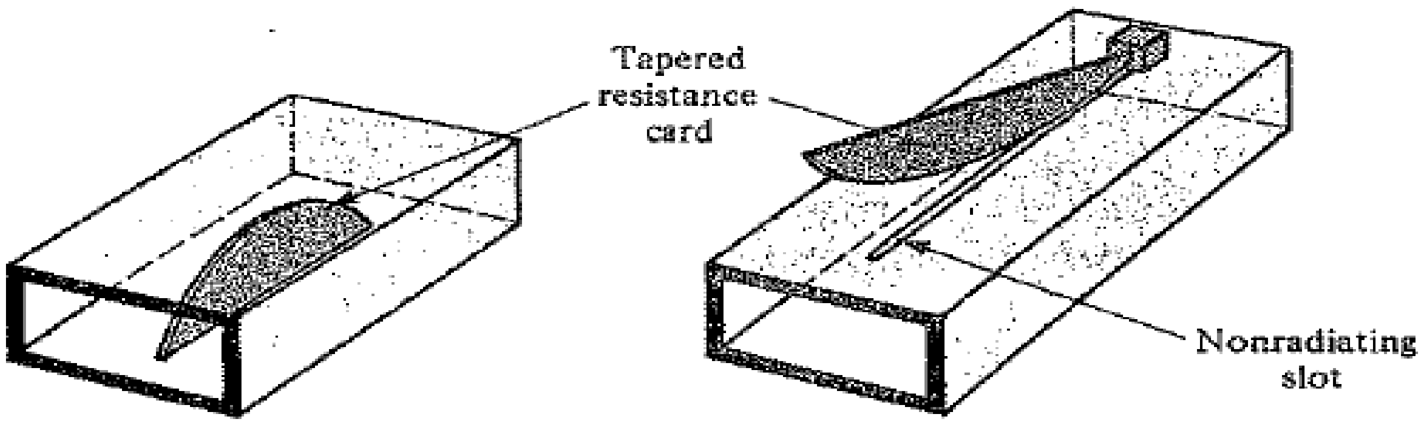

Figure 7–24 Resistive card attenuators in rectangular waveguide.

low input and output SWR over the useful waveguide band. Maximum attenuation per length is achieved by having the card parallel to the electric field and at the center of the guide where the TE_{10} electric field is maximum. The conductivity and dimensions of the card are adjusted, usually by trial-and-error, to obtain the desired attenuation value. The attenuation is a function of frequency, generally becoming greater with increasing frequency. In high-power versions, ceramic-type absorbing materials are used instead of the resistive card.

A variable version of this attenuator, known as the *flap attenuator*, is shown in part *b* of Fig. 7–24. The card enters the waveguide through the slot in the broad wall, thereby intercepting and absorbing a portion of the TE_{10} wave. The hinge arrangement allows the card penetration and hence the attenuation to be varied from zero to some maximum value, typically 30 dB. With the longitudinal slot centered on the broad wall, none of the TE_{10} wave is radiated.[5]

There are two characteristics of the flap attenuator that make its use awkward in certain applications. First, the attenuation is frequency sensitive which makes it inconvenient to use as a calibrated attenuator. Second, the phase of the output signal is a function of card penetration and hence attenuation. This may result in nulling difficulties when the attenuator is part of a bridge-type network. Despite these disadvantages, the flap attenuator finds widespread use in microwave equipment.

There are two characteristics of the flap attenuator that make its use awkward in certain applications. First, the attenuation is frequency sensitive which makes it inconvenient to use as a calibrated attenuator. Second, the phase of the output signal is a function of card penetration and hence attenuation. This may result in nulling difficulties when the attenuator is part of a bridge-type network. Despite these disadvantages, the flap attenuator finds widespread use in microwave equipment.

Rotary-vane attenuator. A variable attenuator that avoids the disadvantages indicated above is the rotary-vane attenuator (Fig. 7–25). The essential parts consist of three circular waveguide sections, two fixed and one rotatable. Also included are input and output transitions that provide low-SWR connections to standard rectangular guide. The attenuation is controlled by rotation of the center section, minimum loss occurring with $\theta_m = 0$ and maximum loss when $\theta_m = 90°$. The analysis that follows shows that the attenuation is a function of θ_m only. This is a significant advantage since the accuracy of the attenuation value merely requires the precise setting of a mechanical angle. The rotary-vane attenuator is, in fact, so accurate that it is used as a calibration standard in most microwave laboratories.

The principle of operation is based upon the interaction between plane-polarized waves and thin resistive cards. The effect is analogous to that described in Sec.

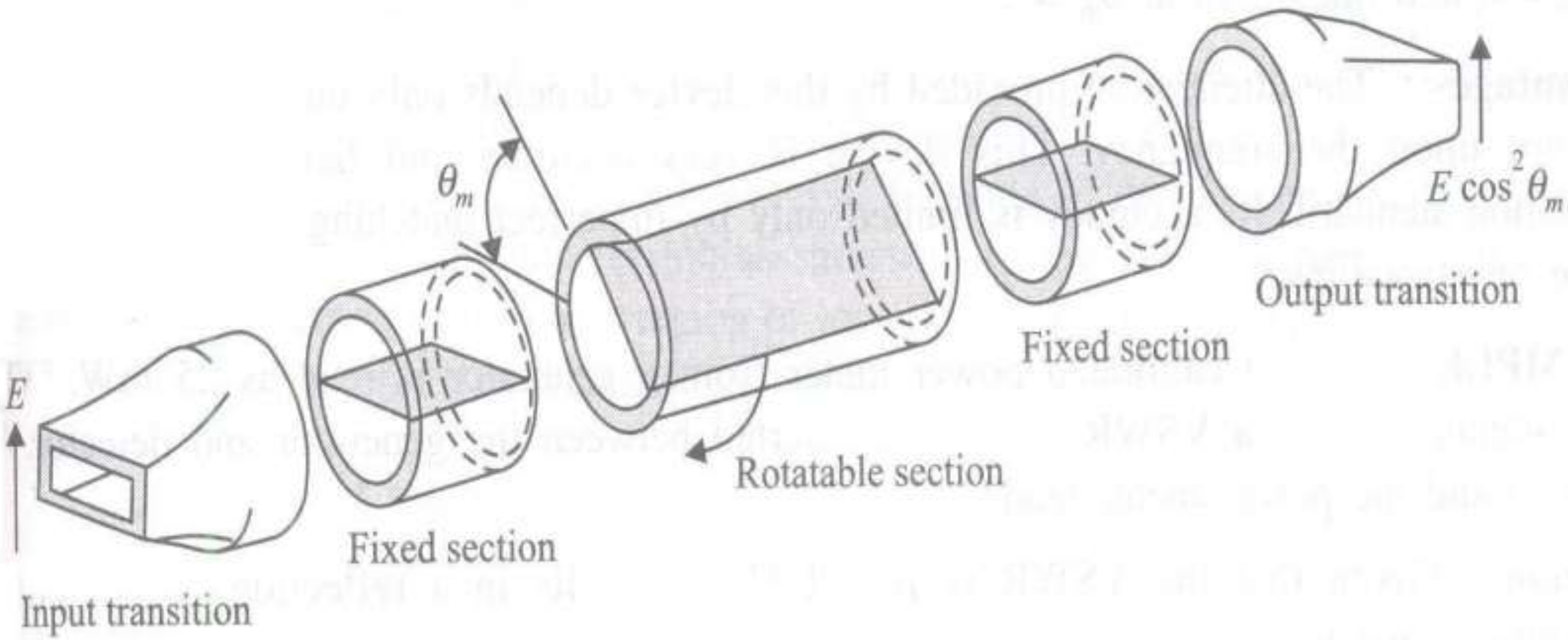

Structural details of Rotary Vane Attenuator

The input transition shown in the figure converts the TE_{10} wave into a vertically polarized TE_{11} wave in circular guide. The electric field associated with the wave is denoted by E. With the input resistance card perpendicular to the electric field, the wave propagates through the first fixed section without loss. When the card in the rotatable section is horizontal ($\theta_m = 0$), the wave passes through it and the output fixed section without loss. Thus for $\theta_m = 0$, the total loss is 0 dB. For any other angle, the component parallel to the rotatable card ($E \sin \theta_m$) is absorbed and the perpendicular component ($E \cos \theta_m$) arrives at the second fixed section with its polarization at an angle θ_m with respect to the vertical plane. This is indicated in the figure. The portion of the wave that is parallel to the output card ($E \cos \theta_m \sin \theta_m$) is absorbed, while the perpendicular component ($E \cos^2 \theta_m$) proceeds to the ouput port via the circular-to-rectangular transition. With power flow proportional to the square of electric field, the fraction of the incident power that is delivered to a matched load is $\cos^4 \theta_m$. Thus the attenuation (in dB) of the rotary-vane attenuator is

$$A_t = 10 \log \left(\frac{1}{\cos^4 \theta_m} \right) \tag{7-12}$$

With a matched generator at the input, the incident power equals the available generator power and therefore the above expression also represents the insertion and transducer loss of the attenuator.

The attenuator can be set for any desired loss value by turning the rotatable section to the appropriate angle θ_m. Its accuracy is determined by the precision with which the angle θ_m can be set (Prob. 7–19). Since A_t is a function of θ_m only, its value is the same at all frequencies within the useful waveguide band, an important advantage in many applications.

Another useful characteristic of the rotary-vane attenuator is that the phase of the output signal is independent of the attenuation setting. The reason is that in order for a signal to arrive at the output, its electric field must have been perpendicular to all three cards. Thus, if $\beta_\perp$ represents the phase constant of the circular guides when the electric field is perpendicular to the card and l the overall length of the three sections, then the total phase delay through the circular sections is $\beta_\perp l$, which is independent of θ_m and hence A_t.

With power proportional to the square of electric field, the fraction of the incident power absorbed by the three resistance cards is 0, $\sin^2 \theta_m$ and $\sin^2 \theta_m \cos^2 \theta_m$,

respectively

Fixed Waveguide Attenuator

Fixed waveguide attenuators typically include a resistive film such as glass placed inside of the waveguide. As shown in ***Figure 2***, the resistive card is placed at the center, parallel to the longitudinal axis and to the maximum electric field with each end tapered sharply to point directly at the incoming wave in order to minimize reflections due to discontinuities. The length of the material is typically two wavelengths (2ƛ) while the length of the tapered portion is about a half a wavelength (ƛ/2). In essence the bulk resistive material accounts for a uniform insertion loss across select frequencies while the taper is fine tuned for a lower VSWR.

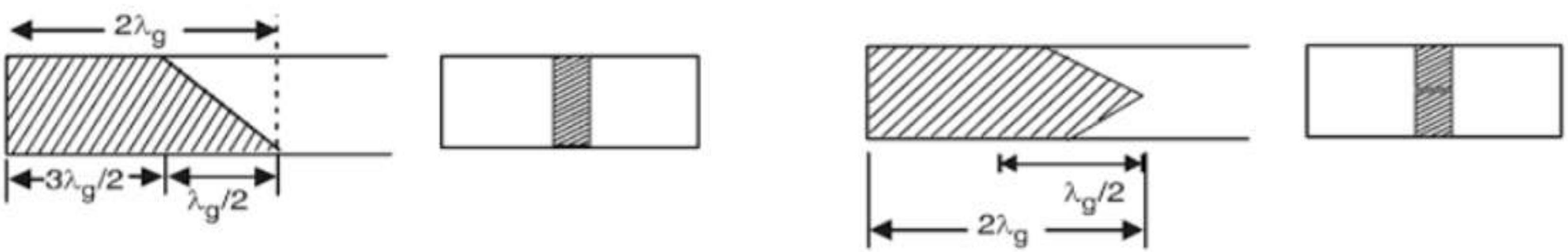

Figure 2: The resistive element causes attenuations while the taper minimizes reflections. The taper shape can vary with a single taper or a double taper.

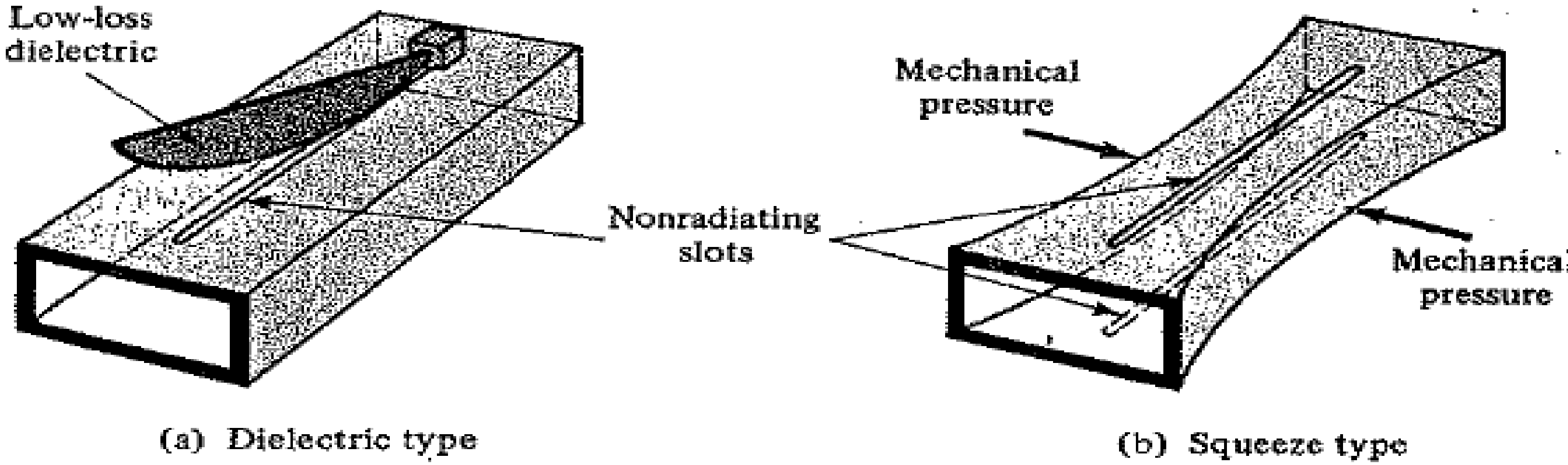

Figure 7–26 Variable phase shifters in rectangular waveguide.

Another version of the dielectric phase shifter employs a pair of thin rods to move the dielectric slab from a region of minimum electric field to one of maximum field

Squeeze-type phase shifter. The phase shifter shown in Fig. 7–26b uses a change in guide width to vary λ_g. The broad walls of the guide contain long nonradiating slots. A clamping arrangement applies pressure to the narrow walls as shown, which reduces the guide width a. This increases λ_g resulting in a decreased phase delay through the waveguide section.

Rotary phase shifter. Because of its accuracy, the rotary phase shifter is used as a calibration standard in most microwave laboratories. Its operation was first described by Fox (Ref. 7–19). A sketch of the unit is shown in Fig. 7–27. Externally it looks very similar to the rotary-vane attenuator. Like the attenuator, its accuracy depends upon the precise rotation of a circular waveguide. The essential parts of the phase shifter are three circular waveguide sections, two fixed and one rotatable. The fixed sections are quarter-wave plates, while the rotatable one is a half-wave plate. Their properties were explained in Sec. 7–1d. In the discussion that follows, it is assumed that they are of the dielectric type shown in Fig. 7–11a.

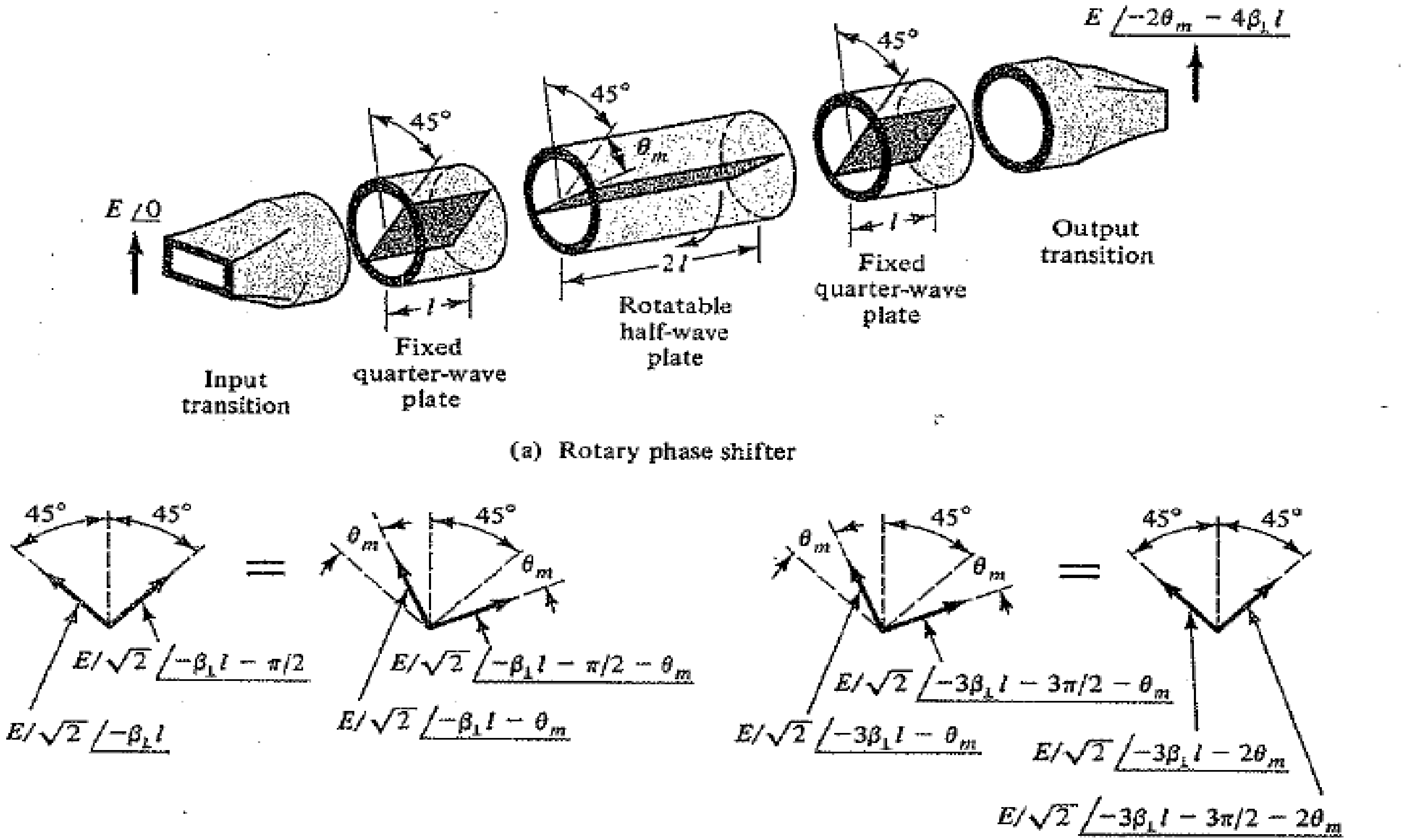

(a) Rotary phase shifter

(b) Vector-phasor components at the input to the rotatable section

(c) Vector-phasor components at the output of the rotatable section

Figure 7–27 The rotary phase shifter and its vector-phasor representation.

to replace these components by two other components, one perpendicular to the dielectric slab in the rotatable section and one parallel to it. Both sets of components are shown in part *b* of Fig. 7–27. The equivalence of these two sets was verified in Sec. 2–5 (see Fig. 2–19). With the length of the half-wave plate equal to $2l$, the perpendicular and parallel components are further delayed $2\beta_\perp l$ and $2\beta_\perp l + \pi$, respectively. The resultant components are shown in part *c* of the figure. This now represents a counterclockwise circularly polarized wave. As before, these components may be replaced by an equivalent set that are perpendicular and parallel to the *output* dielectric slab. Their vector-phasor represenation is shown on the right side of part *c* in Fig. 7–27. Propagation through the output quarter-wave plate delays these components an additional $\beta_\perp l$ and $\beta_\perp l + \pi/2$, respectively. As a result, the value of the output components are

$$E/\sqrt{2}\underline{/-4\beta_\perp l - 2\theta_m} \qquad \text{and} \qquad E/\sqrt{2}\underline{/-4\beta_\perp l - 2\pi - 2\theta_m}$$

With the waves in phase, vector addition results in a vertically polarized output wave of value $E\,\underline{/-4\beta_\perp l - 2\theta_m}$, which is shown in part *a* of Fig. 7–27. Thus, the analysis verifies that rotating the center section an angle θ_m causes the output to be phase delayed an additional $2\theta_m$. Also, with the orientation of the output transition as shown, the vertically polarized wave is delivered to the output port. Since its magnitude equals that of the input wave, the rotary phase shifter is, in principle, lossless for all values of θ_m. Commercial units are available with less than 1.0 dB loss and SWR values below 1.30.

The vector-phasor method of analysis used here is very helpful in understanding the operation of many microwave components. As explained in Sec. 2–5, it makes use of the fact that for sinusoidal signals, the propagating wave can be described by a vector-phasor. In most cases, it represents the transverse electric field of the propagating mode.

Faraday rotation

The Faraday effect is a fundamental property of ferrite materials that are magnetized parallel to the direction of propagation.

A ferrite is a nonmetallic material (though often an iron oxide compound) which is an insulator, but with magnetic properties similar to those of ferrous metals

When electromagnetic waves travel through a ferrite, they produce an RF magnetic field in the material, at right angles to the direction of propagation if the mode of propagation is correctly chosen. If an axial magnetic field from a permanent magnet is applied as well, a complex interaction takes place in the ferrite.

common ferrites are manganese ferrite ($MnFe_2O_3$), zinc ferrite ($ZnFe_2O_3$)

Microwave Isolators

An *isolator* is a nonreciprocal transmission device that is used to isolate one component from reflections of other components in the transmission line.

An ideal isolator completely absorbs the power for propagation in one direction and provides lossless transmission in the opposite direction.

Thus the isolator is usually called *uniline*.

Isolators:

Ferrite isolators may be based either on Faraday rotation, which is used for powers up to a few hundred watts, or on resonant absorption, used for higher powers. The Faraday rotation isolator, shown in Figure 10-40, will be dealt with first.

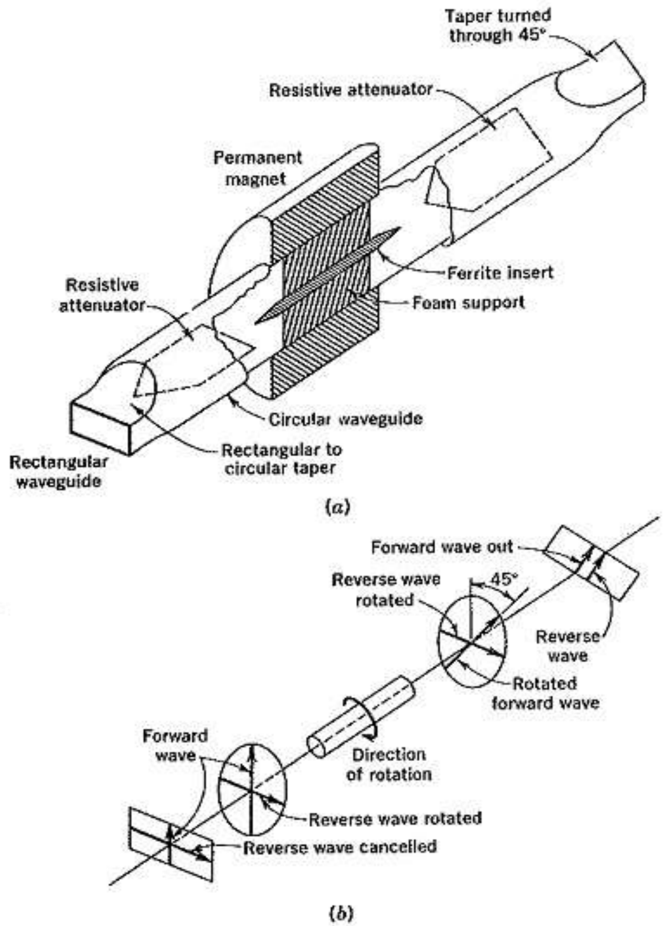

FIGURE 10-40 Faraday rotation isolator. (a) Cutaway view; (b) method of operation.

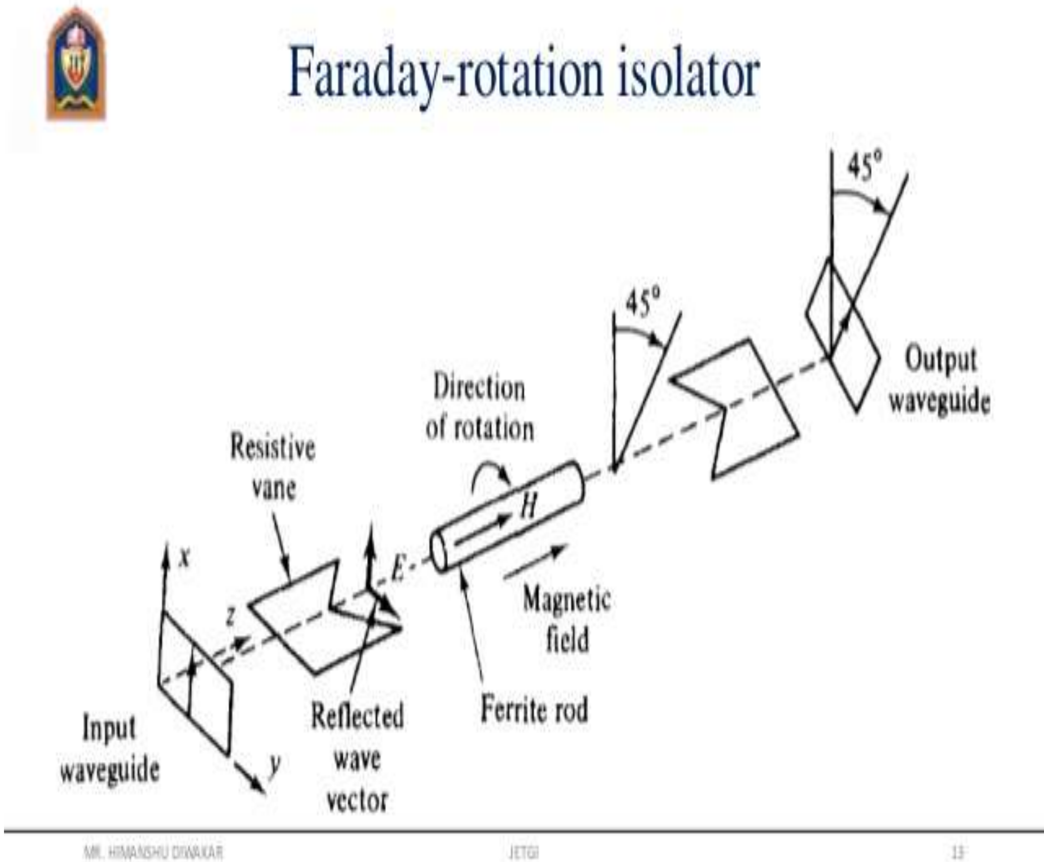

The isolator consists of a piece of circular waveguide carrying the $TE_{1,1}$ mode, with transitions to a standard rectangular guide and $TE_{1,0}$ mode at both ends (the output end transition being twisted through 45°). A thin "pencil" of ferrite is located inside the circular guide, supported by polyfoam, and the waveguide is surrounded by a permanent magnet which generates a magnetic field in the ferrite that is generally about 160 A/m. A typical practical X-band (8.0 to 12.4 GHz) device may have a length of 25 mm and a weight of 100 g without the transitions. Because the dc magnetic field (well below that required for resonance) is applied, a wave passing through the ferrite in the forward direction will have its plane of polarization shifted clockwise (through 45˚ in practical Waveguide Isolator and Circulators) by the time it reaches the output end. This wave is then passed through the suitably rotated output transition, and it emerges with an **insertion loss** (attenuation in the forward direction) between 0.5 and 1 dB in practice. It has not been affected by either of the resistive vanes because they are at right angles to the plane of its electric field; this is shown in Figure 10-40b.

A wave that tries to propagate through the isolator in the reverse direction is also rotated clockwise, because the direction of the Faraday rotation depends only on the dc magnetic field. Thus, when the wave emerges into the input transition, not only is it absorbed by the resistive vane, but also it cannot propagate in the input rectangular waveguide because of its dimensions. This situation is shown in Figure 10-40b. It results in the returned wave being attenuated by 20 to 30 dB in practice (this reverse attenuation of an isolator is called its isolation). Such a practical Waveguide Isolator and Circulators will have an SWR not exceeding 1.4, with values as low as 1.1, which is sometimes obtainable, and a bandwidth between 5 and 30 percent of the center frequency.

- Isolators are generally used to improve the frequency stability of microwave generators, such as klystrons and magnetrons, in which the reflection from the load affects the generating frequency.
- In such cases, the isolator placed between the generator and load prevents the reflected power from the unmatched load from returning to the generator.
- As a result, the isolator maintains the frequency stability of the generator.

- Isolators can be made by inserting a ferrite rod along the axis of a rectangular waveguide as shown in above Figure.
- The input resistive card is in the *y-z* plane, and the output resistive card is displaced 45° with respect to the input card. The dc magnetic field, which is applied longitudinally to the ferrite rod, rotates the wave plane of polarization by 45°.
- The degrees of rotation depend on the length and diameter of the rod and on the applied dc magnetic field.
- An input TE10 dominant mode is incident to the left end of the isolator. Since the TE10 mode wave is perpendicular to the input resistive card, the wave passes through the ferrite rod without attenuation.
- The wave in the ferrite rod section is rotated clockwise by 45° and is normal to the output resistive card. As a result of rotation, the wave arrives at the output end without attenuation at all.
- On the contrary, a reflected wave from the output end is similarly rotated clockwise 45° by the ferrite rod.
- However, since the reflected wave is parallel to the input resistive card, the wave is thereby absorbed by the input card.
- The typical performance of these isolators is about 1-dB insertion loss in forward transmission and about 20- to 30-dB isolation in reverse attenuation.

Circulators:

A circulator is a ferrite device somewhat like a rat race. It is very often a four-port (i.e., four-terminal) device, as shown in Figure 10-42a, although other forms also exist. It has the property that each terminal is connected only to the next clockwise terminal. Thus port 1 is connected to port 2, but not to 3 or 4; 2 is connected to 3, but not to 4 or 1; and so on. The main applications of such circulators are either the isolation of transmitters and receivers connected to the same antenna (as in radar), or isolation of input and output in two-terminal amplifying devices such as parametric amplifiers.

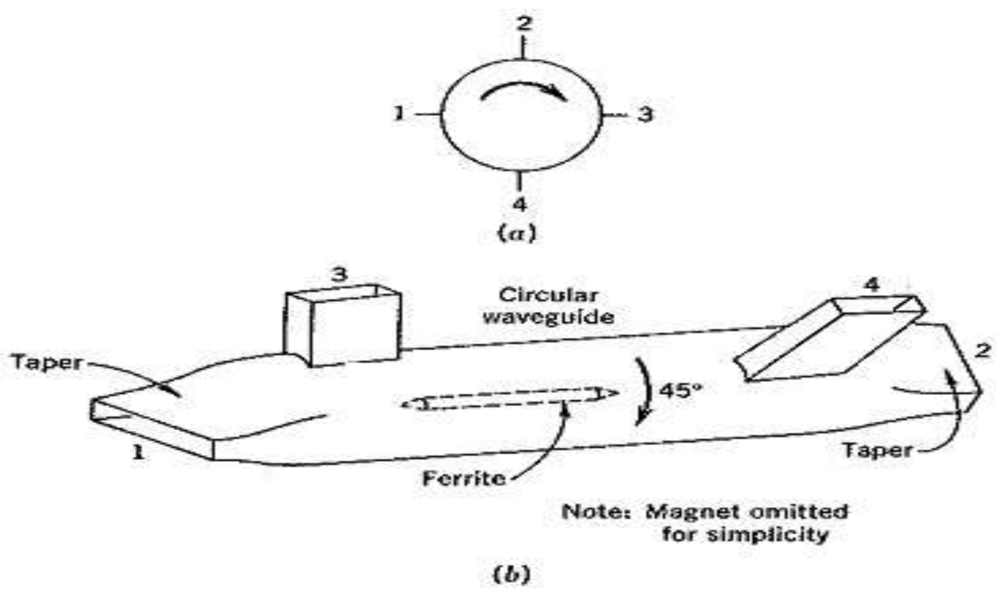

FIGURE 10-42 **Ferrite circulator. (a) Schematic diagram; (b) Faraday rotation four-port circulator.**

four-port Faraday rotation circulator is shown in Figure 10-42. It is similar to the Faraday rotation isolator already described. Power entering port 1 is converted to the $TE_{1,1}$ mode in the circular waveguide, passes port 3 unaffected because the electric field is not significantly cut, is rotated through 45° by the ferrite insert (the magnet is omitted for simplicity), continues past port 4 for the same reason that it passed port 3, and finally emerges from port 2, just as it did in the isolator. Power fed to port 2 will undergo the same fate that it did in the isolator, but now it is rotated so that although it still cannot come out of port 1, it has port 3 suitably aligned and emerges from it. Similarly, port 3 is coupled only to port 4, and port 4 to port 1. This type of circulator is power-limited to the same extent as the Faraday rotation isolator, but it is eminently suitable as a low-power device. However, since it is bulkier than the Y (or wye) circulator (to be described), its use is restricted mostly to the highest frequencies, in the millimeter range and above. Its characteristics are similar to those of the isolator.

High-power circulators are fairly similar to the resonance isolator and handle powers up to 30 MW p

Microwave Circulators

A *microwave circulator* is a multiport waveguide junction in which the wave can flow only from the nth port to the $(n + 1)$th port in one direction as in figure

Although there is **no restriction** on the number of ports, the four-port microwave circulator is the most common.

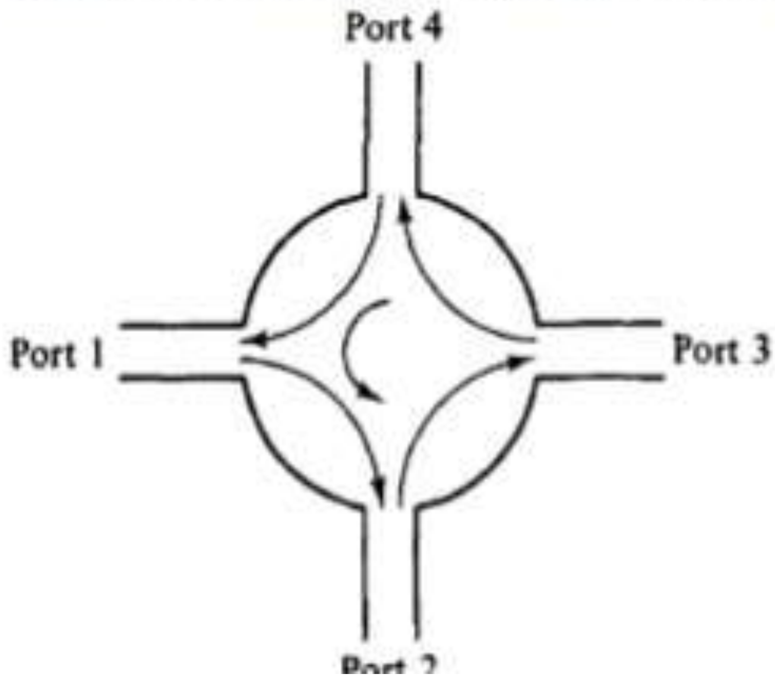

One type of four-port microwave circulator is a combination of two 3-dB side-hole directional couplers and a rectangular waveguide with two nonreciprocal phase shifters as shown in Fig.

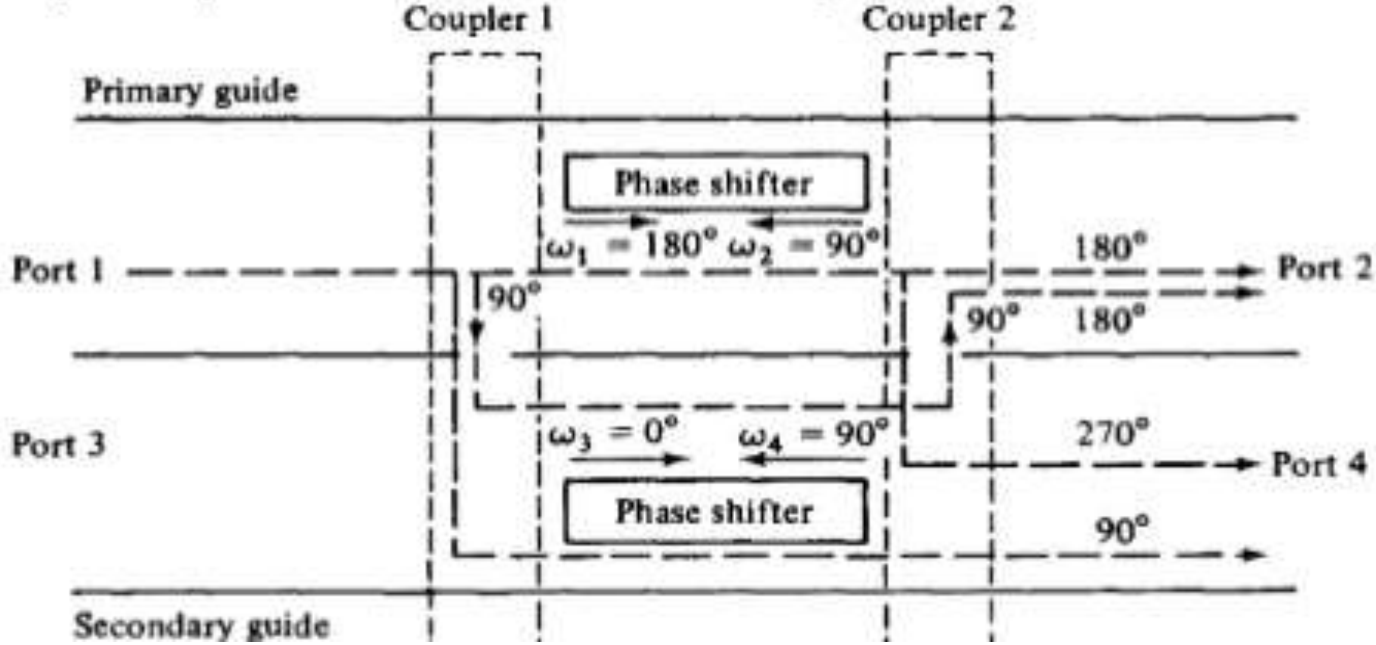

- Each of the two 3-dB couplers in the circulator introduces a phase shift of 90° and each of the two phase shifters produces a certain amount of phase change in a certain direction as indicated.

- Since the two waves reaching port 4 are out of phase by 180°, the power transmission from port 1 to port 4 is zero.

- In general, the differential propagation constants in the two directions

$$\omega_1 - \omega_3 = (2m + 1)\pi \qquad \text{rad/s}$$

$$\omega_2 - \omega_4 = 2n\pi \qquad \text{rad/s}$$

- where m and n are any integers, including zeros.

Many types of microwave circulators are in use today. However, their principles of operation remain the same.

A perfectly matched, lossless, and nonreciprocal four-port circulator has an S matrix of the form

$$\mathbf{S} = \begin{bmatrix} 0 & S_{12} & S_{13} & S_{14} \\ S_{21} & 0 & S_{23} & S_{24} \\ S_{31} & S_{32} & 0 & S_{34} \\ S_{41} & S_{42} & S_{43} & 0 \end{bmatrix}$$

Q- FACTOR OF A CAVITY

1. OBJECTIVE: Measurement of the Q-Factor of a Cavity.

Apparatus

1. Gunn/Klystron source
2. Isolator
3. Variable attenuator 20db.
4. Wave meter.
5. Slotted line
6. Tunable detector 2 Nos
7. VSWR meter.

2. THEORY:

The microwave cavities are basically of two types:

a) Transmission type

b) Absorption type

The transmission type cavity transmits maximum power at resonant frequency and absorption type absorbs the power at the resonant frequency. Cavities are used both as circuit elements and as measuring instruments.

The Q-factor of a cavity has the same meaning as the Q of a resonant circuit lower frequency. It is defined as

$$Q = w\frac{Maximum\ Energy\ stored}{Power\ Loss}$$

Energy stored in the cavity depends on the volume, and the power loss depends on the losses in the conducting walls of the cavity. Approximate value of the Q of the cavity is

$$Q = \frac{V}{A\,S}$$

A = Surface area

S = Skin depth.

V = Volume of the cavity

The intrinsic or unloaded Q_L is greater than the total or loaded Q which includes the effect of coupling mechanism. The loaded Q_L of a cavity may be measured very simply by observing the shape of its resonance curve as a function of frequency. The Q_L of the cavity is determined from

$$Q_L = \frac{f_0}{f_2 - f_1}$$

F_0 resonant frequency.

F_1 & F_2 the 3 dB points.

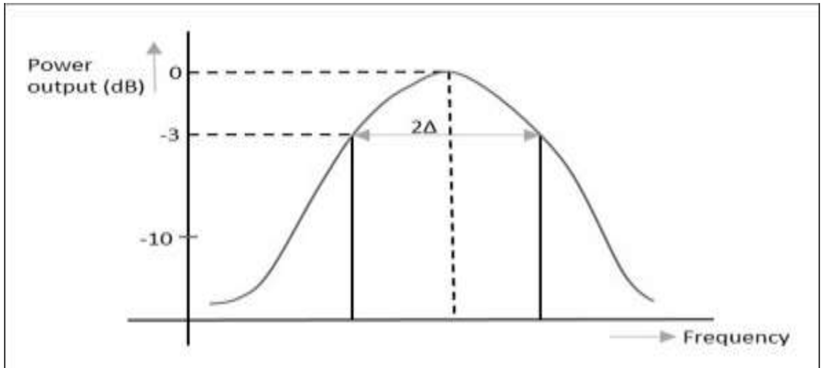

Resonance Curve

3. PROCEDURE:

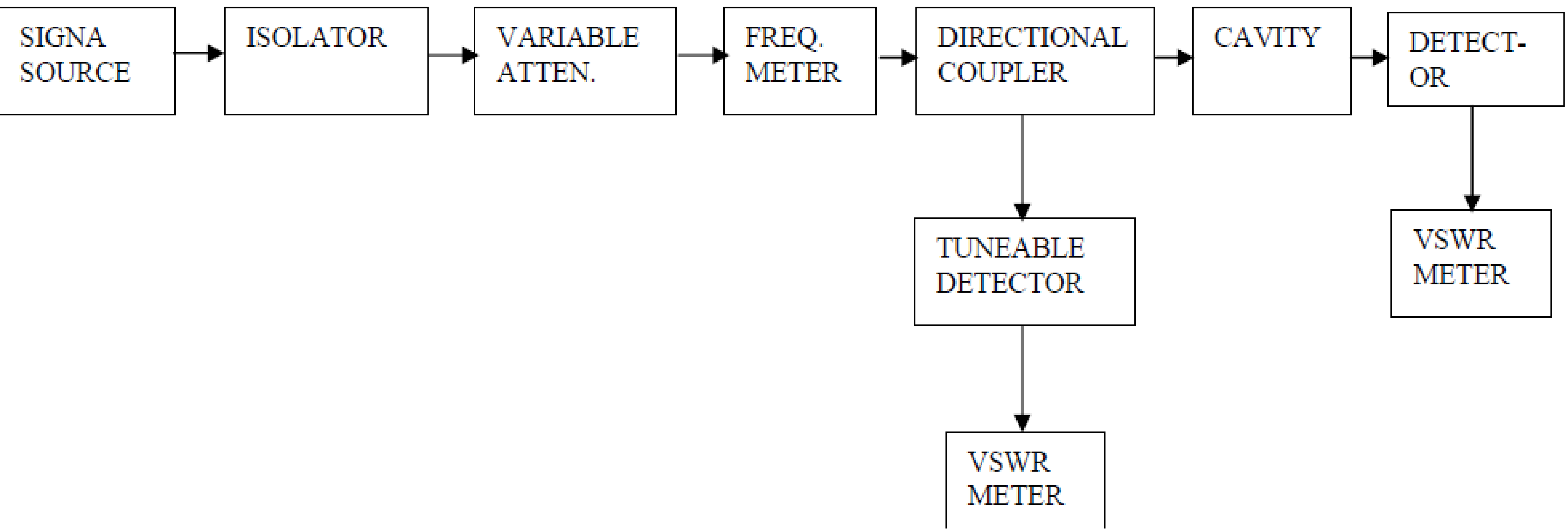

1. Set the microwave bench as shown in the figure.
2. Set the cavity of any position. Set the source frequency output shows a dip if it is a absorption type of vice-versa.

3. keeping the input power to the cavity constant (by using variable attenuator, if necessary), measure the frequencies $(F_1 \& F_2)$ of signal source setting where the output power changes by 3 dB from the resonant frequency value.
4. The graph between frequency and power output may also be drawn.
5. Calculate the value of Q using the given formula. Repeat the different cavity settings.

4. PRECAUTIONS:

1. For calculating Q-factor of the cavity of particular resonant frequency, the cavity position should remain unchanged?
2. For a cavity which has a high/good Q-factor, the signal source should be very stable and it should have capability of frequency variation of at least one megahertz.
3. A tunable detector should be used and it should be tuned for each operating frequency.